

Investigations on peritoneal dialysis
by mathematical modeling and in
vitro/vivo experiments

Dissertation
zur Erlangung des Grades
des Doktors der Naturwissenschaften
der Naturwissenschaftlich-Technischen Fakultät
der Universität des Saarlandes

von
Bernd Eberle

Saarbrücken

2022

Tag des Kolloquiums:	14. April 2023
Dekan:	Prof. Dr. Ludger Santen
Berichterstatter:	Prof. Dr. Christian Wagner Prof. Dr. med. Matthias W. Laschke
Vorsitz:	Prof. Dr. Jochen Hub
Akad. Beisitzer:	Dr. Brigitta Loretz

Abstract

Peritoneal dialysis (PD), which places less stress on the cardiovascular system, is an alternative to the commonly applied hemodialysis (HD) for patients with kidney disease. Each patient should have a treatment plan tailored to his/her individual needs in terms of filling volume, concentration of OA, and length of stay. In practice, this is usually done during ongoing treatment through ongoing adjustment and individualization, as testing to obtain patient-specific information is often too infrequently performed. State of the art research to describe transport processes during PD is the so-called biophysical "TPM". In the context of this work concepts and methods are developed, which may improve the currently used treatment scheme in humans. The software available on the market is mainly designed for substance parameters and less suitable to adjust the patient to a sustainable euvolemic hydration status. Most tests used to determine the patient's membrane parameters do not provide sustainable usable information on the ultrafiltration volume to be achieved per cycle. Biophysical models and methods should be readily applicable and characterize the specific patient. PD devices with intraperitoneal pressure measurement, body composition monitors or dry weight concepts as known from HD could be used to optimize treatment.

Kurzfassung

Die Peritonealdialyse (PD), die das Herz-Kreislauf-System weniger belastet, ist für nierenkranke Patienten eine Alternative zur Hämodialyse (HD). Für den Patienten sollte ein Behandlungsplan erstellt werden, der auf individuelle Bedürfnisse hinsichtlich Füllvolumen, Konzentration des osmotischen Agens und Verweildauer zugeschnitten ist. In der Praxis erfolgt dies meist während der laufenden Behandlung durch fortwährende Anpassung, denn Tests zur Gewinnung patientenspezifischer Informationen werden oft zu selten durchgeführt. Stand der Forschung zur Beschreibung der Transportprozesse während der PD ist das sogenannte biophysikalische "Drei-Poren-Modell". Im Rahmen dieser Arbeit wurden Konzepte und Methoden entwickelt, welche das aktuell verwendete Behandlungsschema am Menschen verbessern könnten. Die auf dem Markt erhältliche Software ist hauptsächlich auf Stoffparameter ausgelegt und weniger geeignet, um den Patienten nachhaltig auf einen euvolemischen Hydratationsstatus einzustellen. Die meisten Tests zur Bestimmung der Membranparameter des Patienten liefern keine nachhaltig verwendbaren Informationen über das pro Zyklus zu erreichende Ultrafiltrationsvolumen. Biophysikalische Modelle und Methoden sollten leicht anwendbar sein und den spezifischen Patienten charakterisieren. PD-Geräte mit intraperitonealer Druckmessung, Body-Composition-Monitore oder Dry-Weight-Konzepte, wie sie von der HD bekannt sind, könnten zum Optimieren der Behandlung Verwendung finden.

List of abbreviations

CAPD	Continuous Ambulatory PD
Da	Dalton
NaCl	Sodium chloride
PD	Peritoneal Dialysis
OA	Osmotic Agent
BCM	Body Composition Monitor
UFV	Ultrafiltration volume
IPP	Intraperitoneal pressure
IPV	Intraperitoneal volume
TPM	Three Pore Model
APD	Automated PD
CTA	Cellulosetriacetat
HD	Hemodialysis
MTAC	Mass transfer coefficient
PET	Peritoneal Equilibration Test
POL	PatientOnLine
UF	Ultrafiltration
CKD	Chronic kidney disease

Content

Chapter 1: Brief introduction, literature review and motivation	1
Chapter 2: Basics concepts and mathematical modeling	3
2.1 PD	3
2.2 Mathematical description	8
2.3 Quality assurance tests.....	14
2.4 State of the art in medical software applications	17
2.5 Targets and main problems for patients on PD	18
Chapter 3: Mathematical model approaches and preparatory <i>in vitro</i> experiments.....	20
3.1 Empirical model approach.....	20
3.2 Abstraction of the biophysical model approaches	23
3.3 Simplified biophysical model approaches	28
3.4 <i>In vitro</i> test setup <i>Bvatar</i>	34
Chapter 4: <i>In vivo</i> test setup, material and animal study design	37
4.1 <i>In vivo</i> test setup for the animal experiments	37
4.2 Material.....	39
4.3 Protocol and study design.....	39
Chapter 5: Experimental results and discussion of the <i>in vivo</i> study results.....	44
5.1 Preliminary testing and general findings	44
5.2 Study observations.....	47
5.3 Plasma glucose concentration and osmolarity	51
5.4 Dialysate and plasma osmolarity	53
5.5 Osmolarity and UFV dependency	55
5.6 Pressure / Volume - characteristics	56
5.7 Calculation of the relative hydration in percent	61
5.8 Relationship of IPP and UFV during the dwell.....	65
5.9 Pressure change during the dwell for different dialysates and corresponding volume estimated from the P/V characteristics	69
Chapter 6: Comparison of the experimental results to the model approaches	70
6.1 Empirical model using the experimental data obtained.....	70
6.2 Biophysical model	76
Chapter 7: Summary and outlook.....	78
7.1 Summary.....	78
7.2 Outlook	78
Literature	80
Appendix	87

Chapter 1: Brief introduction, literature review and motivation

Peritoneal dialysis (PD) is used as a blood purification method for the treatment of renal insufficiencies. A distinction is made between acute and chronic kidney failure. Acute renal failure is a decline of the excretory functions of the kidney occurring within a few hours to days and is normally a reversible deterioration of the renal function. Acute kidney failure can occur in the context of multi-organ failure or, for example, after an accident due to lack of volume and shock. Chronic kidney disease (CKD) is usually caused by inflammatory kidney indisposition. The course of CKD is rather insidious and not reversible compared to acute kidney failure. To differentiate between acute and chronic kidney failure, various clinical examinations as well as medical interviews during the disease must be carried out. For example, a smaller kidney that is examined by ultrasound can be a sign of CKD. In addition, urine indices, such as urine osmolality, urine-sodium concentration or urea elimination are used, as well as urea and creatinine concentration in the blood. In addition to other treatment options, such as hemodialysis (HD) and kidney transplantation, PD is a relatively gentle method. With PD treatment it is possible to avoid high toxin concentrations due to the continuous detoxification. Through a catheter implanted in the abdominal cavity the dialysis solution is infused to the patient, where it is in direct contact with the peritoneum. The dialysate solution contains an OA drawing metabolic waste products and excess body water from the patient's blood through interstitium and the peritoneal membrane inside the abdominal cavity. After the treatment, the dialysis solution with the containing toxins and the removed body water is passed through the catheter into a waste bag. The peritoneum is a semi-permeable membrane that is responsible for the exchange of fluids and substances by blood and lymph vessels. To generate an osmotic gradient, an osmotically active substance with high concentration compared to the patient's blood must be contained in the PD solution [1-4].

Commercially available OAs are glucose, icodextrin and amino acids. For this purpose, a schedule for every specific patient must be created depending on his individual needs. The steady state of prescribing the transport processes in PD is the so called three pore model (TPM), which is a mathematical and biophysical model of fluid and mass transport during a PD cycle [5-7].

Software commercially available today including some parts of the TPM approaches is favorable for theoretical considerations, but is lacking to describe the ultrafiltration during the treatment in practical situations [8-11].

Also, the used membrane tests like the peritoneal equilibration test (PET) to determine the membrane parameters of the patient provide neglectable information about the ultrafiltration volume and are not performed sufficiently frequent. The remove of toxins in PD is no longer critical and therefore some established quality assurance tests exist to guarantee the removal of the waste products from the body, which could not any longer be removed by the kidneys [12-13].

New model approaches to simulate the PD treatment of a specific patient should be easy to use in practical situations. The detection of alterations of the peritoneum during a long period on PD by characterization of the peritoneal membrane with patient-specific transport parameters need to be considered. To determine these parameters, new membrane test methods using

intraperitoneal pressure to acquire the needed data for every treatment cycle will be favorable [2, 10-14].

The cause of overhydration or dehydration is the biggest problem in PD today which needs to be investigated to avoid drop out and transfer to HD (HD). To keep the patient on a healthy hydration status, the treatment scheduling needs to compensate continuously for a bunch of influencing factors. The main factors are fluid intake, urinary output or residual renal function and the specific peritoneal membrane of the patient [2-3].

The scope of this thesis, which was carried out in cooperation with Fresenius Medical Care Deutschland GmbH, is to improve and individualize the PD treatment. With knowledge from literature and a dedicated lab test setup, called *Bvatar*, the transport phenomena and processes during PD are investigated. Further, an animal study and practical empirical and biophysical models are developed. These approaches should be used in the future to give the opportunity to create a controlled treatment schedule, which keeps the individual patient on a euvolemic hydration state. A new medical software application, which uses all the introduced new concepts combined with body composition monitoring (BCM) measurements in a feedback control system, could continuously reschedule the treatment plan to keep the patient on steady state and optimize the treatment. Further new concepts to improve the treatment are to use new OAs, improve the internet of things (IoT) for devices and integrate them to a so-called expert system inside a medical software application (MSA) [17].

Chapter 1 contains the basics and mathematical models to describe PD, existing biophysical models, membrane and established quality assurance tests are described. The next chapter introduces the experimental part with the *in vitro* test setup called “*Bvatar*” and the model approaches and hypotheses. The following chapters 4 to 6 thematize the animal experiments at the Institute for Clinical and Experimental Surgery, Saarland University, Homburg. The various results are discussed followed by a first evaluation of the model approaches. The last chapter gives some insights into future applications of the model in combination with a feedback control system.

Various patent application ideas listed in the Appendix came up in the context of this project. The first patent application deals with an empirical model approach to optimize ultrafiltration prediction and detection of peritonitis. Other authors involved are Vaibhav Maheshwari (previous Renal Research Institute, New York City, left the company) and Paul Chamney (Fresenius Medical Care United Kingdom). The second patent application describes a simplified biophysical model approach for ultrafiltration based on continuous intraperitoneal pressure measurement and various methodologies for application in practice. The model could be modified to deal with all available OAs. Other authors involved here are also Paul Chamney, Vaibhav Maheshwari and David Jörg (Fresenius Medical Care Deutschland).

Further patent applications invented during this thesis are the Wearable Artificial Kidney on PD concepts (WAK-PD) and a novel bimodal dialysis solution, which is a mixture of polyglucose and trehalose. An animal study in cooperation with Carl Öberg was conducted at the University of Lund in Sweden to investigate sodium removal in PD. Further a first trial with patients was planned and executed at the Renal Research Institute in New York City.

Chapter 2: Basics concepts and mathematical modeling

In this section the basic principles of PD and the biophysical concepts of existing model approaches are introduced. Further, the commonly used treatment modalities and quality assurance tests are explained.

2.1 PD

PD uses the patient's peritoneum as a dialysis membrane to clean the blood from uremia toxins. The peritoneum is a tissue with a good capillary blood supply that lines the abdominal cavity and surrounds many organs. The peritoneal membrane acts as the body's own exchange membrane because its pores are semipermeable to certain substances, respectively they allow them to pass through and retain others. For PD, a catheter must be implanted into the patient's abdominal cavity, through which the dialysate solution can be filled and drained. This solution is in contact with the peritoneal membrane in the abdominal cavity for several hours. Due to the concentration gradient between the capillary vessels of the peritoneum and the dialysis solution, the metabolic waste products from the blood pass through the various pores of the peritoneum into the dialysate. Another important task of PD is to remove excess water from the patient's body by ultrafiltration. One of the main problems with PD is to maintain a healthy water balance during long time treatment of the patient. To produce an osmotic gradient, the dialysis solution must contain a higher content of soluble substances than the patient's blood plasma. Many dialysates contain glucose in varying concentrations as an osmotic agent (OA) because it is a naturally occurring substance in the human organism and therefore highly biocompatible. Other commercially available OA are icodextrin (Baxter) and amino acids. To enable permanent blood clearance, the dialysis fluid must be drained after a certain time and replaced with fresh solution, which need to be repeated a few times per day. Due to its small size, glucose can diffuse through the peritoneum into the body, which causes the crystalloid osmotic pressure gradient to decrease. This additionally leads to a decrease in ultrafiltration due to the lower concentration gradient. The glucose enters the patient's bloodstream and gets metabolized rapidly. The patient can carry out most of the treatment at home and is therefore less dependent on dialysis centers or clinics compared to HD. However, the risk of infection from the implanted catheter is a disadvantage, since sterility must be considered when exchanging the dialysate. In long-term use, PD can lead to changes in the peritoneum, lipid metabolism disorders due to glucose uptake and protein loss [2-3, 6, 15, 21-24].

Structure of the peritoneal membrane

A prerequisite for the treatment of CKD with PD is an intact peritoneum. This membrane functions as a semipermeable membrane during the treatment and consists of various parts. The average anatomical surface area is between 1.5 and 2 m^2 but varies greatly depending on gender, age and body dimensions. Only a part of the peritoneum is involved in the fluid and mass exchange (approx. 0.5 to 1 m^2 effective surface area), since factors, such as dialysate volume, distribution and blood circulation in the peritoneal membrane, play an important role. In the peritoneal membrane, the blood vessels and capillaries are embedded in the interstitium, a connective tissue-like matrix structure [2, 24, 35-38].

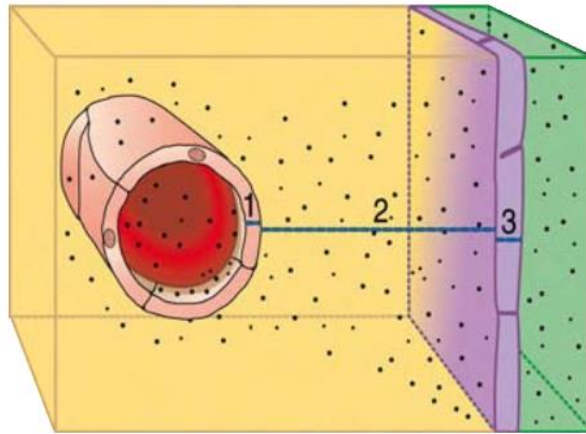


Figure 2-1: Peritoneal membrane composition of blood capillaries consisting of endothelial cells (1), the interstitial matrix (2) and the mesothelial cell layer (3) [2].

The transport of substances during PD takes place from the blood capillaries (Figure 2-1 (1)) through their endothelial cell layer and basement membrane through the interstitium (Figure 2-1 (2)) and the outer unicellular mesothelial cell layer (Figure 2-1 (3)) towards the peritoneal cavity. In the TPM according to Bengt Rippe, a distinction is made between three types of pores (Figure 2-2) [2, 7].

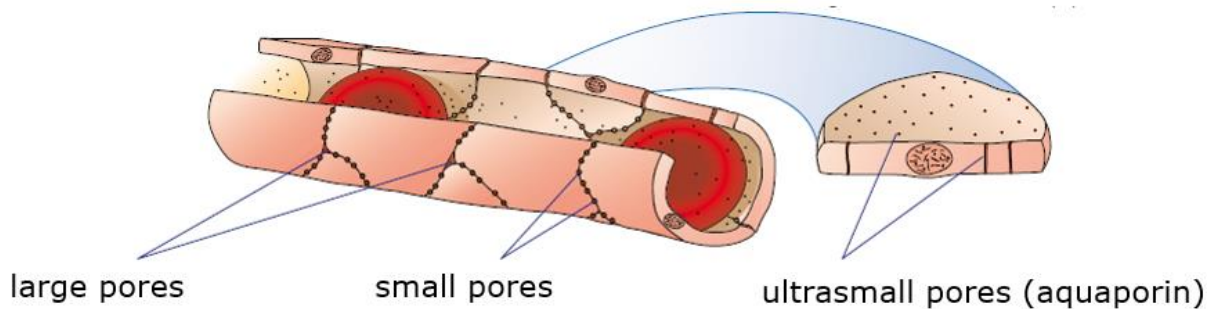


Figure 2-2: TPM composition of the peritoneal membrane by large, small and ultrasmall pores [2]

- Ultrasmall pores also called aquaporins ($r < 0.25$ nm), permeable only to water [2].
- Small pores ($r = 4 - 5$ nm) with a proportion of approx. 99.5% form the main component of the number of all pores, permeable to water and small molecular substances, such as glucose, urea, creatinine and electrolytes [2].
- Large pores ($r > 25$ nm) with a proportion of $< 0.5\%$ are additionally permeable for macromolecular substances, such as proteins [2].

The mainly continuous endothelial cell layer of the blood vessels is the main barrier. There are gaps between the endothelial cells with a diameter of 4 to 5 nm, as well as a small number of gaps with a diameter of approx. 25 nm. The continuous endothelium of the capillaries also contains ultra-small water-selective channels (transcellular pores) with a diameter of ~ 0.25 nm. The trans-peritoneal transport processes are performed by diffusion, osmotic ultrafiltration, convective mass transport and reabsorption of fluid from the abdominal cavity by the lymphatics. In addition to the blood vessels, the interstitium also contains lymph vessels through which a lymphatic absorption of dialysis solution from the abdominal cavity takes place. Aquaporins play an important role in PD in the use of low molecular weight OAs, as water transport by the water channels depends on the number of particles [2, 23, 26-27].

Transport processes through semipermeable membranes

For HD the artificial filter membrane is well characterized by manufacturing and the membrane parameters are known and can be determined with validated industrial test methods. The patient gets a new dialysis filter for every treatment and because of the known transport characteristics of the membrane the removal of water and toxins is well predictable. If PD is used, the filter membrane is in fact the peritoneum of the patient with different membrane parameters for each patient, which change during the time of PD treatment due to alteration of the peritoneal membrane or peritonitis events. During dialysis treatment, the peritoneal membrane transports fluids and substances due to the concentration gradient, respectively the osmotic pressure. In contrast in HD with a pump the needed pressure gradient, time and volume flow can be calculated to fit the patient's individual needs. In PD this is much more difficult and therefore a distinction must be made between the following transport processes:

- Diffusion (electrolytes, glucose, uremia toxins)
- Ultrafiltration (water)
- Convection (mainly serum ingredients)

Further changes of the peritoneal membranes transport characteristics occurring in course of the treatment over a longer period of time are neovascularization and fibrosis, whereby these tissue alterations need to be handled by skillful adaptation of the treatment schedule by the nephrologist to fit the varying needs of the patient [2-3, 43, 46].

Continuous ambulatory PD and automated PD

There are different types of procedures to perform PD available on the market. In Continuous Ambulatory PD (CAPD), the dialysis solution is introduced and withdrawn manually, whereas in Automated PD (APD), a machine called cycler is used. For CAPD, the volume of the dialysate of around 1.5 to 2.5 L remains in the abdominal cavity for around 4 to 8 hours. The changes take place on average three to five times a day. With APD, the cycler changes the dialysate and thus controls factors, such as the inflow quantity, dwell time and outflow. Flexibility in the PD schedule allows for adjustment to various lifestyles of PD patients. There are some important differences between APD and CAPD in terms of the removal of excess body water and toxins, as the retention times in APD procedures are usually shorter since the changes could be preceded automatically during the overnight treatment. PD treatment with glucose as the OA has the highest ultrafiltration rate at the beginning of the treatment (short dwell behavior) due to the high crystalloid osmotic gradient. If an APD method is selected, the ultrafiltration performance can be increased by the shorter residence time while at the same time reducing glucose absorption. The removal of toxins depends on the dialysate flow, the molecule size and the peritoneum of the patient. In general, however, the removal of low-molecular uremia toxins, such as urea, can be increased by a higher ultrafiltration rate in APD with a cycler, but the sodium loading, resulting from short dwells, may cause additional problems for the patient. A major advantage of APD to CAPD is that cyclers are often equipped with software for interpreting the PD process. With the help of this software, the treatment process can be stored on a patient card and, conversely, a treatment scheme can be stored on the card, which is then provided by the cycler to the patient automatically. The therapy form of

adapted APD with a cycler (for example sleep-safe harmony) allows the combination of cycles with short dwell times and small filling volumes as well as cycles with long dwell times and large filling volumes. The catheter, for filling and draining the peritoneal cavity, which is permanently implanted in the patient's abdominal cavity, is supplied with dialysis solution by a tube system [2, 25-34].

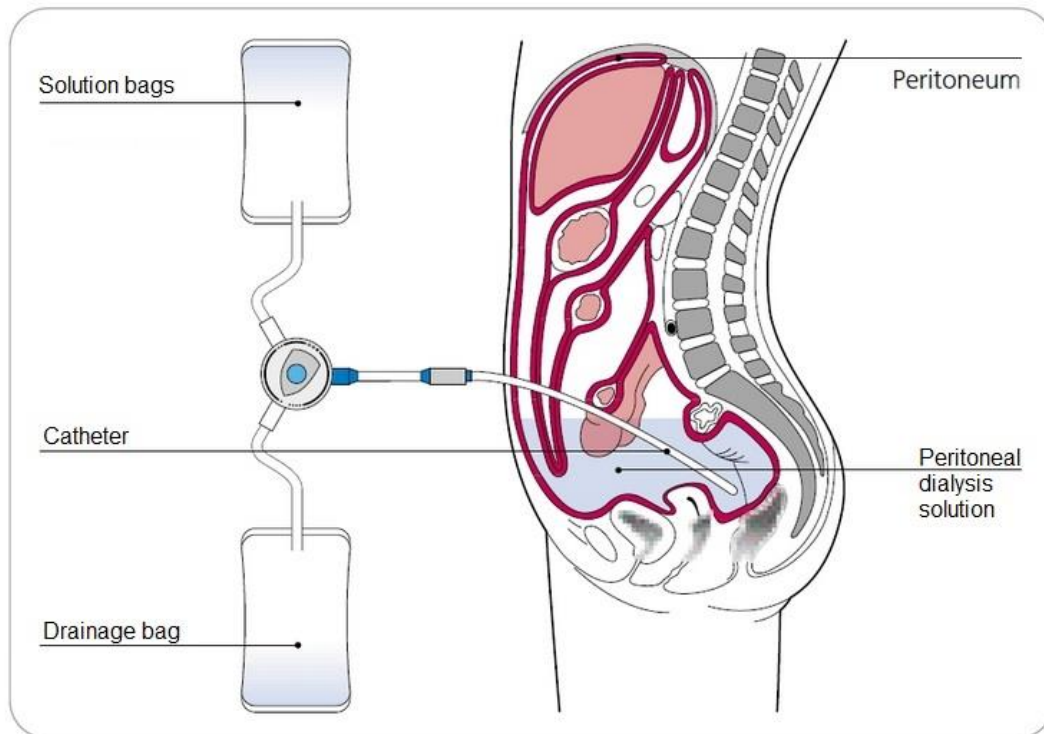


Figure 2-3: Functional principle of CAPD. The solution bag is positioned in a higher position to allow the dialysate to flow by gravity through the catheter inside the abdominal cavity. The dialysis solution is in contact with the peritoneum during the dwell phase. At the end of the treatment a drainage bag is positioned below the catheter to let the solution flow out again [1].

Due to the position of the dialysis bag, the solution flows through gravity into the peritoneal cavity and remains there for a defined time in cause of CAPD treatment, which may differ due to different membrane configurations of the patient's peritoneum. After the specified time has elapsed, the solution is drained again by skillfully positioning the waist bag and also using gravity (Figure 2-3) in comparison to APD, where a pump is used respectively [2-3, 29, 33].

Composition of PD solutions

PD solutions contain various compositions, which are based on blood plasma in their concentration and additionally contain an osmotically effective agent.

The main components of a PD solution are:

- Electrolyte mixture (calcium, magnesium, sodium, chloride)
- Buffer (lactate, bicarbonate)
- OA (glucose, icodextrin and amino acids)

Table 2.1-I clearly shows that the concentration gradient between the glucose concentration in the dialysis solution and the blood plasma is responsible for the transport processes involved in chapter 0 and that the osmotic gradient results from this concentration gradient [2-3, 5, 15].

Table 2.1-I: Composition of a dialysis solution compared to the blood plasma of a human [2-3, 5].

Active pharmaceutical ingredients	CAPD solution [mmol/L]	Blood plasma reference range [mmol/L]
Sodium (Na ⁺)	134	135 - 150
Calcium (Ca ²⁺)	1.75	1.1 - 1.3
Magnesium (Mg ²⁺)	0.5	0.7 - 1.6
Chloride (Cl ⁻)	103.5	98 - 112
Potassium (K)	-	3,5 - 4,5
Hydrogen carbonate (HCO ₃ ⁻)	-	22 - 26
Lactate	35	-
Glucose	83.2 - 235.8	3.05 - 6.1

The task of the PD solution is to withdraw uremia toxins, such as creatinine ($C_4H_9N_3O_2$; 131.13 g/mol), and urea (CH_4N_2O ; 60.06 g/mol) and excess body water from the patient's blood into the dialysate. In addition, the dialysis solution should balance the patient's acid-base and electrolyte level. One of the requirements for a PD solution is biocompatibility, so it is as compatible as possible for the patient and does not cause long-term damage to the peritoneum. Regarding the sodium concentration, there are new approaches to reduce the concentration in the PD solution to achieve a positive effect on blood pressure and overhydration (so-called "low sodium solutions"). Lactate is used as the standard buffer system in the single-chamber bag for PD solutions with a pH value in the range of 5.5, to reduce the formation of glucose degradation products (GDP) during sterilization, as these could have a damaging effect on the peritoneal membrane. Studies have shown that the formation of GDPs increases the higher the pH of the solution to be sterilized. GDPs are mainly responsible for the formation of so-called advanced glycation end products (AGEs), which are deposited in the vessels of the peritoneum and are a possible cause for the increase in peritoneal permeability and thus for long-term ultrafiltration failure. The dialysis solutions from Fresenius Medical Care and other manufacturers (Baxter e.g.) contain glucose as an OA. Also, other PD solutions with a glucose polymer (Icodextrin, Extraneal®, Baxter) and amino acids (Nutrineal®, Baxter) are available on the market. The use of glucose as an OA has several advantages and disadvantages for the PD patients. Glucose is a substance known to the body and can be completely metabolized to H₂O and CO₂ by the organism after absorption. Especially for diabetic patients, the additional caloric load is a problem. In addition, a permanently high glucose load, the GDPs and the resulting AGEs have a negative effect on the peritoneum, resulting in structural and functional changes. The mesothelial cell layer, which is responsible for defense mechanisms and acts as an additional barrier, is ablated. Further consequences are the formation of fibrotic tissue, which also changes the barrier properties over time and the formation of new capillary vessels. This so-called neovascularization increases the proportion of the total pore surface area, whereby the glucose is absorbed more quickly and thus the osmotic pressure decreases even faster [2, 6, 15, 26, 31, 37-42, 58].

2.2 Mathematical description

Basic principles

Diffusion describes the movement of solutes and molecules, from a location of high concentration to a location of low concentration, to achieve concentration equilibrium. The first Fick'sche diffusion law and the Stokes-Einstein equation describe the dependencies of the diffusion rate on the different factors [24, 44, 46].

$$D_i = \frac{k_B T}{6 \pi r_{H,i} \eta}$$

Equation 2-1

Table 2.2-I: Description of the used terms and the corresponding unit.

Term	Description	Unit
k_B	Boltzmann constant	$\left[\frac{J}{K} \right]$
T	Temperature	$[K]$
η	Dynamic viscosity of the solvent	$[Pa \cdot s]$
$r_{H,i}$	Hydrodynamic radius of the i-th solute	$[m]$
D_i	Diffusion coefficient of the i-th solute	$\left[\frac{m^2}{s} \right]$

$$J_{D,i} = \frac{dn_{D,i}}{dt} = -D_i S \frac{\Delta c_i}{\Delta x}$$

Equation 2-2

Table 2.2-II: Description of the used terms and the corresponding unit.

Term	Description	Unit
S	Surface area	$[m^2]$
$J_{D,i}; \frac{dn_{D,i}}{dt}$	Particle flow of the i-th solute through diffusion	$\left[\frac{mol}{s} \right]$
Δc_i	Concentration difference between the compartments of the i-th solute	$\left[\frac{mol}{m^3} \right]$
Δx	Thickness of the membrane	$[m]$
t	Time	$[s]$

The particle flow J_D is therefore proportional to the surface area S , depending on the concentration difference, increases with increasing temperature T and decreases with increasing molecular radius r and increasing viscosity of the solvent η . In PD, for example, urea, which is present in the blood in high concentrations due to inadequate kidney function, diffuses into the dialysate until the concentration balance is achieved. The glucose contained in the dialysate diffuses in the opposite direction from the abdominal cavity into the blood capillaries. If one also considers the transport processes and physiological conditions, further effects play a role. The speed of diffusion depends on the permeability of the peritoneum. If the permeability is

high, the diffusion of urea from the blood into the dialysate, for example, is promoted, but drainage is made more difficult because the OA diffuses from the dialysis fluid into the blood plasma and the osmotic pressure gradient decreases. At low permeability the diffusion of molecules is more difficult, which leads to a better ultrafiltration performance, as the osmotic gradient is maintained longer [24, 44, 46].

To simplify the Equation 2-2, it is possible to introduce the permeability as a membrane coefficient.

$$P_i = \frac{D_i}{\Delta x}$$

Equation 2-3

Table 2.2-III: Description of the used terms and the corresponding unit.

Term	Description	Unit
P_i	Permeability of the i-th solute	$\left[\frac{m^3}{s}\right]$

$$J_{D,i} = \frac{dn_i}{dt} = -P_i S \Delta c_i$$

Equation 2-4

Ultrafiltration describes the transport of fluid from the peritoneal blood capillaries through the semipermeable pores into the dialysis fluid. The solvent transport through membranes is based on a pressure gradient. The equation of Hagen-Poiseuille (Equation 2-5) is used to describe the volume flow through homogeny porous membranes [24, 44, 46]:

$$J_V = \frac{dV}{dt} = \frac{\pi r^4 \Delta P}{8 \eta l}$$

Equation 2-5

Table 2.2-IV: Description of the used terms and the corresponding unit.

Term	Description	Unit
$J_V; \frac{dV}{dt}$	Volume flux	$\left[\frac{m^3}{s}\right]$
r	Inner radius of the pore	$[m]$
l	Length of the pore	$[m]$
ΔP	Pressure difference	$[Pa]$

If all terms concerning the membrane are combined to one parameter, the hydraulic conductivity L_p as in Equation 2-6 is obtained:

$$J_V = \frac{dV}{dt} = L_p S \Delta P_{sum}$$

Equation 2-6

Table 2.2-V: Description of the used terms and the corresponding unit.

Term	Description	Unit
$L_p S$	Hydraulic conductance	$\left[\frac{m^3}{s Pa} \right]$
ΔP_{Sum}	Sum of all pressure differences across the membrane	$[Pa]$

In order to generate the osmotic pressure gradient along the peritoneal membrane, glucose is often used as an OA. The osmotic pressure difference is calculated by Equation 2-7.

$$\Delta\pi_i = R T \Delta c_i$$

Equation 2-7

Table 2.2-VI: Description of the used terms and the corresponding unit.

Term	Description	Unit
R	Gas constant	$\left[\frac{kg m^2}{s^2 mol K} \right]$
$\Delta\pi_i$	Osmotic pressure difference produced by the i-th solute	$[Pa]$

According to Starling's Law, the effective filtration pressure depends on the hydrostatic and osmotic pressure differences between inside and outside the peritoneal cavity. In PD all these effects need to be combined with each other and the lymph absorption also needs to be considered (Equation 2-8) [7, 24].

$$J_V = \frac{dV}{dt} = -L_p S \left(\Delta P_H - \sum_{i=1}^N \sigma_i \Delta\pi_i \right) - L$$

Equation 2-8

Table 2.2-VII: Description of the used terms and the corresponding unit.

Term	Description	Unit
σ_i	Reflection coefficient of the i-th solute	$[-]$
ΔP_H	Hydrostatic pressure difference between blood and cavity	$[Pa]$
$\Delta\pi_i$	Osmotic pressure difference between blood and cavity for the i-th solute	$[Pa]$

The ultrafiltration rate or volume flow J_V is thus dependent on the osmotic pressure difference $\Delta\pi$, the hydrostatic pressure difference ΔP , the effective surface area S of the peritoneum and the hydraulic conductivity L_p of the peritoneal membrane and the reflection coefficient σ . The ultrafiltration performance depends not only on the osmotic concentration gradient, but also on the diffusion of the osmotically active substance through the peritoneal membrane into the blood plasma. Convective mass transport refers to the transport of dissolved substances with the ultrafiltered liquid through the membrane. The convection depends on the volume flow, the concentration of the dissolved substance as well as the reflection coefficient (σ) and the concentration of the substance. The reflection coefficient is a measure of the ability of the substance to pass through the membrane and can be described mathematically as the quotient of the concentration of a substance in the ultrafiltrate to the concentration in the plasma

and can therefore assume values between 0 and 1. A value of 0 would mean that the substance passes unhindered through the membrane. Fluid resorption of dialysis solutions has two different causes. The first is due to the diffusion of glucose from the dialysis fluid into the blood, where it is metabolized and thus leads to a reversal of the pressure gradient, since the osmotic pressure of the blood proteins is greater than that produced by the dialysis solution. Additionally, resorption via lymph vessels at the peritoneum takes place. These equations are very similar to the model by Pyle and Popovich [24, 40, 44, 45, 46].

TPM concepts

The TPM [according to Bengt Rippe] describes the fluid and mass transport at the peritoneum and is today the state of the art and was modified and optimized further [by Carl Öberg]. The membrane is not considered as a homoporous membrane, but the pores of the blood vessels are divided into three different types of pores, as mentioned in Section 0. In the classical three-pore model, the blood vessel is regarded as the only barrier separating the two compartments blood and dialysate. According to this model, the blood vessels contain 1.5 % aquaporins, approx. 5 % large pores and 93.5 % small pores. The three different types of pores run parallel and are considered having a cylindrical shape. The fluid transport depends on the hydraulic conductivity of the membrane, the osmotic pressure difference, the hydrostatic pressure difference, and the reflection coefficients. The difference between the Pyle-Popovich model and the TPM is that the reflection coefficients for the three types of pores are specifically included in the model and weighted according to the percentage of pores [7, 10-11, 40, 44-46].

Table 2.2-VIII: Parameters, respectively the values used for simulation with the TPM.

Parameter	Term	Value
Small pore radius	r_S	47 Å
Large pore radius	r_L	250 Å
Fractional small pore UF-coefficient	α_S	0.935
Fractional transcellular pore UF-coefficient	α_C	0.015
Fractional large pore UF-coefficient	α_L	0.05
Mol radius of sodium (and chloride)	r_{NaCl}	2.3 Å
Mol radius of urea	r_U	2.6 Å
Mol radius of glucose	r_G	3.7 Å
Mol radius of albumin	r_{Prot}	35.5 Å
UF – coefficient	$L_p S$	$0.082 \frac{mL}{min \text{ mmHg}}$
Osmotic conductance to glucose	$L_p S \sigma_G$	$3.5 \frac{\mu L}{min \text{ mmHg}}$
Unrestricted pore area over unit diffusion distance	$\frac{A_0}{\Delta x}$	27.000 cm
PS (MTAC) for glucose	PS_G	$15.5 \frac{mL}{min}$
Peritoneal lymph flow	L	$0.3 \frac{mL}{min}$
Trans-peritoneal hydrostatic pressure gradient	ΔP	9 mmHg
Trans-peritoneal oncotic pressure gradient	$\Delta \pi_{Prot}$	22 mmHg

Parameter	Term	Value
Dialysis fluid instilled	V_0	2.050 mL
Peritoneal residual volume	V_R	300 mL
Serum urea concentration	$C_{P,Urea}$	$20 \frac{mmol}{L}$
Serum sodium (and corresponding anion) conc.	$C_{P,NaCl}$	$140 \frac{mmol}{L}$
Dialysis fluid sodium conc.	$C_{D,NaCl}$	$132 \frac{mmol}{L}$
Serum glucose conc.	$C_{P,G}$	$6.5 \frac{mmol}{L}$

Table 2.2-IX: Parameters, respectively the values for PS_i and σ_i used for simulation with the TPM.

	$PS_i \left[\frac{mL}{min} \right]$	$\sigma_i [-]$
Sodium chloride	18.8	0.0262
Urea	16.2	0.0293
Creatinine	13.5	0.0338
Glucose	10.2	0.043
Albumin	0.086	0.895

The main model equations are shown here:

$$V(t + \Delta t) = V(t) + L_p S \Delta t [\Delta P(V) - \sigma_{Prot} \Delta \pi_{Prot} - \sigma_G \Delta \pi_G(t) - \sigma_U \Delta \pi_U(t) - 2 \sigma_{NaCl} \Delta \pi_{NaCl}(t)] - L \Delta t$$

Equation 2-9

$$\Delta P(V) = \Delta P(V_0) - \frac{V_t - V_0}{490}$$

Equation 2-10

$$\Delta \pi_i = R T (C_{P,i} - C_{C,i}(t))$$

Equation 2-11

$$C_{C,i}(0) = \frac{V_0 C_{D,i} + V_R C_{P,i}}{V_0 + V_R}$$

Equation 2-12

Table 2.2-X: Description of the used terms and the corresponding unit.

Term	Description	Unit
$C_{C,i}$	Concentration of the i-th solute in the peritoneal cavity	$\left[\frac{mmol}{L} \right]$
$C_{P,i}$	Concentration of the i-th solute in the blood plasma	$\left[\frac{mmol}{L} \right]$
$C_{D,i}$	Concentration of the i-th solute in the fresh dialysate	$\left[\frac{mmol}{L} \right]$
$\sigma_{S,i}$	Reflection coefficient for the i-th solute and small pores	$[-]$
$\sigma_{L,i}$	Reflection coefficient for the i-th solute and large pores	$[-]$

According to the three-pore model, the transport of dissolved molecules only takes place via small and large pores of the blood vessels. The small pores transport a substance both diffusively due to the concentration difference between blood and dialysate and by convective mass transport. In contrast, macromolecules are mainly transported by convection through the large pores. Under the assumption that the blood concentration remains constant over time and that no absorption of substance takes place by the lymph vessels, the flow can be described using the following equations.

$$V(t + \Delta t) C_{C,i}(t + \Delta t) = C_{C,i}(t) V(t) + Cl_i (C_P - C_D(t)) \Delta t$$

Equation 2-13

The clearance of solute could be calculated in the TPM with the following equations:

$$Cl_i = \frac{J_{V_s} (1 - \sigma_{S,i})}{1 - e^{-Pe_i}}$$

Equation 2-14

$$Pe_i = \frac{J_{V_s} (1 - \sigma_{S,i})}{PS_i}$$

Equation 2-15

The volume flow through the small pores J_{V_s} depends on the percentage share α_s , the hydraulic conductivity and area as well as on the hydrostatic and osmotic pressure difference and the specific reflection coefficients $\sigma_{i,s}$.

$$J_{V_s} = \alpha_s L_p S \left(\Delta P(V) - \sigma_{Prot,S} \Delta \pi_{Prot} - \sigma_{G,S} \Delta \pi_G(t) - \sigma_{U,S} \Delta \pi_U(t) - 2 \sigma_{NaCl,S} \Delta \pi_{NaCl}(t) \right)$$

Equation 2-16

The volume flow across the large pores J_{V_L} depends on the percentage α_L , the hydraulic conductivity and area as well as on the hydrostatic and osmotic pressure difference and the specific reflection coefficients $\sigma_{i,L}$, whereby for low-molecular substances this is close to 0. Since the hydrostatic pressure difference and colloid osmotic pressure difference have a major influence on the flow through the large pores.

$$J_{V_L} = \alpha_L L_p S \left(\Delta P(V) - \sigma_{Prot,L} \Delta \pi_{Prot} - \sigma_{G,L} \Delta \pi_G(t) - \sigma_{U,L} \Delta \pi_U(t) - 2 \sigma_{NaCl,L} \Delta \pi_{NaCl}(t) \right)$$

Equation 2-17

The volume flow through the ultra-small pores J_{V_c} depends on the percentage α_c , the hydraulic conductivity and area as well as on the hydrostatic and osmotic pressure difference. The reflection coefficient at the ultra-small pores is one for all substances, since only water can diffuse through the pores.

$$J_{V_c} = \alpha_c L_p S \left(\Delta P(V) - \Delta \pi_{Prot} - \Delta \pi_G(t) - \Delta \pi_U(t) - 2 \Delta \pi_{NaCl}(t) \right)$$

Equation 2-18

$$\gamma = \frac{r_{Solute}}{r_{Pore}}$$

Equation 2-19

In general, the reflection coefficient σ depends on the pore size and the molecule size and is calculated within the three-pore model according to Equation 2-20.

$$\sigma_{i,L} = \frac{16}{3} \gamma^2 - \frac{20}{3} \gamma^3 + \frac{7}{3} \gamma^4$$

Equation 2-20

$$\sigma_i = \alpha_c + \alpha_s \sigma_{i,S} + \alpha_L \sigma_{i,L}$$

Equation 2-21

$$J_V = J_{V_s} + J_{V_L} + J_{V_c} - L$$

Equation 2-22

For the volume flow between dialysate and blood vessels, the following equations can thus be defined (Equation 2-16 to Equation 2-18), whereby these always result in one flow equation (Equation 2-22) [7].

$$\alpha_c + \alpha_s + \alpha_L = 1$$

Equation 2-23

Further, as described by Öberg et al., the volume and mass changes during fill and drain procedure could be also considered for theoretical purposes as [11]:

$$\frac{dV}{dt} = J_V = J_{V_s} + J_{V_L} + J_{V_c} - L + J_{Fill} - J_{Drain}$$

Equation 2-24

Table 2.2-XI: Description of the used terms and the corresponding unit.

Term	Description	Unit
J_{Fill}	Fresh dialysate inflow rate during the fill phase	[L/min]
J_{Drain}	Cavity volume outflow rate during the drain phase	[L/min]
$\frac{dV}{dt}$	Rate of change in cavity volume with time during the cycle	[L/min]

2.3 Quality assurance tests

Quality assurance tests should be performed regularly during the course of treatment to make sure that the removal of uremia toxins, excess body water and salt is sufficient [51-52].

Peritoneal membrane tests

In practice, various membrane test methods have been invented to make a direct statement about the transporter category of the patient or to calculate membrane parameters in combination with medical software applications (MSA). The Peritoneal Equilibration Test (PET) is the preferred test method to evaluate the ultrafiltration performance and peritoneal transport characteristics of a patient's low molecular weight substances (glucose, uremia toxins). The PET is currently still the most frequently used method today, as only simple calculations are necessary to interpret the results. Nevertheless, sometimes during the whole treatment this test is performed

only once or none. The Figure 2-4 schematically shows the procedure of the "standard PET" with a 2.3% glucose solution. A volume of 2 liters is transferred to the patient, dialysate samples are taken at times 0, 2 and 4 hours and a blood sample is taken after 2 hours. In addition, the weight of the dialysate drained is determined after 4 hours to draw conclusions about the ultrafiltration performance [13, 48-49].

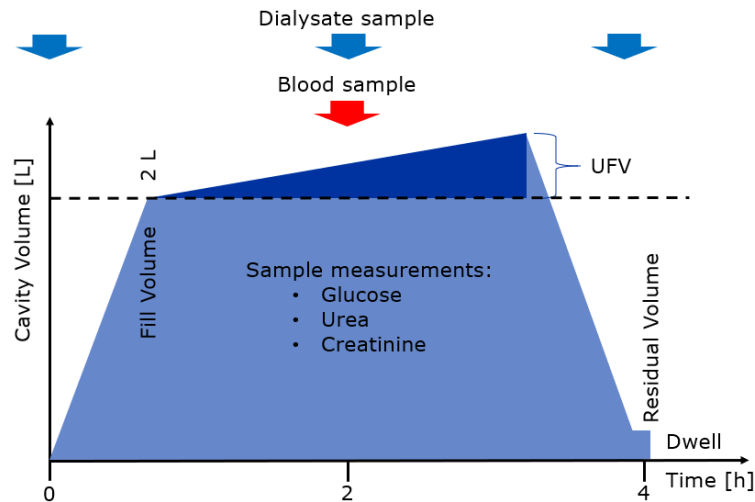


Figure 2-4: Schematically representation of the PET procedure. A volume of 2 liters is transferred to the patient, dialysate samples are taken at times 0, 2 and 4 hours and a blood sample is taken after 2 hours. In addition, the weight of the dialysate drained is determined after 4 hours to draw conclusions about the ultrafiltration performance (created by information from [3, 12-13, 47-49]).

In the evaluation of the data, the ratio of the concentration between dialysate and plasma (D/P) of the two indicator substances urea and creatinine is determined to be able to make a statement regarding clearance of toxins. The literature also describes that the ratio D/P of sodium in PET is determined. Further the ratio between dialysate and dialysate initial concentration is determined from glucose (D/D₀) to draw conclusions about the glucose absorption (Figure 2-5) [3, 12-13, 47-52].

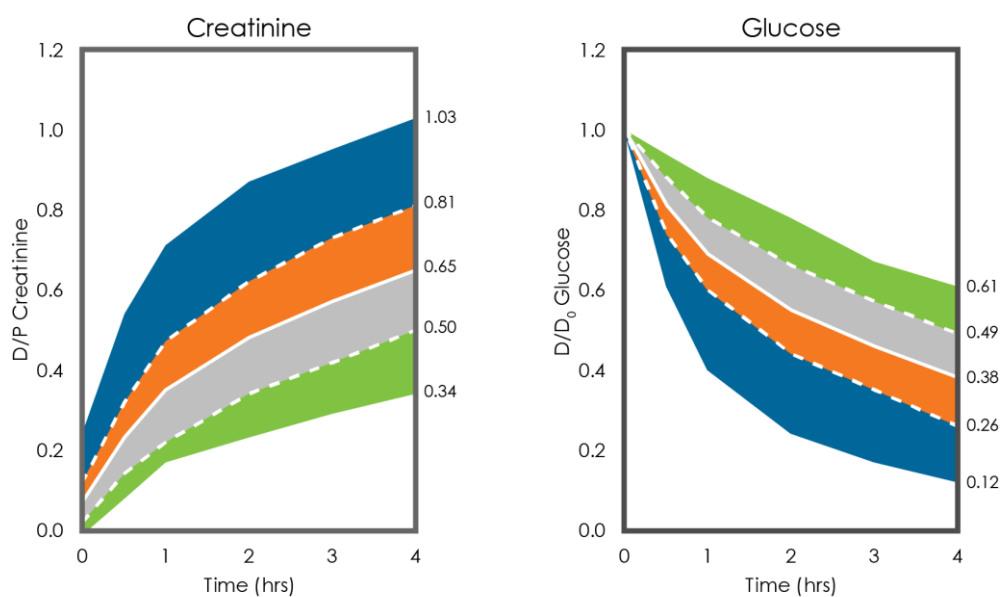


Figure 2-5: Exemplary evaluation of the PET, here green for low, grey for low average, orange for high average and blue for high transporter type of the patient [3, 12-13, 47-52].

The results are then evaluated according to Twardowski's classification that a statement can be made about the transport behavior of the patient's peritoneal membrane. Figure 2-5 shows that in a fast transporter type the ratio D/P of creatinine increases faster and glucose is absorbed faster. The rapid absorption of glucose in fast transporters usually results in moderate to poor ultrafiltration. It also schematically shows the categorization of creatinine and glucose, distinguishing between slow (green), moderately slow (grey), moderately fast (orange) and fast (blue) transporter types. The reasons for a fast transporter type may have anatomical causes, such as an increased effective peritoneal exchange area, inflammation of the peritoneum (Peritonitis) or neovascularization. The cause of fibrosis would work the other way around [48-52].

Dialysis dose

Peritoneal and renal clearance are added to the pool of collected information to find the suitable dialysis dose for the patient by the nephrologist. Options to influence the dialysis dose are changing dwell time, fill volumes and/or dialysate OA concentration (OA) or the OA itself. The target parameter for urea clearance is a weekly Kt/V of more than 1.7. The European Best Practice Guidelines additionally require a creatinine clearance of more than 45 L/week/1.73 m² for APD. While there is no upper limit for urea clearance in HD, it was shown in PD that a peritoneal Kt/V of more than 2.1 compared to a peritoneal Kt/V of 1.7 to 2.0 was rather associated with worse outcome. Reasons for this effect could be that a high peritoneal Kt/V is purchased with a high dialysate turnover and then the disadvantages of dialysate exposure outweigh the advantages of higher dialysis clearance. If the creatinine excretion in urine and dialysate (urine creatinine × urine quantity + dialysate creatinine × dialysate outlet) is determined at the same time, the collection accuracy and compliance of the patient can be monitored. Total creatinine excretion in steady state is independent of kidney function and dialysis dose. Creatinine excretion is determined by muscle mass. If suddenly significantly higher creatinine excretion values are found, this is an indication that the patient has performed fewer than the ordered bag changes [31, 50-55].

Volume control

UFV for a patient on PD is calculated from the difference between dialysate fill and drain volume. However, this seemingly simple balance sheet calculation contains several sources of error. The most common error is that it is assumed that a 2 L bag contains exactly 2 L of PD solution. The fact is that the bags contain a larger amount of dialysate 2100-2200 mL per 2 L bag. If this overfill is not considered, the daily ultrafiltration is overestimated. Other sources of error are weighing before or after the flush and varying residual volumes. The aim should be to withdraw at least 1 L of fluid per day (peritoneal ultrafiltration plus renal excretion), as this is associated with better survival. But this is rarely useful if no individual target for the UFV dependent on the individual patients needs could be set and rearranged from day to day treatment because the hydration of the patient is underlying somehow pronounced fluctuations [53-57, 59-61].

2.4 State of the art in medical software applications

Currently, different MSA's with various membrane transport model approaches are used in practice, variants, or combinations of the Pyle-Popovich model, Kedem-Katchalsky or Tree-Pore-Model. Each of these software modules, as PD Adequest® (Baxter), PatientOnLine (Fresenius Medical Care), PACK PD (Fresenius Medical Care) or Synergy (former Gambro, now Fresenius Medical Care) requires results from practical membrane assays to integrate the specific membrane parameters into the models. The first variants of PD Adequest were based on the Pyle-Popovich model, whereby the TPM was included in the meantime. Thus, parameters such as MTAC, which depends on the filling volume and treatment time, the substance-specific reflection coefficient, and the lymphatic absorption, are integrated in the software. PD Adequest 2.0 calculates specific MTAC's and other patient-specific parameters from the results of the PET test, which are then incorporated into the software. These include the effective peritoneal surface area, the volume flow and the ultrafiltration. As input parameters for the software PACK PD as well as for software called PatientOnLine (POL) it is necessary to perform the peritoneal function test (PFT). PACK PD is based on a simplified model variant of the Pyle-Popovich model and POL on an extended variant. The net ultrafiltration volume can be determined by using the cycler or simple weighing after each treatment. However, to determine the clearance of uremia toxins, it is necessary to determine concentrations in blood plasma and dialysate. Since realization in routine applications is difficult, it is necessary to realize an adapted treatment using membrane models and software, which are working well regarding clearance, but less accurate for ultrafiltration [8, 27, 77].

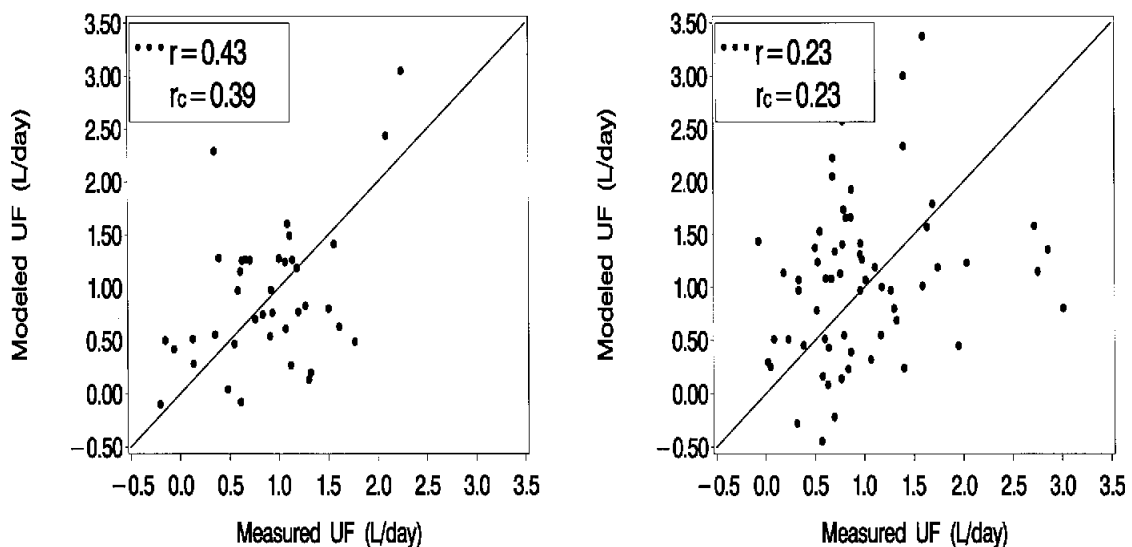


Figure 2-6: A multinational clinical validation study of PD Adequest 2.0 Representation of predicted/modeled UF in L/day vs. measured UF in L/day (CAPD, left; APD, right) [8].

These MSA-based on models do not deliver sufficient prediction capability regarding UFV. Figure 2-6 shows results of a validation study regarding PD Adequest 2.0. The measured UF per day is plotted against the modeled UF per day. Reaching that all points are on the straight line should be the target for the models, but also the newest MSA on the marked is far away from precision in UF prediction [8].

2.5 Targets and main problems for patients on PD

In PD treatment today, the removal of waste products from the body could be handled well with the used membrane test methods and quality assurance concepts. The goal of the removal of uremia toxins is simply minimizing the concentration in the blood to the lowest value possible. To keep the sodium concentration on a steady state around 140 mmol/L, the patient must pay attention to his salt intake and if needed stick to diet. Another possibility is using LoNatra PD solutions with lower sodium concentrations instead of standard PD solutions to remove more sodium per cycle. The missing point is the optimization of the treatment regarding UFV to keep the patient on target steady state hydration status (Figure 2-7).

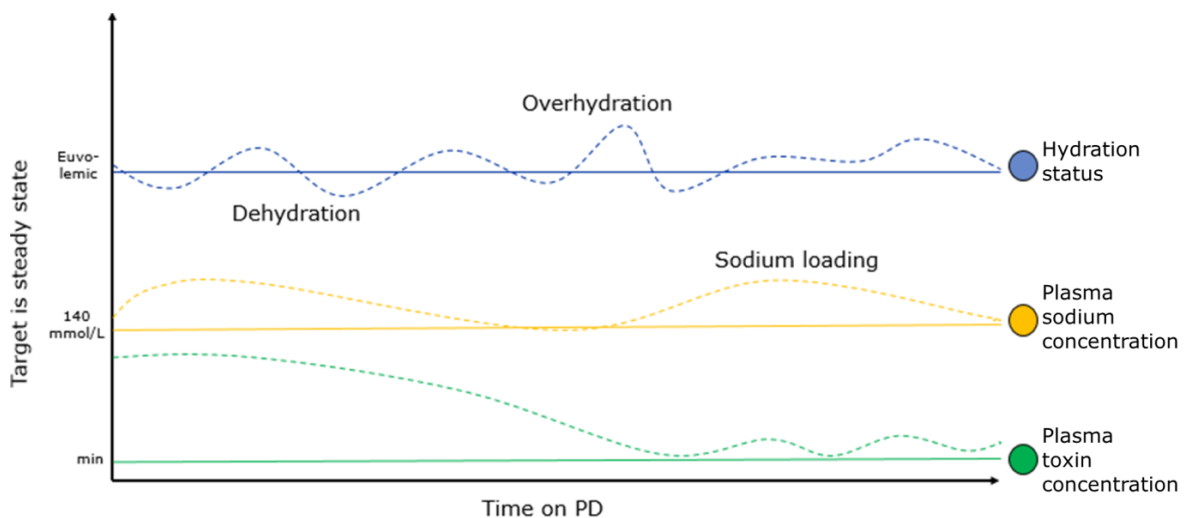


Figure 2-7: Treatment target in PD regarding hydration, sodium loading and uremia toxin removal (created by information from [46, 50, 58-61]).

The software applications available on the market could not provide sufficient prediction capability to keep the patient on target steady state hydration status. Most of the patients are overhydrated because of the reduced kidney function. The treatment is, however, regarding UFV to get the target hydration status, trial and error based. These treatment schedules, which need to be rescheduled various often, are running the patient from overhydration to dehydration and after modifications of the treatment schedule vice versa, till some steady state around the optimum is achieved for a period of time and the procedure starts again due to alterations of the peritoneal membrane. With this treatment procedure, the patient's hydration status is shifting from one extreme to another till it's causing problems to the welfare with following investigation in the clinic. The target optimum hydration status is in a small range and if the patient is long term on unhealthy hydration levels the risk of mortality increases. To investigate how to set up the treatment for an individual patient is difficult because there is a whole bunch of influencing factors, which are interacting with each other (Figure 2-7).

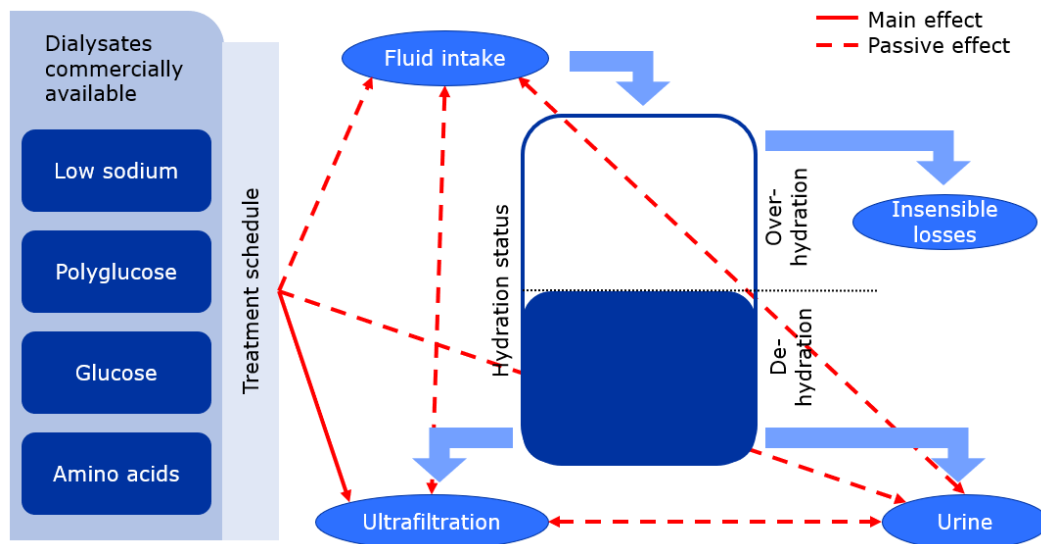


Figure 2-8: Interactions of the main factors influencing the hydration status (created by information from [46, 50, 58-61]).

On the one hand there are the treatment-related factors prescribed by the nephrologist like treatment schedule, the dose of the dialysate and its ingredients, which have a direct effect on the UF-volume. Low sodium (LoNatra) solutions additionally may reduce the thirst, resulting in a reduced fluid intake. On the other hand, are the patient-related influencing factors, which are dependent on the residual kidney function, resulting in the urine output and the characteristics of the peritoneal membrane, which influences the UF volume. Additionally, the fluid intake and the insensible losses can have a main effect on the hydration status. The treatment, which directly influences the hydration status per UF, can deal some side effects passively to the urinary output. To deal with these problems and treat the patient in the right way, new concepts are needed:

- Fast and long-lasting ultrafiltration performance and prediction capabilities
- Low absorption of the OA by blood and lymph vessels, especially for glucose
- No or minimal toxic, allergic, metabolic effects with optimized clearance
- Ideally complete metabolism of the absorbed OA

In order to evaluate such concepts with regard to their ultrafiltration and clearance performance, animal experiments, *in vitro* experiments or computer simulations are used in practice. To get investigable information of the patient hydration a Body Composition Monitor (BCM) can be used [54, 58, 61-65].

Chapter 3: Mathematical model approaches and preparatory *in vitro* experiments

The goal of the research and development process during this project and the study conducted are explained in more detail in this section. The main simplifications of the biophysical model approach, the empirical model approach and the concept of the pressure/volume-characteristics (P/V-characteristics) are introduced. Further, these are shown as an introduction applied on the *in vitro* test system called *Bvatar*.

3.1 Empirical model approach

The ‘dose’ within a PD prescription may be described in terms of 3 variables, namely the fill volume, the composition of the instilled dialysate, especially the mass of the OA (e.g., Glucose, Polyglucose, amino acids), and the duration of the dwell period. Given values of each of these variables lead to specific UFV trajectory. The following part considers empirical model approaches for predicting the intraperitoneal volume in an individual patient and hence the ultrafiltration volume yielded at the time of the drain. In the interests of clarity regarding the terminology, the general scheme shown in Figure 3-1 applies.

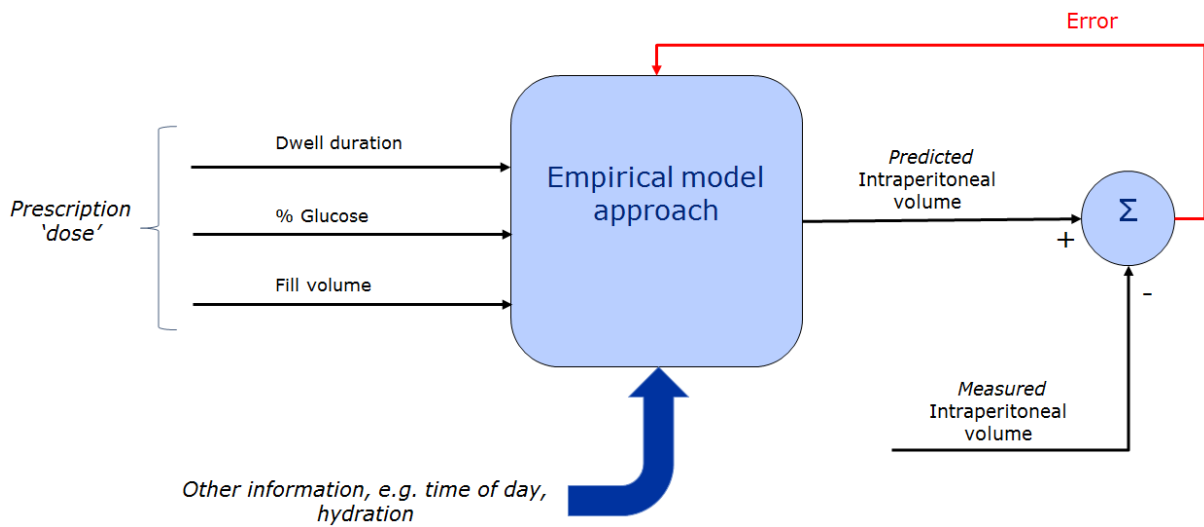


Figure 3-1: General empirical model approach for prediction of UFV.

Table 3.1-I: Description of the used terms and the corresponding unit.

Variable	Description	Unit
t_{dwell}	Dwell time of the dialysate inside the PC	[min]
$C_{Osm}^{PDF}, C_{Osm}^{dialysate}$	Osmolarity of the dialysate used	[mOsm/L]
V_{fill}	Fill volume of the dialysate initial to the dwell	[L]
V_{drain}	Drain volume of the dialysate after the dwell	[L]
$V_{UFmeasured}$	Measured UFV at the end of the cycle, net amount of fluid removed	[L]

Variable	Description	Unit
$V_{UF_{predicted}}$	Predicted UFV at the end of the cycle, net amount of fluid removed	[L]

While the dose is considered one of the main predictors, other information may be introduced to further improve accuracy, such as the time of day or the hydration status considering dry weight concepts or BCM measurements. The ‘Error’ accounts for unknown or unpredictable effects leading to a difference between the measured and predicted UFV. It is the minimization of the error, which is the basis for establishing the parameters of the empirical model approaches. This implies that measurements of UFV are generally needed to improve the prediction accuracy of the empirical model, but this can be realized easily after every treatment cycle.

Linear regression model

A monotonic linear regression model predicts the UFV from input variables considered to be independent. The variables dialysate osmolarity (C_{Osm}^{PDF}), dwell duration (t_{dwell}), and the fill volume (V_{fill}) for example. The measured UFV, which is calculated by subtraction of the fill volume from the drained volume, may be determined by the relationship of the following form:

$$V_{UF_{measured}} = a + b t_{dwell} + c C_{Osm}^{dialysate} + d V_{fill}$$

Equation 3-1

Besides the dose variables and their coefficients b , c , d , an offset term a is introduced. In the context of experimental design, we have three factors (ascribing to main effects) and one response, representing a simple method to predict UFV. The parameters a , b , c and d are unique to the specific patient. Multiple prescriptions lead to a matrix of doses variables and may be represented as:

$$\begin{bmatrix} V_{UF_{measured}}(1) \\ V_{UF_{measured}}(2) \\ V_{UF_{measured}}(3) \\ \dots \\ V_{UF_{measured}}(n) \end{bmatrix} = \begin{bmatrix} 1 & t_{dwell}(1) & C_{Osm}^{dialysate}(1) & V_{fill}(1) \\ 1 & t_{dwell}(2) & C_{Osm}^{dialysate}(2) & V_{fill}(2) \\ 1 & t_{dwell}(3) & C_{Osm}^{dialysate}(3) & V_{fill}(3) \\ \dots & \dots & \dots & \dots \\ 1 & t_{dwell}(n) & C_{Osm}^{dialysate}(n) & V_{fill}(n) \end{bmatrix} \cdot \begin{bmatrix} a \\ b \\ c \\ d \end{bmatrix}$$

Equation 3-2

After four (the number of parameters in this regression model) PD cycles in this case, the system of equations becomes over determined and the parameters a , b , c and d may be obtained by standard regression methods as least squares for example. The monotonic model does not capture the inherent non-linearity of the UFV response. Typically, the UFV undergoes a rise after PD fluid instillation, reaching a peak in the first few hours of the dwell before fluid absorption causes UFV to decrease again [18-20].

Linear and non-linear regression model with interactions

The linear model can capture only the first monotonic increase part. A modified model structure is:

$$V_{UF_{measured}} = a + b t_{dwell} + c C_{Osm}^{dialysate} + d V_{fill} + e t_{dwell} C_{Osm}^{dialysate} + f C_{Osm}^{dialysate} V_{fill} + g V_{fill} t_{dwell} + h V_{fill} t_{dwell} C_{Osm}^{dialysate}$$

Equation 3-3

In the updated model, 8 parameters [a - h] are introduced with more degrees of freedom to capture also the nonlinearities of the interactions between the input variables and the intraperitoneal volume response. The error term *a* in the model accounts for disturbance effects from unknown factors. Examples of unknown factors may be the time of the day or the patient's activity during the dwell. Other disturbances can be patient hydration status, food intake, time elapsed into the dwell e.g., which may be explicitly included into the model structure or lumped into the error term *a*, if no information is available [18-20].

Design of experiments (DoE)

Let's assume that only three factors (control variables) need to be considered: (1) Dwell time, (2) Osmolarity, (3) Fill volume, and the rest will be captured in the error term *a*. If the patient treatment is perturbed with multiple combinations of dwell time, osmolarity and fill volume, multiple values for the UFV can be obtained, which can provide an estimate of the patient-specific parameter vector (for the chosen model structure). For example, data of discreet glucose concentrations (directly linked to the osmolarity), time and fill volumes could be collected.

Table 3.1-II: Example of variation possibilities for the perturbation approach.

Dwell time [min]	120	180	240
Dialysate OA concentration [%]	1.5	2.3	4.25
Fill volume [L]	1.5	2	2.5

In the above example, 3 factors and 3 different levels for each factor, result in total experiments $3 \times 3 \times 3 = 27$ experiments based on full factorial design paradigm. The number of experiments can possibly be reduced using fractional factorial experimental design by conducting only orthogonal experiments [18-20].

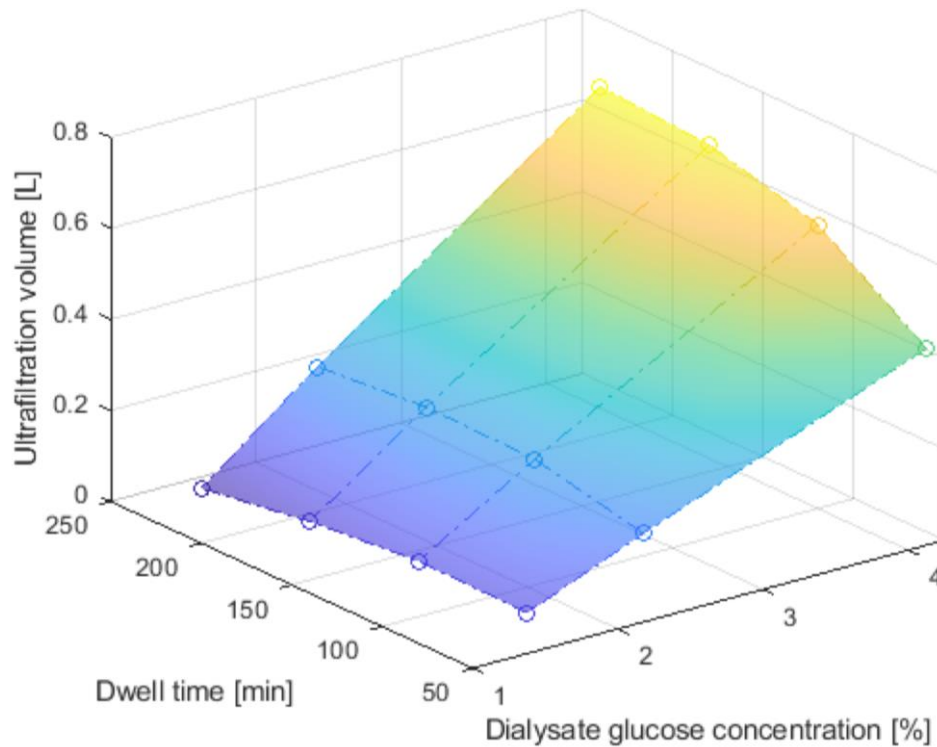


Figure 3-2: An example of designed experiments with only varying the glucose in the dialysate (1.5 %, 2.3 %, 4.25 %) and the Dwell time (60 min, 120 min, 180 min, 240 min) results in a mapping of these variables against the UFV and represents the influences and interactions. For this mapping, the Rippe TPM was used to simulate UFV dependent on dialysate % and dwell time as introduced in section 0 (created by data produced with the TPM) [7].

For generation of the input data for the empirical model approach a modified TPM simulation was used. The model fitted to these data could be used to afterwards predict treatment cycles for various dose variables. The accuracy could be improved, if more influencing factors are fed to the model (hydration, daytime e.g.), if these have a significant influence on the UFV. Once the model for an individual patient is set, the optimal dwell time for a given glucose concentration and fill volume to achieve the desired UFV can be identified. One assumption here is that a patient peritoneal membrane's characteristic stays constant over a period of time (weeks or months). If the membrane characteristics change, the model predictions will differ from the measured values of the UFV. Thus, it can also be used as an early detection tool to indicate some physiological changes, such as peritonitis. Therefore, the model should be continuously updated by the collected data from routine treatment. This will provide robust predictive capability of the model and takes the steady state concepts of regression learner as machine learning tools into account [17-20].

3.2 Abstraction of the biophysical model approaches

In a first consideration a 2nd and 3rd pool was added to the TPM, especially for blood reservoir and interstitium. Based on evaluations regarding the applicability of this consideration in practice, the decision was made, to use a reduced biophysical model with at least the processes mentioned in Figure 3-3.

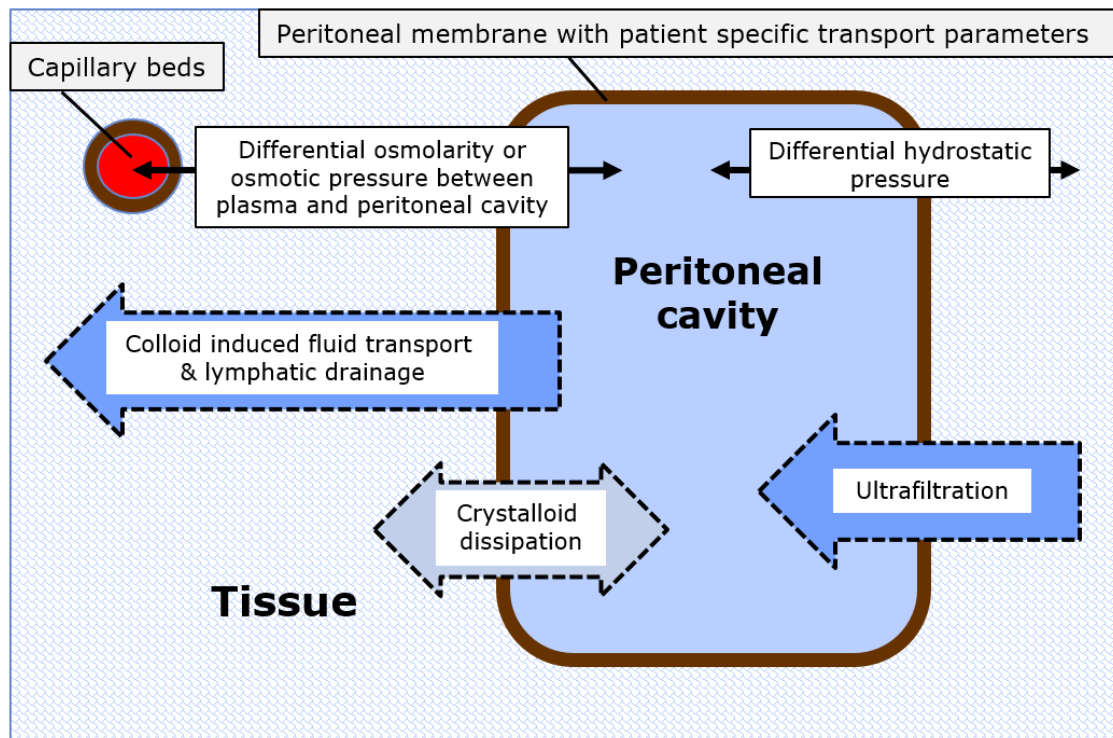


Figure 3-3: Schematic representation of the main transport processes during PD.

The system of ordinary differential equations (ODE's) with the minimum number of parameters consists of 2 ODE's and 4 parameters. Main transport phenomena considered are dissipation of crystalloids by diffusion and convection and the change in intraperitoneal volume (IPV) due to ultrafiltration and absorption. IPV could be reabsorbed by lymph and colloid induced osmotic pressure (by blood proteins). Additionally, the hydrostatic pressure gradient through the peritoneal membrane drives fluid transport. The biophysical model approaches could be modified for various scenarios and OAs (OA). Regarding the study conducted only the biophysical models dealing with glucose as crystalloid OA are introduced [7, 45, 54, 67].

Osmolarity and crystalloid osmotic pressure

The TPM consists (chapter 2.4) of one ODE for every solute, which is considered to influence the transport kinetics during PD. However, with the assumptions made for the model parameters, the patient-specific membrane characteristic is not considered, and suitable parameter identification seems impossible. To simplify the model, the sum of all crystalloid osmotically active molecules, also known as osmols are used as an agglomerated patient-specific parameter. An aggregated reflection coefficient $\tilde{\sigma}$, representing the overall average effect of different types and relative densities of pores present in the peritoneal cavity is introduced. The aggregated reflection coefficient is specific to an individual patient and is assumed to be constant on short term. The approximation yields a simplified expression for the effective differential crystalloid osmotic pressure,

$$\Delta\pi_{Osm}^{Eff} = \sum_m \sum_i \sigma_{i,m} \cdot RT (C_i^{PC} - C_i^{Pls}) \approx RT \tilde{\sigma} \sum_i (C_i^{PC} - C_i^{Pls}) = \tilde{\sigma} RT (C_{Osm}^{PC} - C_{Osm}^{Pls})$$

Equation 3-4

where

$$C_{Osm}^{PC} = \frac{N_{Osm}^{PC}}{V^{PC}} = \sum_i C_i^{PC}$$

Equation 3-5

and

$$C_{Osm}^{Pls} = \sum_i C_i^{Pls}$$

Equation 3-6

A further main simplification is merging of the concentration of the solutes in the peritoneal cavity and blood plasma to the osmolarity C_{Osm}^{PC} and C_{Osm}^{Pls} .

Table 3.2-1: Description of the used terms and the corresponding unit.

Term	Description	Unit
$\tilde{\sigma}$	Aggregated reflection coefficient (all solutes considered) dependent on the active pores in the individual patient	[-]
RT	Product of universal gas constant and temperature	[kg·m ² ·S ⁻² ·mol ⁻¹]
C_{Osm}^{Pls}	Osmolarity of the blood plasma	[mOsmol/L]
C_{Osm}^{PC}	Osmolarity of the peritoneal cavity volume	[mOsmol/L]
$\Delta\pi_{Osm}^{Eff}$	Effective crystalloid osmotic pressure gradient only considering osmols	[mmHg]
C_i^{Pls}	Concentration of the i-th solute in the blood plasma	[mOsmol/L]
C_i^{PC}	Concentration of the i-th solute in the peritoneal cavity fluid	[mOsmol/L]
$\sigma_{i,m}$	Reflection coefficient for the i-th solute and the m-th pore size	[-]
N_{Osm}^{PC}	Amount of osmotically active molecules in the peritoneal cavity	mOsmol
V^{PC}	Volume inside the peritoneal cavity	L

The number of osmols is dominated by crystalloids especially for glucose-based PD solutions with smaller contributions from urea, creatinine, and physiological electrolytes. Any colloids present have negligible contribution to the number of osmols. The biophysical model approach by contrast is not based on assumptions regarding reflection coefficients of individual crystalloid pore size pairs or the relative proportions of different pores in the peritoneal membrane. Instead, the net contribution of all crystalloids expressed as number of osmols rather than individual crystalloids with the major effect caused by the OA (glucose) is considered.

In a membrane system permeable only to water (for example aquaporins), the reflection coefficient is unity:

$$\Delta\pi_{Osm} = RT (C_{Osm}^{PC} - C_{Osm}^{Pls})$$

Equation 3-7

Table 3.2-II: Description of the used terms and the corresponding unit.

Term	Description	Unit
$\Delta\pi_{Osm}$	Unscaled crystalloid osmotic pressure gradient	mmHg

But for the mixture of various pores present, the osmotic pressure needs to be scaled by the reflection coefficient to the effective osmotic pressure potent through the membrane which is driving the volume flow by:

$$\Delta\pi_{Osm}^{Eff} = \tilde{\sigma} \Delta\pi_{Osm}$$

Equation 3-8

$\Delta\pi_{Osm}$ is the unscaled differential osmotic pressure across the peritoneal membrane caused by the gradient of osmolarity between blood plasma and dialysate, which could be scaled by the aggregated reflection coefficient $\tilde{\sigma}$ to the effective crystalloid osmotic pressure through the peritoneal membrane [7, 24, 67-68].

Pressure / Volume – characteristics

Dialysate introduced into or drained from the peritoneal cavity causes the intraperitoneal pressure (IPP) to change accordingly – the so-called ‘pressure-/volume (P/V) -characteristics’ of the peritoneal cavity could be extracted from these data. This characteristic is shown schematically in Figure 3-4 [14, 30, 69-73].

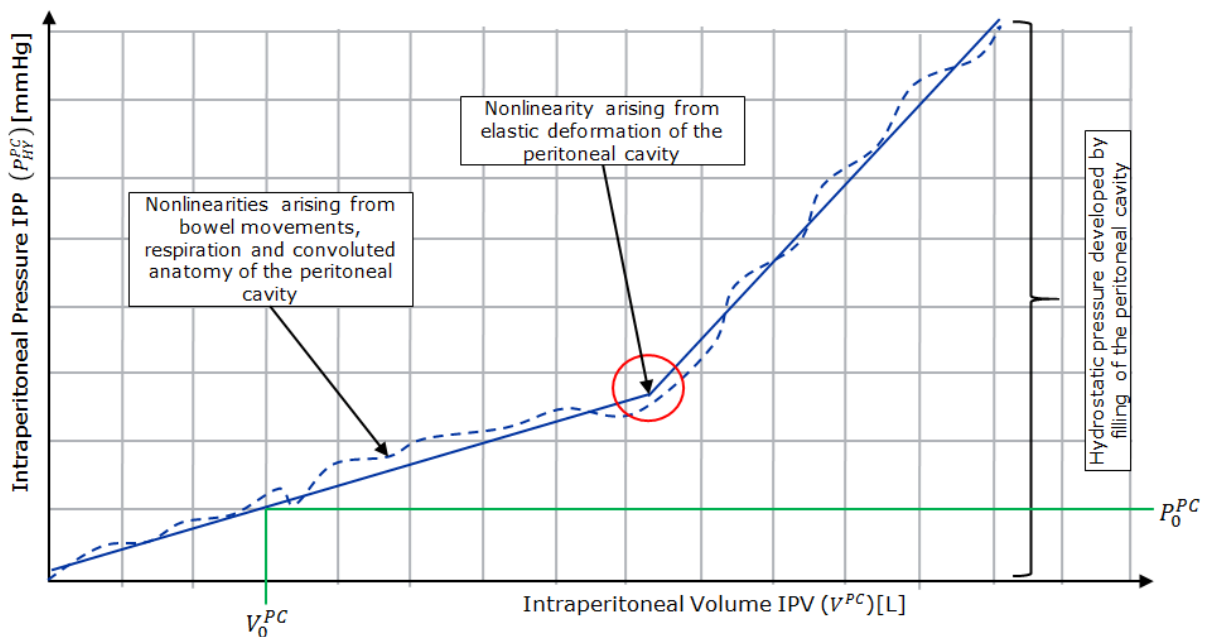


Figure 3-4: Schematic representation of the P/V-characteristics. The intraperitoneal pressure at the peritoneal cavity varies in accordance to the change of intraperitoneal volume during fill, dwell or drain.

The drawback of the P/V-characteristics is that the relationship applies to a patient population rather than the individual patient in previous model approaches. Differences in hydrostatic offsets and the compliance of the peritoneal cavity is likely to vary between patients, especially with different age and body weight (parameters P_0^{PC} and γ , respectively Equation 3-9, differ between subjects) [14, 30, 69-73].

$$\widetilde{P}_{Hy}^{PC}(V_{PC}) = P_0^{PC} + \gamma (V^{PC}(t) - V_0^{PC})$$

Equation 3-9

Table 3.2-III: Description of the used terms and the corresponding unit.

Term	Description	Unit
P_{Hy}^{PC}	Pressure in the intraperitoneal cavity	[mmHg]
P_0^{PC}	Pressure at V_0 respectively empty cavity	[mmHg]
V^{PC}	Volume in the intraperitoneal cavity	[L]
V_0^{PC}	Volume at P_0 respectively empty cavity	[L]
γ	Patient-specific transfer parameter	[mmHg/L]

With the proposed membrane test method including measurement of intraperitoneal pressure (IPP) during fill and drain we can get a patient-specific characteristic [14]:

$$\widetilde{P}_{Hy}^{PC}(V_{PC}) = f(P_{Meas}^{PC}(t), V_{Meas}^{PC}(t))$$

Equation 3-10

Table 3.2-IV: Description of the used terms and the corresponding unit.

Term	Description	Unit
$\widetilde{P}_{Hy}^{PC}(V_{PC})$	Patient-specific relationship between volume in the peritoneal cavity and the resulting intraperitoneal pressure	[mmHg]
$P_{Meas}^{PC}(t)$	Quasi-continuous measurement of the intraperitoneal pressure	[mmHg]
$V_{Meas}^{PC}(t)$	Quasi-continuous measurement of the intraperitoneal volume	[L]

It is proposed that $\widetilde{P}_{Hy}^{PC}(V_{PC})$ is determined for the individual patient during fill, dwell and/or drain phase by acquisition of V_{Meas}^{PC} and P_{Meas}^{PC} , for example via an APD cyclor. This could be a polynomial or spline fitted to the measured data. In later research it has been demonstrated that interstitial pressure, P_{HS}^{Int} is in fact the relevant pressure outside the peritoneal cavity and is scaled by the hydration status of the patient. For the purposes of the current simplified UF prediction model a more general form of $\Delta\widetilde{P}_{Hy}^{PC}(V_{PC})$ may be considered:

$$\Delta\widetilde{P}_{Hy}^{PC}(V_{PC}) = \widetilde{P}_{Hy}^{PC}(V_{PC}) - P_{HS}^{Int}$$

Equation 3-11

Table 3.2-V: Description of the used terms and the corresponding unit.

Term	Description	Unit
P_{HS}^{Int}	Patient-specific interstitial pressure depending on the hydration status of the patient	[mmHg]
$\Delta\widetilde{P}_{Hy}^{PC}(V_{PC})$	Patient-specific pressure gradient between peritoneal cavity and interstitium as a function of the intraperitoneal volume	[mmHg]

In a subject without renal failure, P_{HS}^{Int} is typically in the area of - 3 mmHg. However, renal failure leading to fluid overload and free fluid flow across the interstitial matrix will cause P_{HS}^{Int} to raise a few mmHg above zero [2, 14, 30, 40, 69-73].

3.3 Simplified biophysical model approaches

Our simplified ultrafiltration models describe the dynamics of peritoneal cavity volume V^{PC} and the number of osmols N_{Osm}^{PC} or effective crystalloid osmotic pressure gradient $\Delta\pi_{Osm}^{Eff}$ in the peritoneal cavity based on basic principles of volume and mass balance taking transport processes like diffusion, convection and absorption into account. The dynamics of our model is defined independently for the different phases of the PD cycle, as illustrated in Figure 3-5.

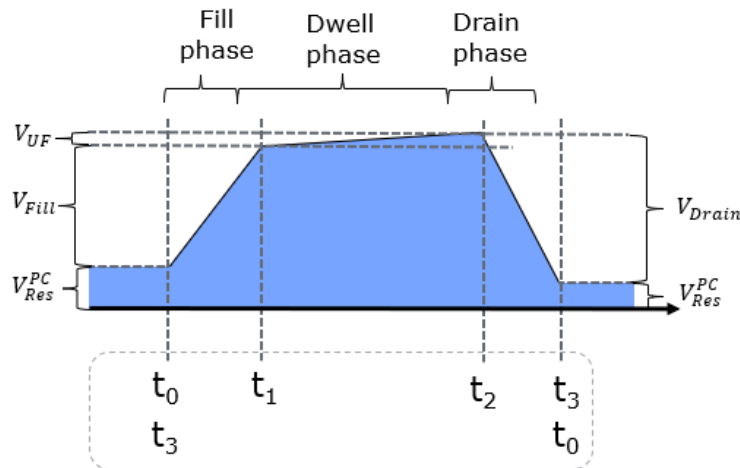


Figure 3-5: Parameterization of the PD cycle. The height of the blue area equals the volume in the peritoneal cavity respectively on the y axis.

To obtain an efficient description, the start and end time points of the phases of a PD cycle and the volume changes during these phases are defined as follows:

Table 3.3-I: Declaration of time points during the PD cycle for the different phases. The end of the drain phase at $t = t_3$ marks the beginning of the fill phase of the next cycle.

PD cycle phase	Start time	End time	Volume change [L]
Fill phase	t_0 Start of the cycle (fill procedure), time point <u>before</u> instillation of PD fluid	t_1	V_{Fill} Fill volume

PD cycle phase	Start time	End time	Volume change [L]
Dwell phase	t_1 Start of the dwell, time point <u>after</u> instillation of PD fluid	t_2	V_{UF} Ultrafiltration volume
Drain phase	t_2 Start of the drain phase <u>before</u> drainage of PD fluid and at the end of the dwell of a PD cycle	$t_3 = t_{end} = t_0$ End of the PD cycle <u>after</u> drainage of PD fluid. Also start of the next cycle (fill procedure), time point <u>before</u> instillation of PD fluid	V_{Drain} Drain volume

ODE system for multiple cycles

In our model, the rate of change in cavity volume is given by the balance of several volume fluxes. Within one PD cycle, the volume rate of change is defined piecewise for different phases of the cycle:

$$\frac{dV^{PC}}{dt} = J_{Mem} - \widetilde{J}_{CL} + \begin{cases} J_{Fill} & t_0 \leq t \leq t_1 \\ 0 & t_1 \leq t \leq t_2 \\ -J_{Drain} & t_2 \leq t \leq t_3 \end{cases}$$

Equation 3-12

and applies to a complete PD cycle, i.e., over the range $t_0 \leq t \leq t_3$ as defined in Figure 3-5. The initial conditions for the cycle are defined at t_0 .

Table 3.3-II: Description of the used terms (parameters) and the corresponding unit.

Term	Meaning	Unit
$\frac{dV^{PC}}{dt}$	Rate of change in cavity volume during the cycle	[L/min]
J_{Mem}	Flow rate through the peritoneal membrane	[L/min]
\widetilde{J}_{CL}	Patient-specific combined volume flow rate due to the differential colloid osmotic pressure across the peritoneal membrane and lymphatic drainage of the peritoneal cavity (assumed to be constant in the short term of weeks)	[L/min]

The flow through the peritoneal membrane denoted as J_{Mem} is the dominating contribution to the total volume flux during the dwell phase, which is driven by hydrostatic and crystalloid osmotic pressure leading to UFV:

$$J_{Mem} = -\widetilde{L}_p S \left[\Delta P_{Hy}^{PC}(V_{PC}) - \widetilde{\sigma} RT \left(\frac{N_{Osm}^{PC}}{V_{PC}} - C_{Osm}^{Pls} \right) \right]$$

Equation 3-13

Table 3.3-III: Description of the used parameters and the corresponding unit.

Parameter	Description	Unit
$\widetilde{L}_p S$	Specific hydraulic conductance. Regarded as the overall flow through the peritoneal membrane per unit pressure	[L/min/mmHg]

Equation 3-13 represents the reduced formulation of the model equations described by Carl Öberg et al. and Rippe et al. [7, 10-11].

The patient-specific parameters in Equation 3-13 are the specific hydraulic conductance $\widetilde{L}_p S$, the aggregated reflection coefficient, and the linear flow \widetilde{J}_{CL} , given by the sum of the lymphatic absorption rate and the volume flux due to colloid osmotic pressure caused by proteins in the blood plasma. The flows J_{Fill} and J_{Drain} are defined over the ranges $t_0 \leq t \leq t_1$ and $t_2 \leq t \leq t_3$, respectively, and are zero-valued elsewhere. Within different phases, the flow rates are constant and given by the rates with which the pump of the cyler fills and drains the patient's cavity during standard treatment. For CAPD respectively, it is the volume infused divided by the time needed for the fill. The rate of change of the number of osmols in the peritoneal cavity during the cycle includes contributions from diffusion, convection (via ultrafiltration) and absorption (lymph and colloid induced convection) as well as the fill and drain behavior, which changes the amount of osmotically active substances,

$$\frac{dN_{Osm}^{PC}}{dt} = -\widetilde{P}_{Osm} S \left(\frac{N_{Osm}^{PC}}{V_{PC}} - C_{Osm}^{Pls} \right) - \widetilde{J}_{CL} \frac{N_{Osm}^{PC}}{V_{PC}} + \begin{cases} J_{Fill} C_{Osm}^{PDF} & t_0 \leq t \leq t_1 \\ 0 & t_1 \leq t \leq t_2 \\ -J_{Drain} \frac{N_{Osm}^{PC}}{V_{PC}} & t_2 \leq t \leq t_3 \end{cases}$$

Equation 3-14

or

$$\frac{dN_{Osm}^{PC}}{dt} = -\widetilde{P}_{Osm} S \left(\frac{N_{Osm}^{PC}}{V_{PC}} - C_{Osm}^{Pls} \right) + (1 - \tilde{\sigma}) J_{Mem} C_{Osm}^{Pls} - \widetilde{J}_{CL} \frac{N_{Osm}^{PC}}{V_{PC}} + \begin{cases} J_{Fill} C_{Osm}^{PDF} & t_0 \leq t \leq t_1 \\ 0 & t_1 \leq t \leq t_2 \\ -J_{Drain} \frac{N_{Osm}^{PC}}{V_{PC}} & t_2 \leq t \leq t_3 \end{cases}$$

Equation 3-15

Table 3.3-IV: Description of the used parameters and the corresponding unit.

Parameter	Description	Unit
$\widetilde{P}_{Osm} S$	Overall permeance of the peritoneal membrane to osmols. May be related to the overall mass transfer area coefficient (MTAC) for all osmols and determines the rate at which solutes permeate the peritoneal membrane by diffusive processes	[L/min]

In this ODE the overall permeance of the peritoneal membrane to osmols is introduced as patient-specific membrane parameter. How the initial conditions for the model are set generally depends on the scenario simulated. For the case of CAPD, there is an unknown in- and outflow

of the dialysate. In this case, it is advisable to start the model at $t = t_1$. If the flows are known (by means of a cyclor with known fill and drain flows, for example), the calculation could start at $t = t_0$.

In conventional CAPD treatments the fill volume (instilled volume) V_{Fill} can be measured by weighing the bag of PD fluid pre- and post-instillation. Under gravity, the fill flow rate J_{Fill} , varies during the fill phase and is not known with any accuracy (unless flow sensing is introduced in the patient line).

In the general case, where a residual volume V_{Res}^{PC} is present in the peritoneal cavity, the number of osmols at the end of the fill phase can be determined as

$$N_{Osm}^{PC}(t_1) = C_{Osm}^{PC}(t_0) V_{Res}^{PC} + C_{Osm}^{PDF} V_{Fill}$$

Equation 3-16

where $C_{Osm}^{PC}(t_0)$ and C_{Osm}^{PDF} are the concentrations of osmols in the peritoneal cavity at time t_0 (start of the fill phase) and the concentration of fresh PD fluid, respectively. Under the assumption that the cavity osmolarity is fully equilibrated with the blood plasma (which is measured rather rarely), $C_{Osm}^{PC}(t_0)$ can be replaced with C_{Osm}^{Pls} and assumed that the plasma osmolarity ends up on a constant level due to metabolization (on the time scale of weeks at least),

$$N_{Osm}^{PC}(t_1) = C_{Osm}^{Pls} V_{Res}^{PC} + C_{Osm}^{PDF} V_{Fill}$$

Equation 3-17

The initial volume in the peritoneal cavity at the end of the fill phase is given by

$$V^{PC}(t_1) = V_{Fill} + V_{Res}^{PC}$$

Equation 3-18

The duration of the fill and drain phases of a PD cycle can easily account for 30 minutes or more during which transport processes could also persist. Consequently, a more general model of PD transport processes determines the initial conditions at the start of the PD cycle ($t = t_0$), rather than solely during dwell phase. The number of osmols at t_0 is given by

$$N_{Osm}^{PC}(t_0) = C_{Osm}^{PC}(t_0) V_{Res}^{PC} \approx C_{Osm}^{Pls} V_{Res}^{PC}$$

Equation 3-19

and the initial volume is

$$V^{PC}(t_0) = V_{Res}^{PC}$$

Equation 3-20

In a PD treatment system, where the fill flow rate J_{Fill} is known, either by a suitable sensor in the patient line or by APD, this flux may be directly included in the governing equations (Equation 3-13, Equation 3-14 & Equation 2-21) describing the transport kinetics. This allows the variation in the number of osmols and cavity volume during fill and drain to be considered. If the peritoneal cavity is completely empty (dry) at the start of the fill phase, then $V_{Res}^{PC} = 0$ [7, 9-11, 75].

ODE system for single cycle (dwell only)

Importantly, this model applies only over the dwell phase and for a fixed fill volume used for the treatment, i.e., in the time range $t_1 \leq t \leq t_2$. In contrast to other models in PD, this model does not describe the rate of change of osmotically active molecules in the peritoneal cavity but provides a direct description of the change in the effective osmotic pressure difference $\Delta\pi_{Osm}^{Eff}$ that drives the fluid flow through the peritoneal membrane.

The reduced biophysical model is given by the following pair of ordinary differential equations,

$$\frac{dV^{PC}}{dt} = -\widetilde{L}_p S \left[\Delta P_{Hy}^{PC}(V_{PC}) - \Delta\pi_{Osm}^{Eff} \right] - \widetilde{J}_{CL}$$

Equation 3-21

$$\frac{d\Delta\pi_{Osm}^{Eff}}{dt} = -\widetilde{K}_{Osm} S \Delta\pi_{Osm}^{Eff}$$

Equation 3-22

Table 3.3-V: Description of the used terms and the corresponding unit.

Parameter	Description	Unit
$\widetilde{K}_{Osm} S$	Patient-specific dissipation coefficient for the crystalloid osmotic pressure gradient	[-]

The rate of crystalloid dissipation during the dwell phase is determined by crystalloid transport across the membrane and the dilution of crystalloids by the ultrafiltration volume appearing in the peritoneal cavity. If the crystalloid dissipation is approximated as a first-order process, the decay constant of the crystalloid osmotic pressure gradient becomes the patient parameter denoted by $\widetilde{K}_{Osm} S$ (as exponential decrease). The additional ODE describing the osmotic pressure gradient $\Delta\pi_{Osm}^{Eff}$ requires an initial condition for the effective osmotic pressure difference at the start of the dwell at $t = t_1$:

$$\Delta\pi_{Osm}^{Eff}(t_1) = \widetilde{\Delta\pi}_{Osm}^{Eff}(C_{Osm}^{PDF})$$

Equation 3-23

Table 3.3-VI: Description of the used terms and the corresponding unit.

Parameter	Description	Unit
$\widetilde{\Delta\pi}_{Osm}^{Eff}(C_{Osm}^{PDF})$	Patient-specific osmotic pressure gradient at the start of the dwell as a function of the dialysate OA concentration (In this model, this initial condition becomes a patient-specific parameter)	[mmHg]

If there is no information available about the characteristic of the patient's membrane at the beginning of the treatment, the aggregate reflection coefficient $\widetilde{\sigma}$ is unknown.

However, the reflection coefficient infer using information about blood plasma and peritoneal cavity fluid osmolarity (C_{Osm}^{Pls} and C_{Osm}^{PC} , respectively) at the start of the dwell. First, a fictitious osmotic pressure gradient $\Delta\pi_{Osm}(t_1)$ under the assumption that the membrane is only permeable to water is calculated (in which case the reflection coefficient is unity).

$$\begin{aligned}
\Delta\pi_{Osm}(C_{Osm}^{PDF}) &= RT (C_{Osm}^{PC}(t_1) - C_{Osm}^{Pls}) = RT \left(\frac{C_{Osm}^{PDF} V_{Fill} + C_{Osm}^{PC}(t_0) V_{Res}^{PC}}{V_{Fill} + V_{Res}^{PC}} - C_{Osm}^{Pls} \right) \\
&= RT \left(\frac{C_{Osm}^{PDF} V_{Fill} + C_{Osm}^{Pls} V_{Res}^{PC}}{V_{Fill} + V_{Res}^{PC}} - C_{Osm}^{Pls} \right) \\
&= RT \Delta C_{Osm}^{PC,Pls} \quad \text{at } t = t_1
\end{aligned}$$

Equation 3-24

Then, the effective osmotic pressure for the semipermeable peritoneal membrane at the start of the dwell dependent on the dialysate OA concentration (C_{Osm}^{PDF}) is given by $\Delta\pi_{Osm}$ scaled by the aggregated reflection coefficient:

$$\Delta\pi_{Osm}^{Eff}(C_{Osm}^{PDF}) = \tilde{\sigma} \Delta\pi_{Osm}(C_{Osm}^{PDF}) \quad \text{at } t = t_1$$

Equation 3-25

The effective osmotic pressure gradient $\Delta\pi_{Osm}^{Eff}(C_{Osm}^{PDF})$, which depends on the dialysate OA concentration, can be obtained by model optimizations with patient data. Using this method to determine $\Delta\pi_{Osm}^{Eff}(t_1)$ and calculate $\Delta\pi_{Osm}(t_1)$ by Equation 3-25 for different glucose concentrations, lead to the aggregated reflection coefficient $\tilde{\sigma}$ as the slope of a linear regression of $\Delta\pi_{Osm}^{Eff}(t_1)$ and $\Delta\pi_{Osm}(t_1)$, see Figure 3-6.

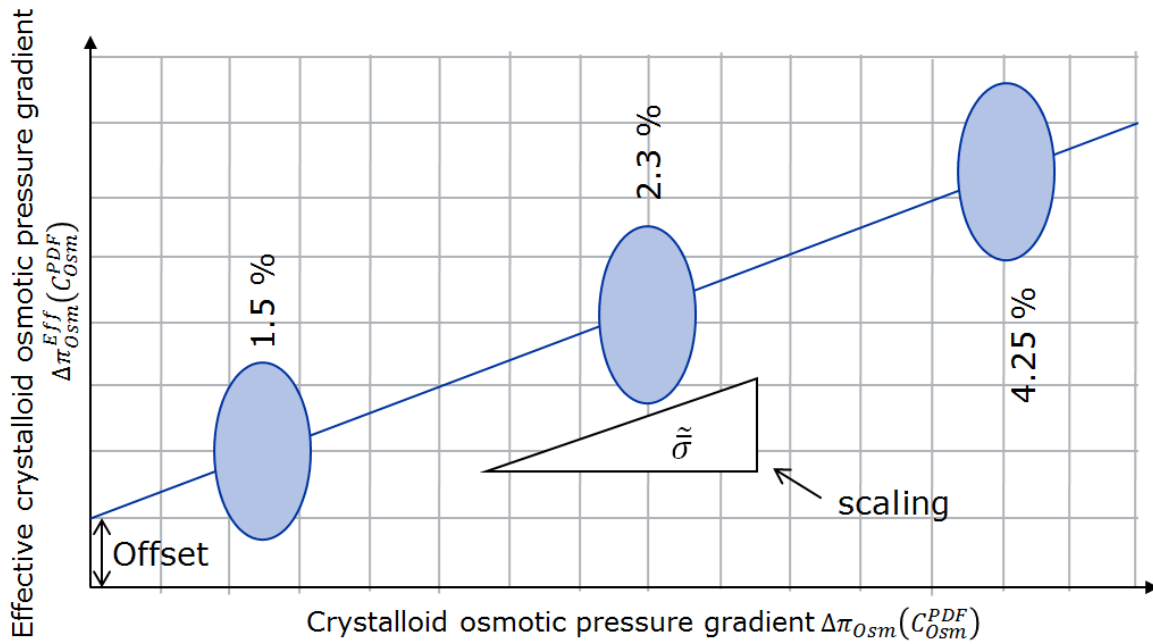


Figure 3-6: Schematic representation of the relationship of the osmotic pressure gradient $\Delta\pi_{Osm}(C_{Osm}^{PDF})$, which is scaled by the effective osmotic pressure gradient $\Delta\pi_{Osm}^{Eff}(C_{Osm}^{PDF})$ by the aggregated reflection coefficient $\tilde{\sigma}$ with offset correction.

$$\Delta\pi_{Osm}^{Eff}(C_{Osm}^{PDF}) = \tilde{\sigma} \Delta\pi_{Osm}(C_{Osm}^{PDF}) + Offset \quad \text{at } t = t_1$$

Equation 3-26

Also, other polynomials which are suitable transfer functions, could be used to capture nonlinearities arising by physiological effects and treatment conditions [7, 9-11, 44].

3.4 *In vitro* test setup *Bvatar*

The *in vitro* test system (called *Bvatar*) was designed and manufactured at Fresenius Medical Care St. Wendel site in collaboration with the in-house training metal-workshop in the past decade. Figure 3-7 shows a schematic representation of the artificial membrane test system equipped with 2 pressure sensors (WIKA CPH6300, 0-100 mbar Pt6200) to detect the pressure gradient from inner to outer media in the riser pipe for experiments made at 37 °C to mimic body temperature.

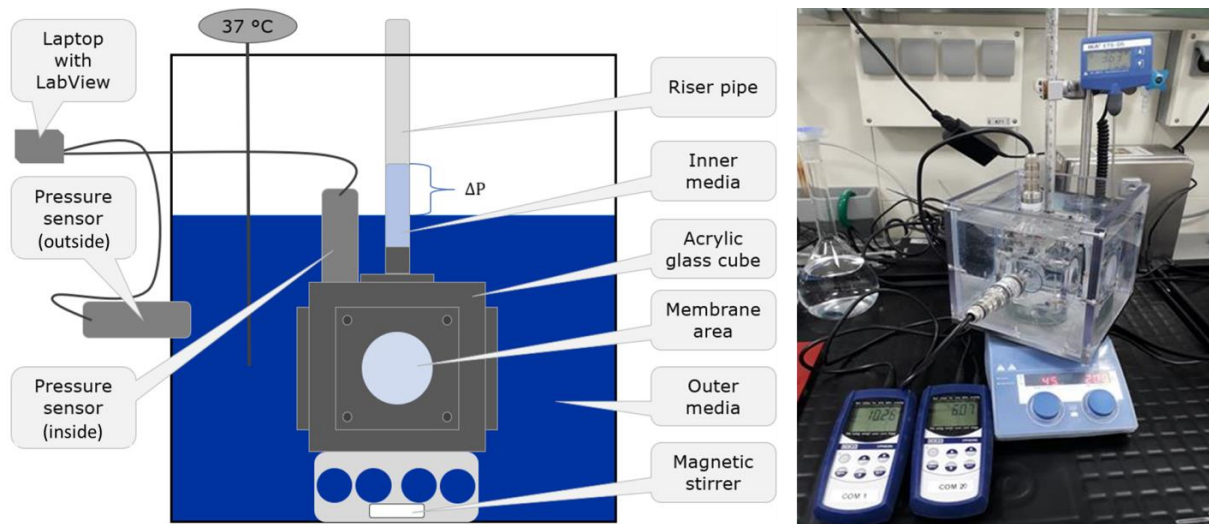


Figure 3-7: Schematic sketch of the *Bvatar* test setup (left) and photograph (right) with two pressure sensors and the possibility to equip with membranes.

It is possible to attach up to four different artificial membranes to the sides of the acrylic glass cube. The membranes are sealed with the help of built-in O-rings and pressed to the side parts. A flange is placed on the upper side of the cube, to which a burette (riser pipe) can be attached. The cube filling volume for the *in vitro* test system was determined in preliminary tests and is approximately 0.101 L in contrast to the volume of the outer beaker, which is 3 L.

In order to carry out experiments using the *Bvatar*, the desired membranes, which are previously soaked in distilled water, or blank sides made of acrylic glass must first be screwed to the side walls provided with seals. The cube is then filled with the desired inner media (for example glucose solution). During the filling, air bubbles inside the cube especially at the membrane surface area ($4 \times 7.067 \text{ cm}^2$, Sartorius 20 kDa Cellulose triacetate) and the pressure sensors must be removed. After filling the cube, the acrylic burette (Nalgene, Thermo Scientific) can be attached. Then, the automated pressure measurement performed by automation via LabView (National Instruments) can be started and the cube must be placed in the outer beaker.

Because of the known dimensions of the riser pipe (25 mL, Inner- \emptyset 0.95 cm), the volume increase due to UF inside the pipe can be calculated from the pressure. With the volume of the cylinder equation [66]:

$$\Delta v(t) = \pi r^2 \Delta h(t)$$

Equation 3-27

and the Pascal's law (hydrostatic pressure):

$$\Delta P(t) = \rho g \Delta h(t)$$

Equation 3-28

the relationship:

$$\Delta V(t) = \left(\pi r^2 / \rho g \right) \Delta P(t) = \gamma_{Bvatar} \Delta P(t) \sim 0.9634 \Delta P(t)$$

Equation 3-29

for the *Bvatar* can be achieved, which is for the setup equal to the P/V-characteristics explained in section 3.2 for the specific patient.

Table 3.4-I: Description of the used terms and the corresponding unit.

Term	Description	Unit
ρ	Density of the solution	[kg/m ³]
g	Ground acceleration	[m/s ²]
$\Delta P(t)$	Pressure change till start, at time t of the experiment	[Pa], [mmHg]
$\Delta v(t)$	Volume change till start, at time t of the experiment	[m ³]
r	Radius of the riser pipe	[m]
$\Delta h(t)$	Height change till start, at time t of the experiment	[m]
$\Delta V(t)$	Volume change till start, at time t of the experiment	[mL]
$\Delta P(t)$	Pressure change till start, at time t of the experiment	[mmHg]
γ_{Bvatar}	<i>Bvatar</i> -specific transfer parameter	[mL/mmHg]

Bvatar model evaluation

The Phenomenological model used by Rippe et al. is given by [7]

$$V(t) = V_0 + a_1 (1 - e^{-k t}) - a_2 t$$

Equation 3-30

The parameters for the different model approaches of Figure 3-8 can be found in the appendix section.

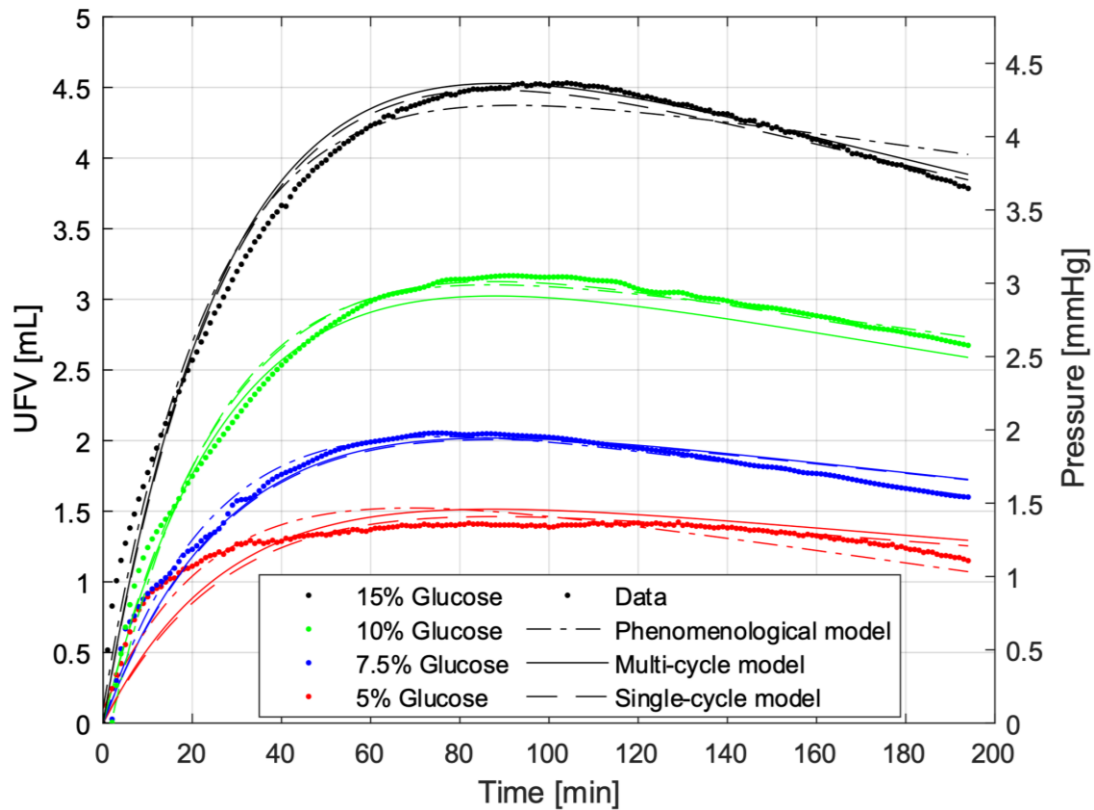


Figure 3-8: Results of Bvatar experiments with different glucose solutions as inner media and water as outer media with 4 small pore membranes (like explained in Section 3.4) and the corresponding model evaluations. The conversion between pressure and volume was made by the relation $V(t) = 0.9634 P(t)$ resulting from the geometry of the riser pipe.

Tracking of membrane characteristics

The biophysical model approaches discussed can be optimized with data of various treatment cycles to get a good estimate of the membrane parameters. The parameters are assumed to be constant in short term (weeks) and can change over time on PD, especially, if the patient got an infection of the peritoneum (peritonitis). In the parameter determination process, only the last day's cycles would be taken into account for optimization, respectively the parameters should be tracked over the time on PD to identify membrane changes. Early detection of peritonitis or other treatment complications represented in the models by uncharacteristic changes in the patient-specific parameter set should be implemented. This may allow the nephrologist to intervene at an early stage. For the empirical model same concepts can apply by taking for example the error of the predicted to the measured UFV into account. The different model approaches explained in more detail in the sections above (section 3.1-3.3) may be combined to get the maximum benefit out of the information delivered by the patients data measured, especially from intraperitoneal pressure and ultrafiltration volume combined with hydration status information. For example, the single cycle biophysical model approach combined with the empirical model approach to take the influence of the fill volume into account. This can be realized, if a 3rd dimension with the fill volume is added to Figure 3-6 (example included in the appendix). With this approach the model capabilities to deal with nonlinearities probably improves. Further, the model can be extended to take other influencing factors into account [75-79].

Chapter 4: *In vivo* test setup, material and animal study design

The execution of the animal experiments with the designated test system and the animal study protocol is described in this chapter. The screening of the hypothesis should provide representative results for the population of rats and should be transferrable also to PD patients. The animal experiments were approved by the local governmental animal protection committee (permit number: 07/2020) and conducted in accordance with the European legislation on the protection of animals (Directive 2010/63/EU) and the NIH guidelines on the care and use of laboratory animals (NIH publication #85-23 Rev. 1985). Female Sprague Dawley rats with an age of 6 to 8 months were used. The animals were housed in a licensed animal facility at the Institute for Clinical & Experimental Surgery (Saarland University, Homburg, Germany). Their day/night cycle was 12 hours. The rats were fed with water and standard pellet food (Altromin, Lage, Germany) *ad libitum*. During the experiments, the rats were anesthetized using isoflurane (~ 2 %) and sacrificed after the study experiment. The rat population consisted of Sprague Dawley rats of female gender in a weight range of 255 to 335 g. The data were recorded within LabView and analyzed with MATLAB (MATLAB for Windows 10, Version 2020b; MathWorks, Natick, Massachusetts, USA), respectively. To evaluate the data, p -values of the data were determined. The significance level was set to $p \leq .05$. The slope of the P/V relationship, needed for further analysis, was calculated by linear regression. To quantify the dependency of UFV and the slope of the P/V characteristic on hydration status or IPP with UFV, a linear mixed effects model was constructed. This enabled quantification of the effects of random variation in measured variables, especially for the random effect of the individual rat (3rd study phase) and of the 3 consecutive cycles. For the 2nd study phase linear regression models are decided sufficient for analysis, since every result accounts for a single individual. All other results were expressed as mean \pm standard deviation of the sample [16].

4.1 *In vivo* test setup for the animal experiments

To perform the *in vivo* animal experiments, a self-constructed test system with various hard and software components was used for data acquisition.

The setup was built by a scale (KERN EG 220-3NM; precision 1 mg) for the fill volume and a second scale for the rat weight measurement before at the start $w(0)$ and after $w(t_3)$ the experiment (KERN PCB1000-1; precision 0.1 g). Further, a pressure transducer (WIKA CPH6300, 0-100 mbar Pt6200, precision 0.01 mmHg) and a 2/2-way servo-controlled electronic diaphragm valve (Bürkert Type 6213) were used. All devices were simultaneously controlled by a LabView computer program. Pressures and weights were recorded at minimum ~20 x per second. The mechanical stand with the weighing system enabling under floor weighing at the fill line (Figure 4-1, black box) was produced by MINITEC GmbH in Schönenberg-Kübelberg and was equipped with the weight scale for the fill. To avoid the passage of air through the fill line inside the abdominal cavity, a self-constructed bubble trap was build. Further, a 3D-printed cage was developed for the catheter to avoid the blockage by the intraabdominal rat tissue during the drain. The experimental setup provided the opportunity to measure the pressure over time inside the catheter line (FESTO plastic tubing PUN-H-4X0.75-NT) during the whole experiment, respectively during fill, dwell and drain phase. It

was also possible to measure the volume mass, which is flowing inside the cavity during fill and the volume leaving the cavity during the drain over time by the weight measurements. The electrical valve was used to automate the fill and drain procedure in order to get a standardized scheme for all individuals.

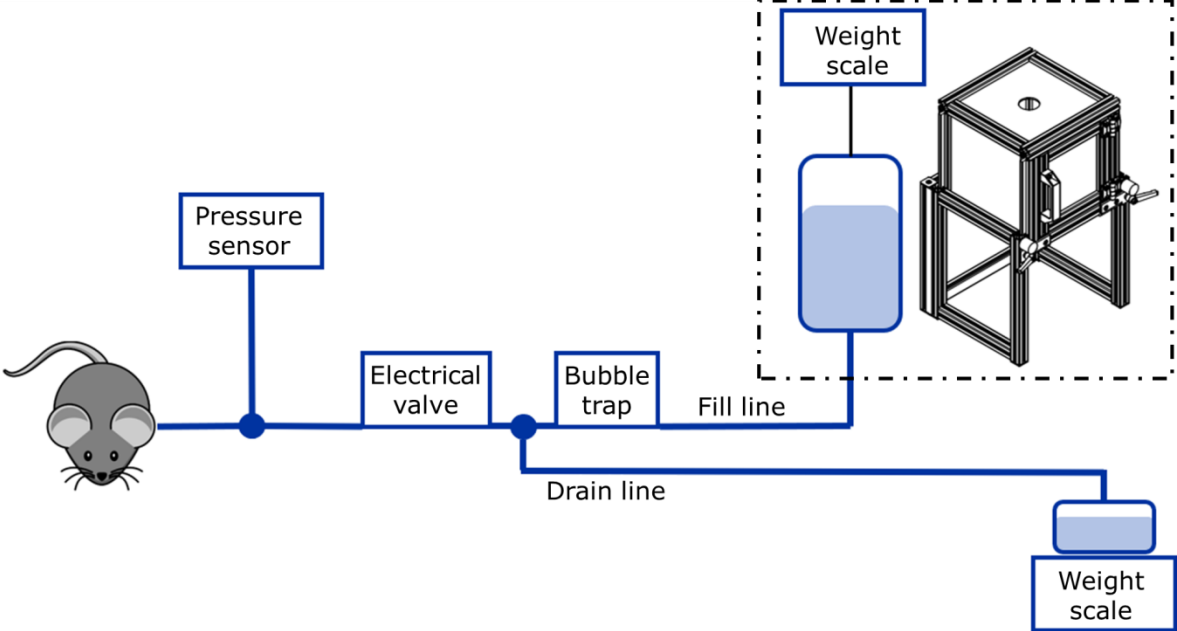


Figure 4-1: Schematic representation of the in vivo test setup to perform the animal experiments. Additionally, quasi continuous pressure measurements in the catheter line and weight measurements of the fluid infused and drained were performed.

Catheter blockage

A problem occurring during the feasibility experiments was the blockage of the catheter holes by interstitial tissue caused by the drainage of the peritoneum by gravity. This issue was solved by development of a 3D printed cage. The catheter cage was added to the tubing to enlarge the surface by uniformly sized and distributed holes.



Figure 4-2: The image on the left side shows the catheter tubing with an open end of the tube diameter and various small holes at the last 2 cm of the tube. The right image shows in contrast the tubing equipped with the 3D printed cage.

With the previously used catheter, it was not possible to achieve sufficient drainage of the abdominal cavity. All holes were covered with tissue due to the negative pressure created by the drainage procedure (Figure 4-2, left). With the modified catheter (Figure 4-2, right), drainage down to less than 1 mL residual volume could be achieved in the majority of cases.

4.2 Material

At discrete time points, samples were taken to investigate blood plasma and dialysate effluent solution. An OSMOMAT 3000 (mOsm/kg H₂O ~ mOsm/L) and an electronic blood glucose meter with a chemically treated, disposable ‘test-strip’ were used. The maximum glucose concentration measurable was 600 mg/dL and the minimum was 10 mg/dL. For measurements of osmolarity, a three-fold determination was used with previous calibration, which was repeated after maximum 15 measurements. During the implantation of the catheter and for taking blood samples a stereomicroscope was used. For the experiments, Balance dialysis solutions in the commercially available Fresenius Medical Care concentrations and an isotonic NaCl solution were used (Table 4.2-I).

Table 4.2-I: Composition of the solutions used for the animal experiments [5]

Active pharmaceutical ingredients [mmol/l]	balance-solution (FRESENIUS MEDICAL CARE)	NaCl 0,9 % (FRESENIUS MEDICAL CARE)
Sodium (Na ⁺)	134	154
Calcium (Ca ²⁺)	1.75	0
Magnesium (Mg ²⁺)	0.5	0
Chloride (Cl ⁻)	101.5	154
Lactate	35	0

Table 4.2-II: Glucose content and osmolarity of the solutions used for the animal experiments [5]

Dialysate Glucose concentration	1.5 %	2.3 %	4.25 %	NaCl
Glucose [mmol/L]	83.2	126.1	235.8	0
Osmolarity[mOsm/L]	358	401	511	308

Table 4.2-I and Table 4.2-II: Glucose content and osmolarity of the solutions used for the animal experiments [5]. Table 4.2-II show the composition of the used solutions regarding buffer, electrolytes and OA [5].

4.3 Protocol and study design

The experimental results represented in Figure 4-3 of an animal study with rats from Lameire et al. in [80] were performed with a fill volume of ~ 28 mL and different OA PD solutions and concentrations (Baxter). The concepts of this study served as basis for the present study design.

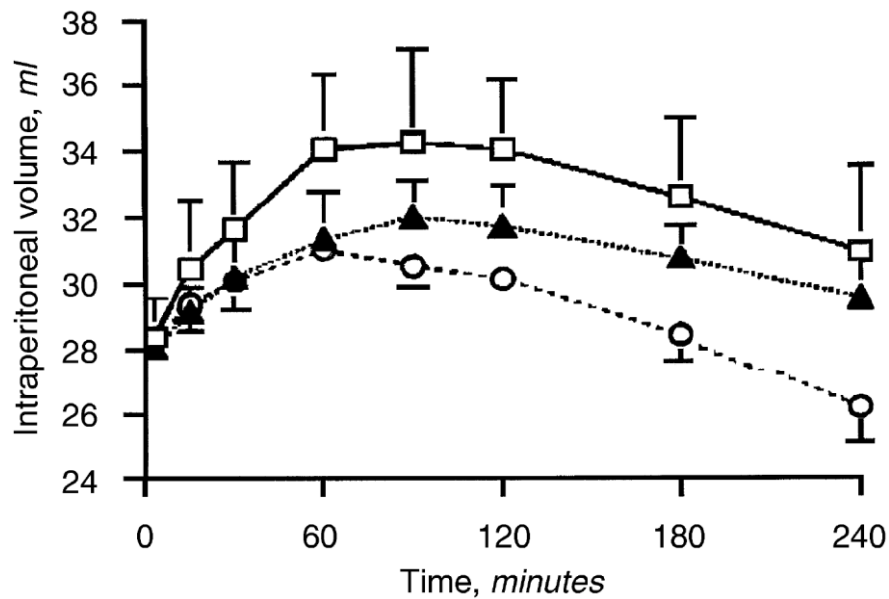


Figure 4-3: Intraperitoneal volume versus dwell time for 3.86% glucose dialysate (□, N = 8), 2.27% glucose dialysate (○, N = 8) and 4% oligopeptides solution (Δ, N = 8). The intraperitoneal volume at the end of the dwell was significantly higher in the 3.86% glucose dialysate and 4% oligopeptide solution groups when compared to the 2.27% glucose dialysate group (both $p < 0.01$), whereas no significant difference was found between the former two groups [80].

In comparison, the following study phases were implemented using pre dwell fill volumes of around 40 mL and to run the dwell phase using around 25 mL as an initial treatment cycle volume leaving space for up to 15 mL UFV. The dialysis solutions introduced in section 4.1 were used in the different phases as mentioned in this chapter. Blood plasma and dialysate samples were analyzed post experiment at the same day or frozen overnight and measured the following day. The maximum time per rat experiment granted from the ethics committee was 240 min, followed by sacrificing the animal. The rat was narcotized (Isoflurane inhalation) during the whole experiment and the catheter was placed at the beginning inside the peritoneal cavity via a small incision, sealed with a suture and observed during the whole experiment for possible leakage occurrence. Blood samples were taken by a jugular vein catheter. The blood sample volume, taken with a syringe, was between 0.4 - 0.5 mL. The drained dialysate was divided in 2 parts. The first part was neglected because of flushing of the tubing system and the second part, was used for further analysis to measure the osmolarity. For flushing, a volume of minimum 12 mL was used for a tubing volume of around 7 mL. To get the complete drain volume both flushed volumes were summed together. At the end of the experiment, after the last drain phase, the residual cavity volume was caught with a syringe after opening the abdominal cavity with a scalpel. After all drains, the volume collected was documented by weighing and the urine excretion was estimated roughly by eye (< 0.1 mL) and was assumed to have neglectable influence on the experiments. Additionally, the weight of the rat was documented before and after the experiment. The plasma was analyzed regarding osmolarity and glucose concentration and the drained fluid regarding osmolarity [80-85].

1st study phase: Pilot phase and feasibility test

The first study phase was mainly for pilot experiments and feasibility test of the concepts mentioned in Chapter 3: and is consequently the basis of the following study phases 2 and 3. In

a first evaluation with a group of 10 animals, we decided to use an isotonic solution and a 4.25 % dialysate to check the extremes, respectively minimum and maximum fluid osmolarity. In this phase, we filled the rat with 40 mL of isotonic solution, followed directly by the drain. Then the cavity was filled again with 25 mL of the 4.25 % balance – solution and a dwell time of 90 to 190 minutes was conducted. After this treatment cycle, the fill and drain procedure from the beginning with the isotonic solution was repeated. At the start of the experiment only a blood sample and after every drain phase samples of drained dialysate and blood were taken, see Figure 4-4.

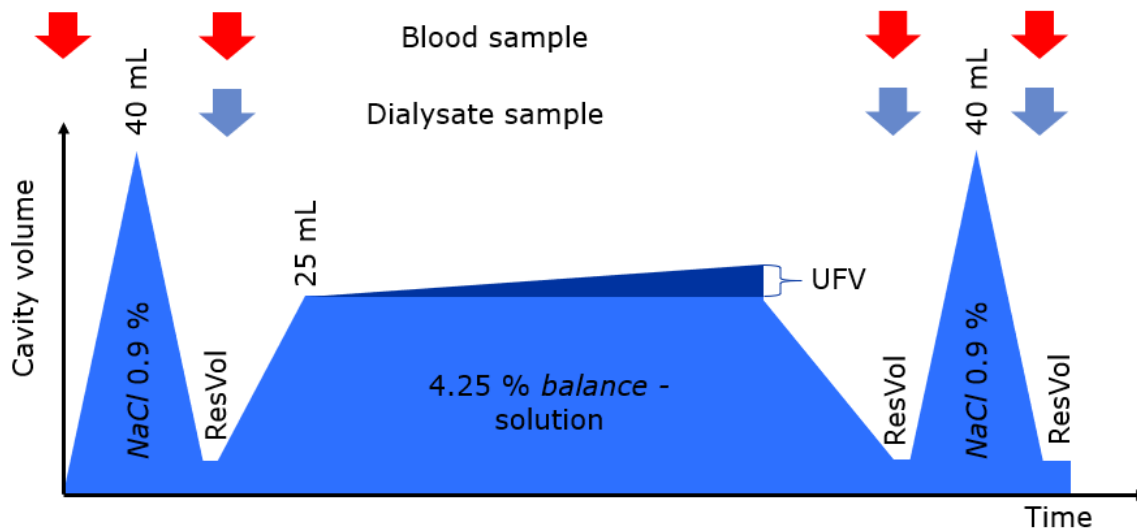


Figure 4-4: Schematic procedure of the experiments of the first study phase

From the results we expected first information about the feasibility of individual P/V characteristics determination, pressure and volume over time behavior and disturbance variables, especially resolution of intraperitoneal pressure, UFV, osmolarity and reproducibility. For the following study parts, modifications should be done to compensate for disturbances and anomalies. The results should also be used to fix the fill volumes and treatment schedule designs for the next study phases. During the execution of this study phase the 3D printed catheter was developed.

2nd study phase: Influence of the OA concentration on ultrafiltration volume

The second study phase was designed to investigate the influence of the different CAPD *balance* solutions on intraperitoneal pressure, UFV and glucose absorption. For this study phase per dialysate solution a number of 9 rats was selected. Here a fixed long dwell behavior with a dwell time of around 200 minutes was used. Also, the dependence of the P/V-characteristics with the OA concentration of the dialysate, the expected correlation of UFV with osmolarity of the dialysate and intraperitoneal pressure with volume for the dwell phase could be evaluated. The resulting intraperitoneal pressure over time curves during the dwell should be transferred to intraperitoneal volume over time using the P/V relationship for the used dialysates. In this study phase a modified fill and drain scheme was used to prevent blockage of the PD catheter due to the negative pressure applied during drainage and additionally by the 3D printed cage for the catheter.

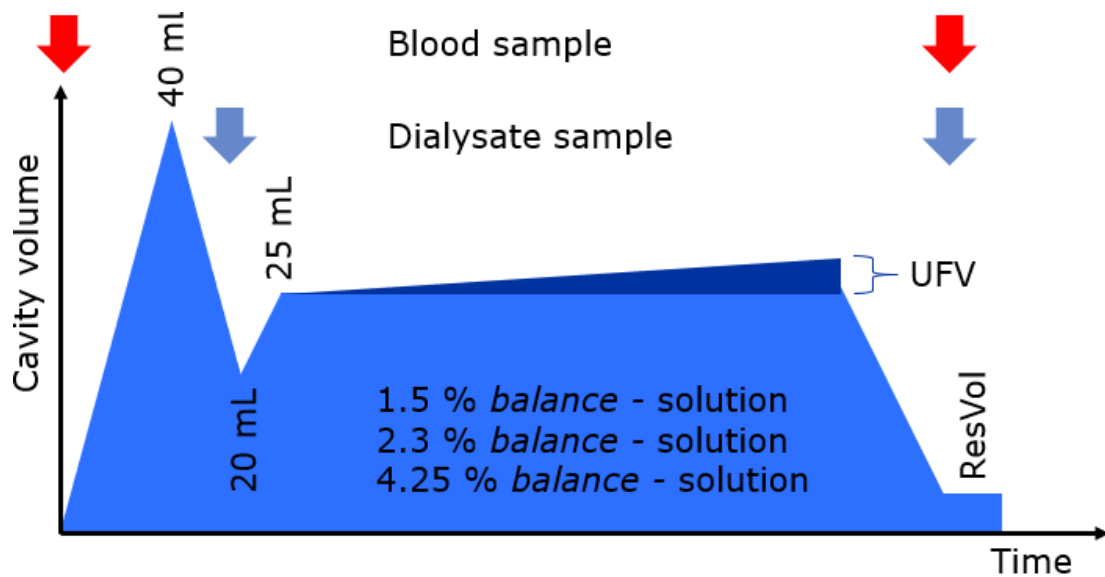


Figure 4-5: Schematic procedure of the experiments of the second study phase

First 40 mL of the desired dialysate got filled inside the cavity, directly followed by drainage of 20 mL, and again filling of 5 mL, resulting in a pre-dwell volume of 25 mL (Figure 4-5). Then the dwell phase occurred, and the cavity got drained completely till only the residual volume was left inside the abdominal cavity. Blood samples were taken only at the beginning and at the end of the experiment. Drained dialysate only got sampled during both drain phases. This study phase was caused by the different dialysates used subdivided in the parts 2.1 for the 1.5 %, 2.2 for the 2.3 % and 2.3 for the 4.25 % *balance*-solution respectively.

3rd study phase: Influence of hydration status on ultrafiltration volume

The third study phase was used to investigate the influence of dehydration on the UFV, this could be hypothetically a reason for ultrafiltration failure, which is a reason for critical dropout rates in PD and transfer to HD. The accounting for the hydration status of the patient could minimize the dropout rate because of wrong interpretation of too low UFV and inaccurate PD treatment. Also, for future model modifications the influence of hydration on intraperitoneal pressure, UFV and glucose absorption would be fundamental. For this study phase a number of 10 rats and the 4,25 % *balance* solution was used. A fixed short dwell behavior with a dwell time of around 60 minutes was applied and repeated 3 times to stepwise dehydrate the rat by UFV's. Also, the dependence of the P/V-characteristics with the hydration of the animal, the expected correlation of UFV with dehydration and intraperitoneal pressure with volume for the consecutive dwell phases could be evaluated.

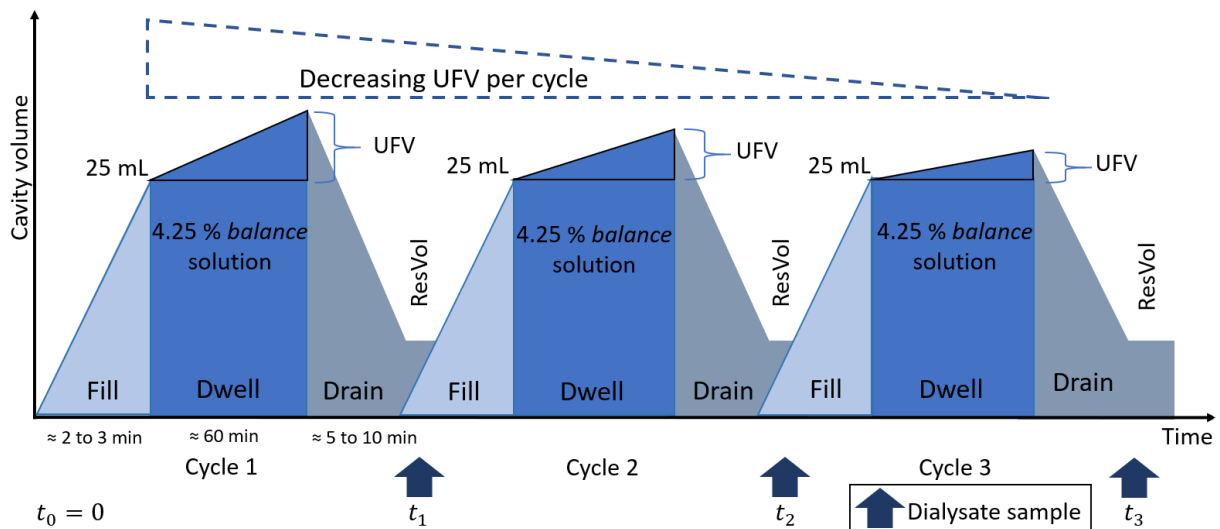


Figure 4-6: Schematic depiction of the experimental protocol. In each cycle, the rat's peritoneal cavity was filled with 25 mL of the fresh dialysate, driven by hydrostatic pressure. During the dwell (approximately 60 min), UFV increased due to the hypertonic dialysate. In the subsequent drain, lasting 5 to 10 min, most of the fluid was drained, except a small residual volume (denoted as ResVol in the Figure). The fill, dwell and drain phases were repeated three times for each rat.

Directly the required 25 mL of the 4.25 % dialysate got filled inside the cavity (Figure 4-5). Then the dwell phase of ~ 60 min occurred, and the cavity got drained completely till only the residual volume was left inside the abdominal cavity. This scheme was repeated 3 times each animal. Blood samples were taken at the beginning of the experiment and at the end of each drain phase. Drained dialysate got sampled during all drain phases. In a real treatment situation, it's not possible to intentionally dehydrate the patient in this order of magnitude, but for the rat experiment, this was possible because the rat gets sacrificed at the end of the experiment and doesn't feel pain or misbehavior because of narcotization.

Chapter 5: Experimental results and discussion of the *in vivo* study results

In this chapter the main results of the study are presented. All diagrams show the full set of animals investigated during the study, except it is mentioned explicitly otherwise.

Table 4.3-I: Declaration for the individual animal and study phase in the following sections

S1 S2, S2.1, S2.2, S2.3 S3, S3.1, 3.2, 3.3	Study phase 1 Study phase 2: 1-1.5%,2- 2.3% and 3-4.24% dialysate Study phase 3: 1- 1.cycle, 2-2.cycle and 3-3.cycle
R1, R2, R3, R4...	Rat experiment identification number

The declaration of the different study phases and animals is done by the abbreviations in Table 4.3-I. In the following sections, if pressure is mentioned, always intraperitoneal pressure is meant. In this section the feasibility results and evaluation of the first study phase is discussed, followed by the results of the second and third study phases. For the calculation of volumes from weight measurements, a conversion factor of 1 g/mL for the density was assumed for simplicity, because the density of the dialysate is varying during the experiments by the change of composition.

The dialysis dose is a combination of the dwell time, fill volume and the dialysate OA concentration used. The dialysate composition is fixed by the product specifications. In comparison, the fill volume and dwell time is dependent on the experimental setup and design. In this section, these important variables and their quality are highlighted.

5.1 Preliminary testing and general findings

The first study phase was used to establish the physiological PD rat model. The pilot experiments delivered bright insides to the problems and mechanisms occurring in the rat's physiological PD system.

Preliminary testing of the Pressure/Volume – dependency

In a first investigation at the beginning of the study, a rat was filled stepwise up to 140 mL cavity volume- The intraperitoneal pressure was recorded continuously during the fill, resulting in a P/V – characteristics (Figure 5-1). For the preliminary testing the isotonic solution was used to minimize the influence of osmotic gradients.

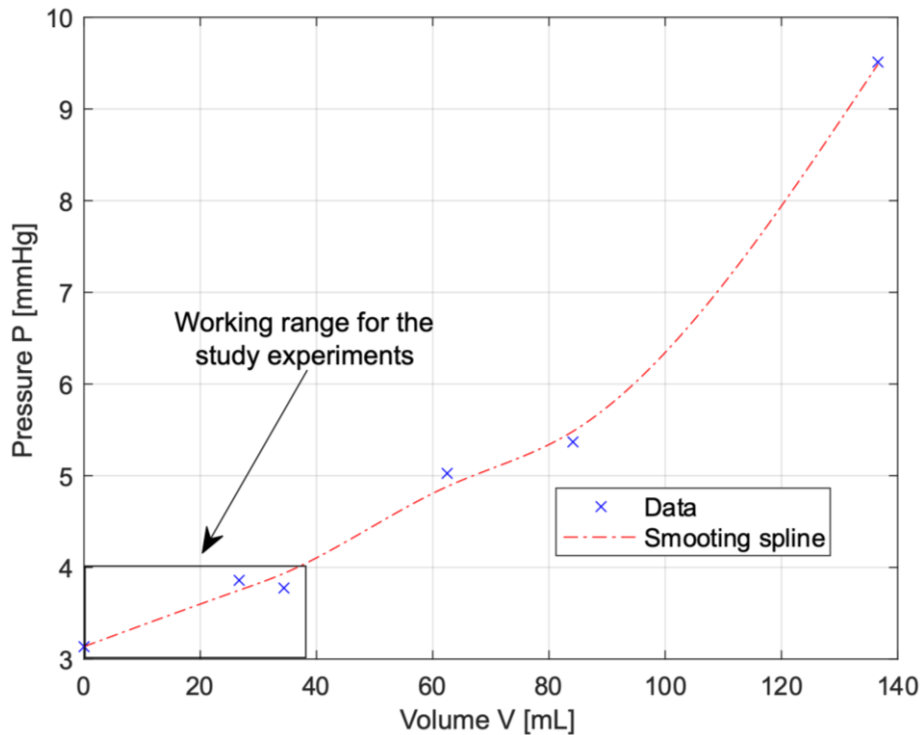


Figure 5-1: P/V characteristic in a single rat of 290 g body weight, over a fill volume range of 0 to approx. 135 mL. Nonlinear behavior was apparent for fill volumes exceeding 80 mL.

The relationship of the P/V-relationship seems to be linear in the range of 0 to 40 mL and was chosen as maximum fill volume for the experiments. Above 80 mL dialysate infusion, the pressure appears to rise more rapidly because the cavity is completely filled and elastic deformation of the abdominal wall causes the pressure to rise.

Variation in urine- and residual volume

For all experiments of the 2nd and 3rd study phase, the excreted urine volume was less or ~ 0.1 mL per individual animal over the whole experiment. During the study ~25 % of the rats had urinary output: The urine volume was neglected for further analysis and was included to the interpolated insensible losses.

The residual volume at the end of each experiment was collected by surgically opening the abdominal cavity and then collected with a syringe. A mean residual volume for study phase 2 and 3 of 0.62 mL resulted from the data collected. If the study phase 2 (1.12 mL) and 3 (0.11 mL) are compared to each other, a difference in the residual volume could be found. A possible reason for this could be the different hydration of the rat due to the different experimental protocols.

Physiological effects

In addition, the frequency of the measurements was investigated to obtain meaningful results for volume inflow and intraperitoneal pressure. The occurrence of physiological influencing factors, especially on the intraperitoneal pressure signal, was identified and needs to be considered over the course of the experiment cycle consisting of fill dwell and drain phase (Figure 5-2).

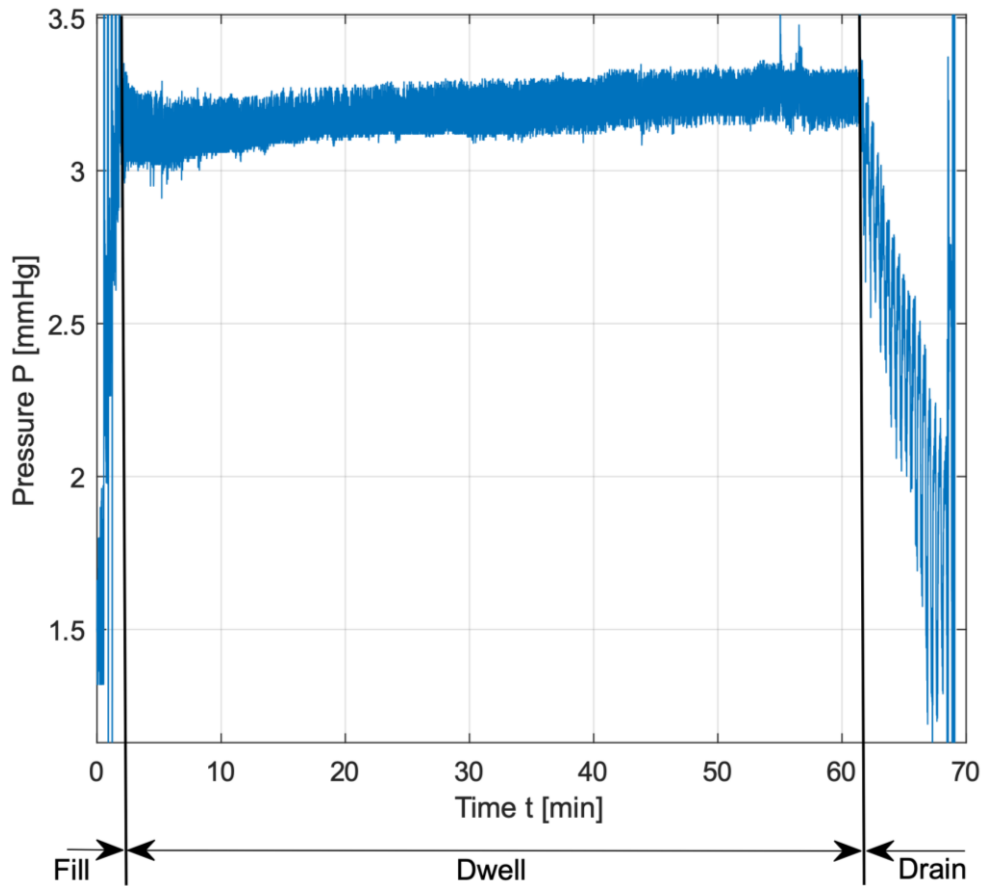


Figure 5-2: Example of the temporal variation in intraperitoneal pressure during the fill, dwell and drain phases of a cycle.

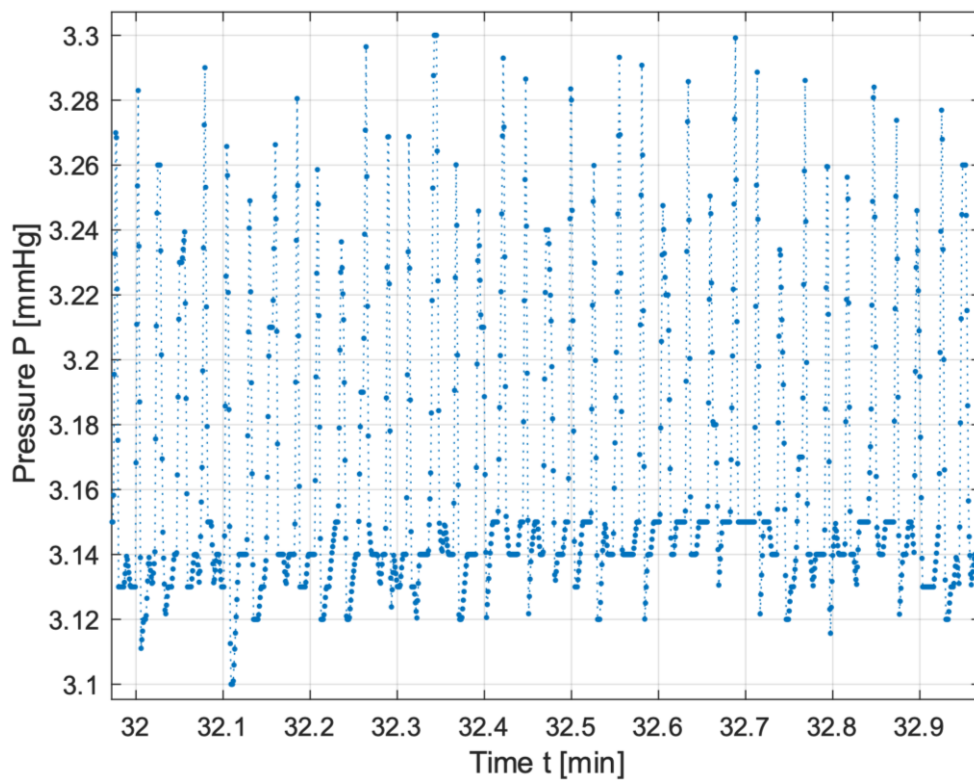


Figure 5-3: The small periodic pressure oscillation due to the respiration of the rat is depicted in magnification of Figure 5-2 for ~ 1 minute. The larger pressure oscillations could be attributed by bowel movements or other physiological effects.

During longer periods (minutes) some fluctuations of the pressure signal could be observed, probably due to bowel movements (Figure 5-3). The frequent periodic pressure oscillations shown in Figure 5-3 are due to the respiration of the animal. To smooth the measured data, high measurement frequencies are required. The data can be smoothed by suitable filters to extract the desired information. To achieve adequate resolution, the weight and pressure signals were measured at the maximum possible frequency for the volume and weight, respectively, at approximately 20 Hz for the pressure signal.

5.2 Study observations

This section mainly reflects the frame variables measured during the study phases 2 and 3 to ensure the quality of the study investigations and compliance with the protocol. For this, the urine volume and residual cavity volume were measured. Additionally, the weight change of the rat through the experiment as well as the deviation in filling and draining the rat by gravity adequately.

Rat weight and weight change

The weight of each rat was noted before and after the experiment, to track the weight loss over time due to insensible losses. These are not captured by the UFV drained after the dwell phase. The initial weight of the rats varied between 330.54 g and 256.17 g for the 2nd and 3rd study phase with different weight losses dependent on the protocols applied to the animals depicted in Figure 5-4.

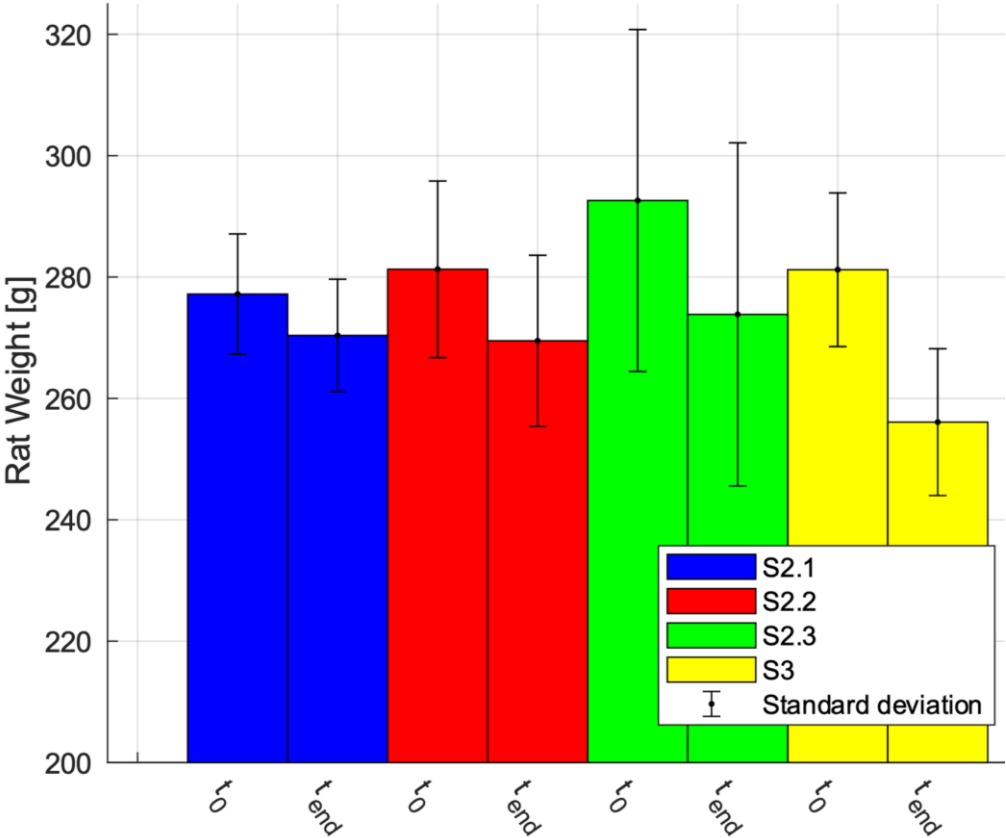


Figure 5-4: Mean rat weight pre and post the experiment for the different study conditions regarding the design of the study phases. Additionally, the standard deviations are shown (from left to right: S2.1, S2.2, S2.3 and S3).

From these data, the weight loss could be calculated, shown in Figure 5-5.

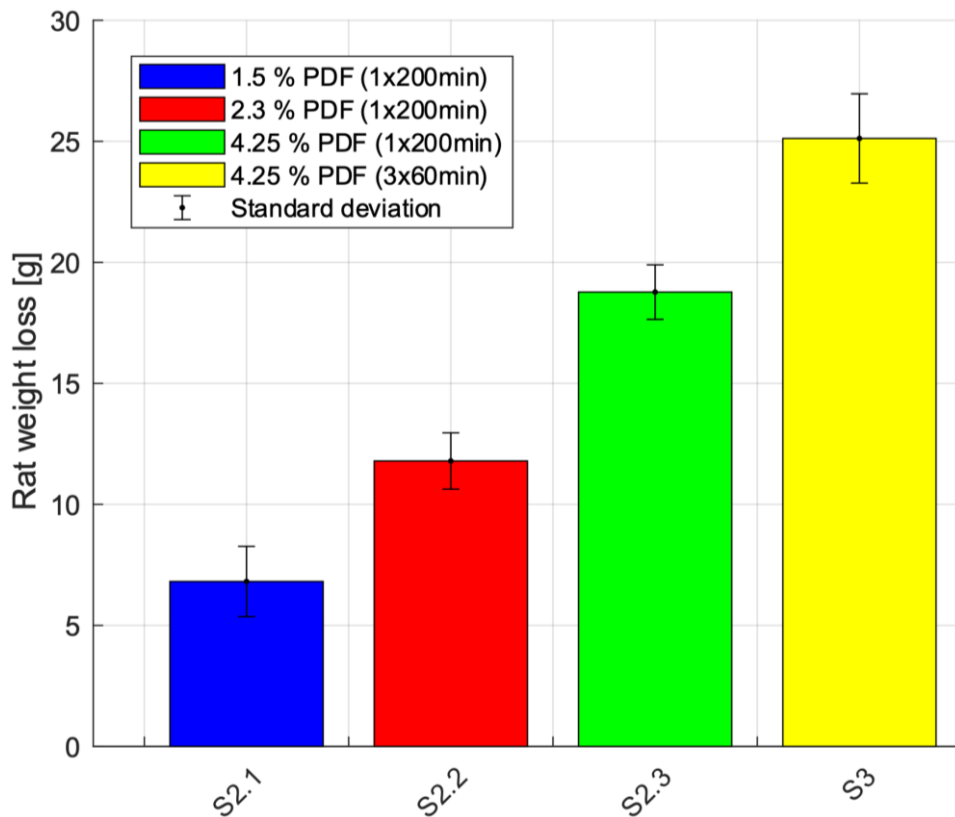


Figure 5-5: Average weight loss during the experiments for the different study phases and corresponding standard deviations (from left to right: 1.5 %, 2.3 %, 4.25 % 200 min and 4.25 % 60 min dwell).

As expected, the weight loss is higher with dialysate glucose concentration and number of the consecutive cycles performed. This depends in majority from the UFV's reached, but independently for all study phases comparable results for the insensible losses could be found (calculation and results explained in more detail at section 0).

Fill volumes

Due to the different study phases, the animals need to be filled and drained in varying regimens dependent on the protocol prior to the dwell.

The automatic fill and drain procedures by gravity controlled by a valve delivered a good control about the fill and drain volume, respectively the initial dwell volume. In the second study phase, pre-dwell in sum ~ 45 mL of dialysate was filled and 20 mL were drained again to achieve the targeted initial dwell volume of 25 mL. To achieve this, first 40 mL was filled, followed by a drain of 20 mL and again filling of around 5 mL to avoid blockage of the catheter, resulting in 25 mL dialysate in the peritoneal cavity for the dwell phase.

For the 3rd study phase, one fill of 25 mL was proceeded (Figure 5-6). Finally, mean initial dwell volumes of 25.15 mL, respectively 24.79 mL for the second and third study phase could be realized with standard deviations of 1.19 mL and 1.15 mL, respectively.

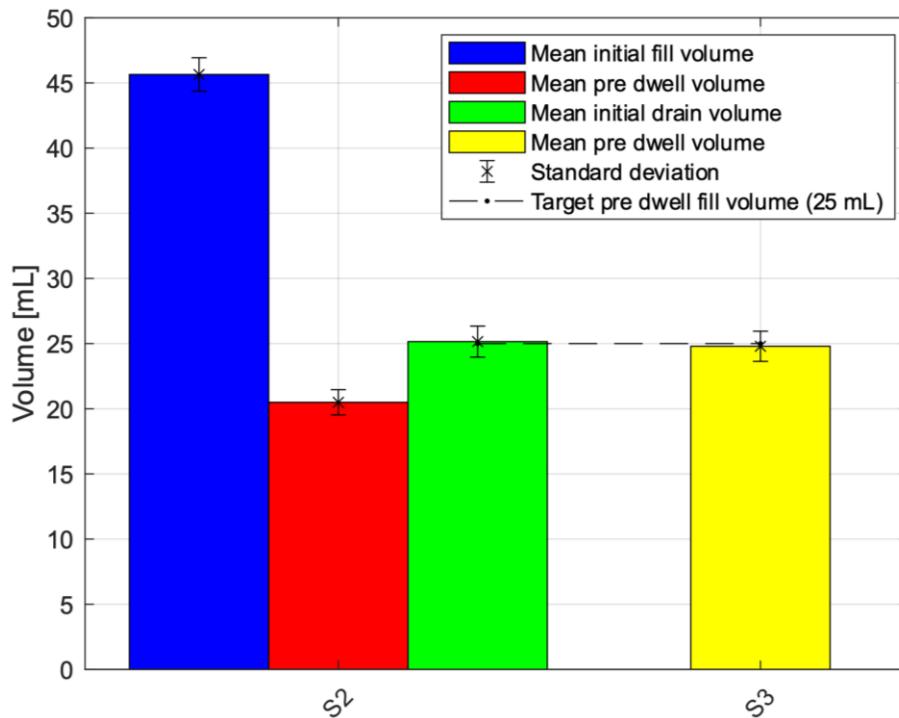


Figure 5-6: Mean fill and drain volumes prior to the dwell phase and initial dwell volumes compared to the target volume and corresponding standard deviations (from left to right: mean initial fill, drain and dwell volume of S2 and mean initial dwell volume of S3).

Drain volumes

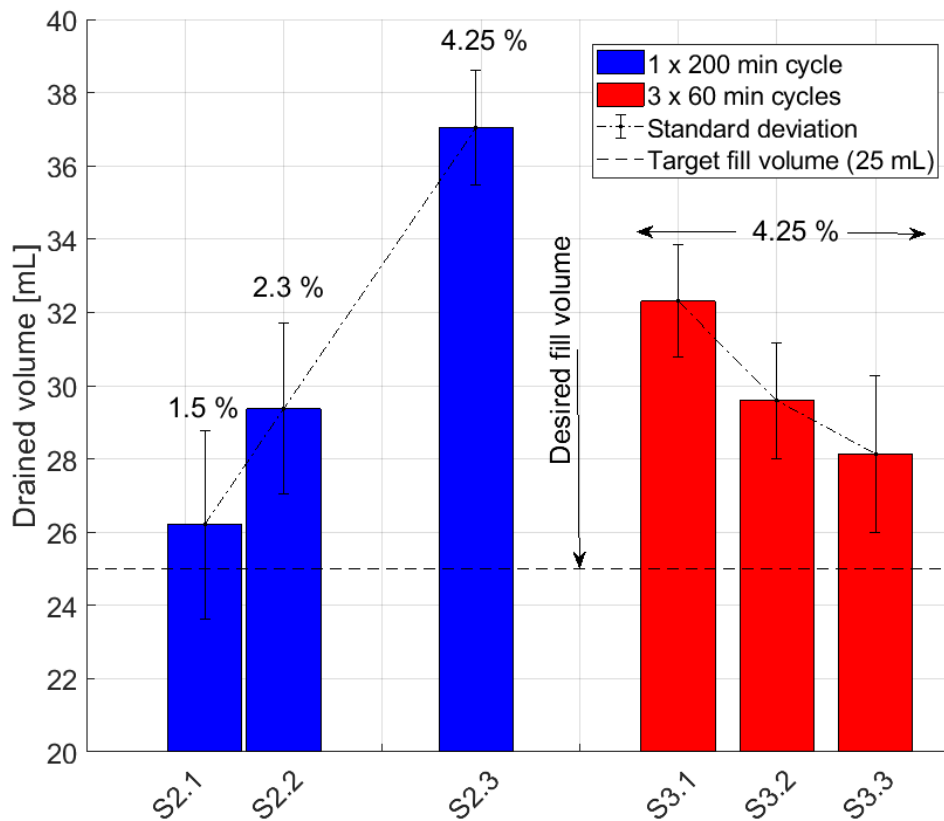


Figure 5-7: Average drain volumes of the different study phases after the dwell phase, corresponding standard deviations. The desired fill volume was marked to reference the obvious increase of volume in the peritoneal cavity by the UFV.

A basic principle known from the literature is the occurring ultrafiltration, which could be detected by the collection of the waste dialysate at the drain. The UFV could be calculated by simply subtracting the fill volume from the drain volume.

The state of the art could be demonstrated for study phase 2, reflecting an obvious increase of intraperitoneal volume dependent on the dialysate glucose concentration used. Further for the 3rd study phase a relationship between the numbers of cycles performed, respectively relative hydration and the UFV, could be identified (Figure 5-7).

Dwell time and UFV

The UFV could be determined from the data shown in Figure 5-7 for every individual animal by simply subtract the fill volume from the drain volume taking the residual volume into account.

$$V_{UF_{measured}} = V_{Drain} - V_{Fill} + V_{Res}^{PC}$$

Equation 5-1

The residual volume is assumed constant for each experiment and was measured at the end of the experiment. The dwell time for each experiment was also known from the continuous pressure readings. The accuracy of the dwell time, respectively the start of the drain was underlying some variation caused by performing treatments in parallel. For the 2nd study phase an average dwell time of ~ 200 min could be achieved as planned, see Figure 5-8.

However, a greater range of dwell times between ~ 170 min and ~ 220 min for various percentage of dialysate's occurred.

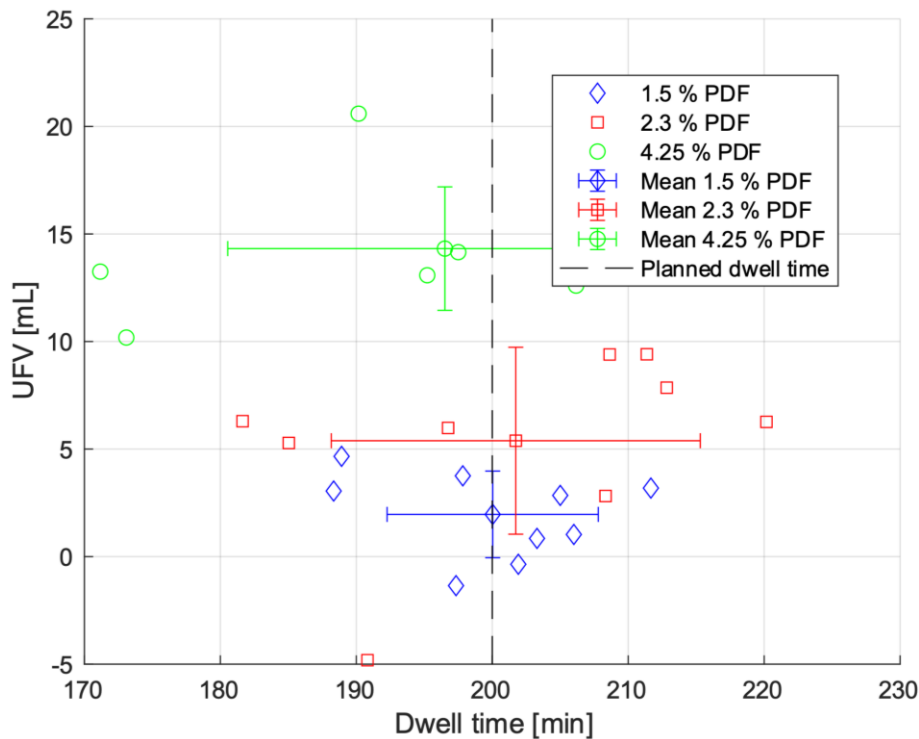


Figure 5-8: Observed UFV per dwell time for the various dialysate's and mean per dialysate glucose concentration with sample standard deviation for the second study phase. After the long dwell time of 200 min for the low glucose concentration dialysates the UFV was negative since in this cases the resorption of fluid was larger than the ultrafiltered volume.

The 3rd study phase had a dwell time of ~ 60 min, see Figure 5-9. However, a range of dwell times between ~ 50 min and ~ 65 min for the different number of consecutive cycles occurred.

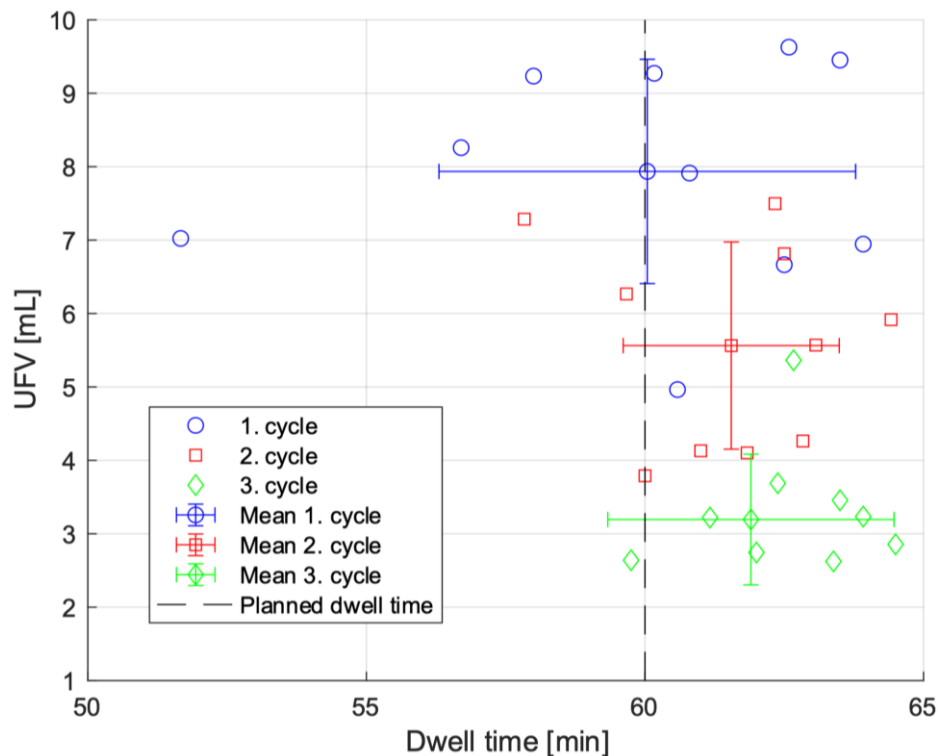


Figure 5-9: Observed UFV per dwell time for the various dialysate's and mean per dialysate glucose concentration with sample standard deviation for the third study phase.

The data shown in this section demonstrates, that the experimental conditions fulfill the requirements for the study regarding dialysis dose, which could be adjusted by dwell time, dialysate OA concentration and fill volume.

5.3 Plasma glucose concentration and osmolarity

The major effect on the fluid transport is driven by the concentration gradient between dialysate and blood plasma. In current clinical practice one problem is a simple and cheap measurement method to determine the glucose content in the dialysate. Like used for diabetes patients, the blood glucose concentration may be easily measured with known concepts and devices. The blood sugar meters are well known devices but the glucose concentrations in the dialysate is far too height (maximum of 600 mg/dL glucose measurable) for reasonable measurement. A suitable compromise, which is the main simplification of the model approaches, are the measurement of blood and dialysate osmolarity to get information about the driving forces of transport processes. To test this hypothesis both values are measured in the blood plasma inside the measurable range for both devices, Osmomat and glucose meter. The long dwells of the 2nd study phase result in only small increases of glucose concentration and osmolarity due to the long dwell and resulting high systematic metabolism of sugar in the blood. Nevertheless, the obtained data in Figure 5-10 lead to a moderate positive correlation ($R = 0.6$) between plasma osmolarity and glucose concentration.

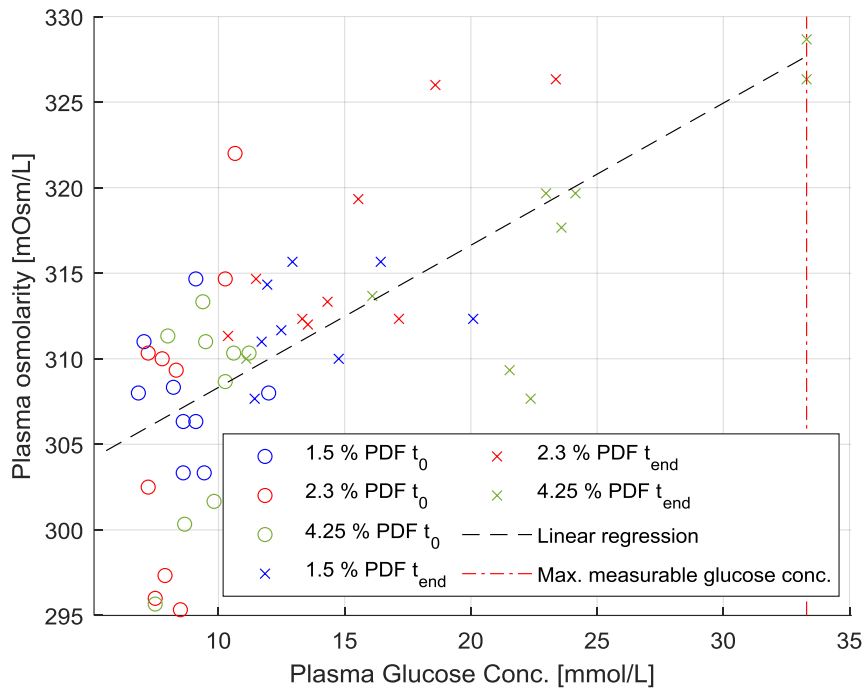


Figure 5-10: Relationship of plasma osmolarity and glucose concentration for the 2nd study phase, respectively for the different dialysates used. Additionally, the resulting linear regression line and the maximum measurable glucose concentration of the glucose meter are shown at the marked red line for 600 mg/dL (33.33 mmol/L).

All values not in the measurable range for the glucose meter for both figures (Figure 5-10 & Figure 5-11) above 600 mg/dL, respectively 33.33 mmol/L, were set to the maximum measurable value for visualization purposes only. For the linear regression and correlation calculation, the values outside the measurable range (maximum measurable glucose concentration: 33.33 mmol/L) at the red line in the figures were excluded.

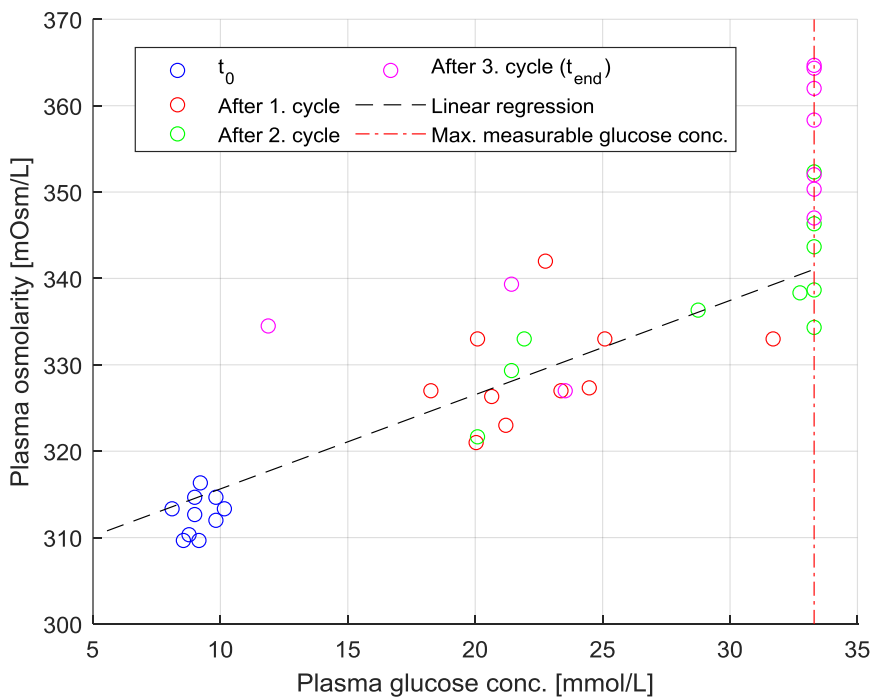


Figure 5-11: Relationship of plasma osmolarity and glucose concentration of the 3rd study phase, respectively before and after the consecutive cycles conducted. Additionally, the resulting linear regression line (black line) and the maximum measurable glucose concentration (red line) by the glucose meter are visualized.

The short dwells of the 3rd study phase accordingly result in a higher glucose load caused by the consecutive cycles with the 4.25 % dialysate after each consecutive cycle performed. The data lead to an obvious positive correlation ($R = 0.83$) between plasma osmolarity and glucose concentration for the 3rd study phase. The results seem to support the hypothesis and the model underlying principles.

The relationship between osmolarity and glucose for later usage needs to account for the offset of osmolarity (Figure 5-11: 304.7 mOsm/L, Figure 5-10: 300 mOsm/L), resulting from the matrix solution, respectively the molecules of the dialysate and plasma (electrolytes, buffers), and eventually effects of other physiological influencing factors. The slope of the linear regression of Figure 5-11 is $1.091 \frac{mOsm/L}{mmol/L}$ and for the Figure 5-10, $0.831 \frac{mOsm/L}{mmol/L}$, respectively, supporting our hypothesis as basis for our simplifications. The transfer between osmolarity and glucose concentration with suitable transfer functions should be feasible.

5.4 Dialysate and plasma osmolarity

During the study phases the drained dialysate and blood plasma osmolarity was measured. The collected dialysate from every drain was measured to get information about the intraperitoneal volume osmolarity. The blood plasma osmolarity was determined before and after every dwell phase. For the 2nd study phase only single cycles with dwells of ~ 200 min and a modified fill scheme were performed with different dialysate's. The 3rd study phase differs due to conducting three consecutive cycles of ~ 60 min with the highest dialysate glucose concentration used. The average blood plasma osmolarity at the start of the experiments was 308 ± 6 mOsm/L. The fresh dialysate osmolarity is specified in the product data sheets, as 358, 401 and 511 mOsm/L, for the dialysate's of 1.5, 2.3 and 4.25 % glucose respectively. The specified osmolarity was crosschecked by measurement of the fresh dialysate with the Osmomat. The difference in the osmolarity of the solutions comes from the different amount of glucose molecules. The matrix solution for all used dialysates is the same (Table 4.2-I). The data presented in this section contain information about the dissipation of osmols, especially glucose through the membrane and the metabolization process of glucose into the blood of the animals.

Single cycle with different dialysate glucose concentration

For the single cycle experiments of study phase 2, the dwells started with a slightly lower osmolarity as the fresh dialysate solution caused by the fast dissipation at the beginning the highest concentration gradient between blood and dialysate is present. The modified fill scheme with filling of 40 mL, drainage of 20 mL and filling of 5 mL again allows for this dissipation. This could be seen in all parts of the 2nd study phase represented in Figure 5-12.

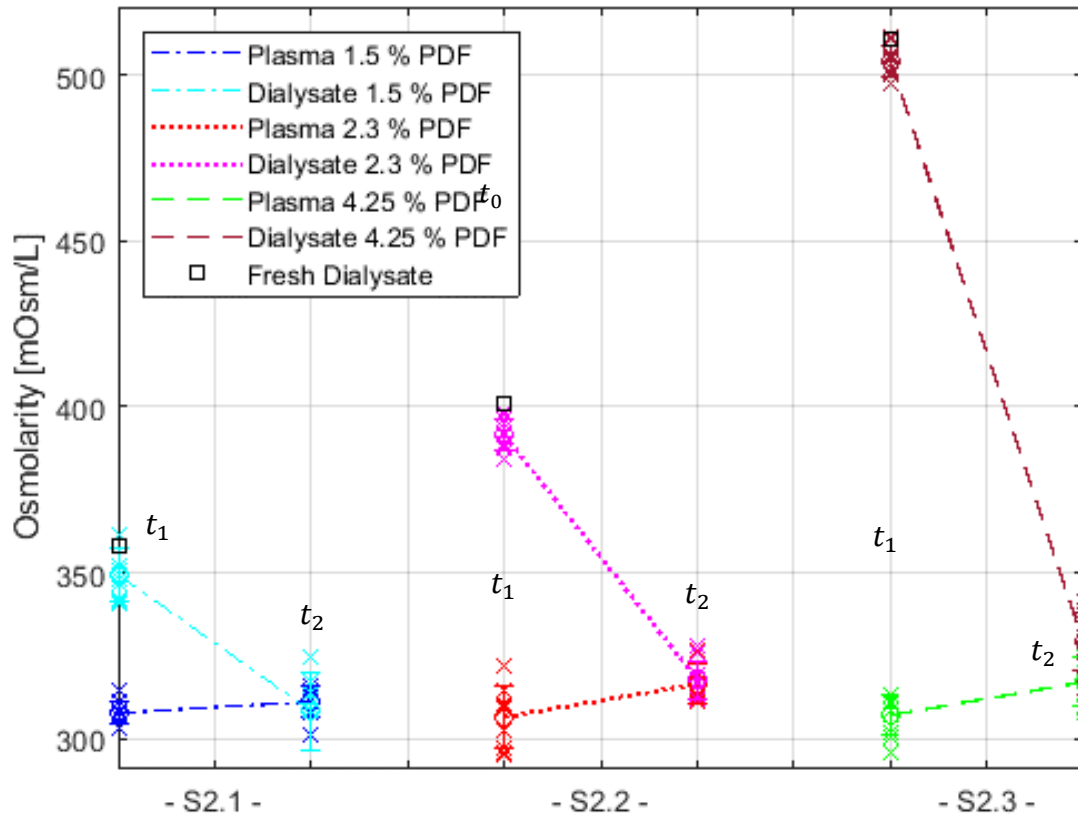


Figure 5-12: Change in osmolarity from the start of the experiment t_0 (black \square), respectively the start of the dwell at t_1 (o) distinguished by the dialysate % used. For all study parts an equilibration of osmolarity between dialysate and blood plasma could be found.

The data could be interpreted to mean that at higher osmolarity, there is a higher gradient or dissipation rate, loading the animals' blood plasma with glucose. However, the glucose is metabolized. The plasma osmolarity would increase at the end of the cycle, since the metabolization rate, although scaled by the glucose blood concentration, is somehow limited.

Three consecutive cycles with high dialysate glucose concentration

For the multicycle experiments, the consecutive cycles (dwells) started with an osmolarity of 511 mOsm/L given by the fresh dialysis solution. At the underlying 3rd study phase no modified fill scheme was used, so the cavity was directly filled up to 25 mL followed by the dwell phase. This fact was used for the 3rd study phase, respectively the consecutive cycles and is represented in Figure 5-13.

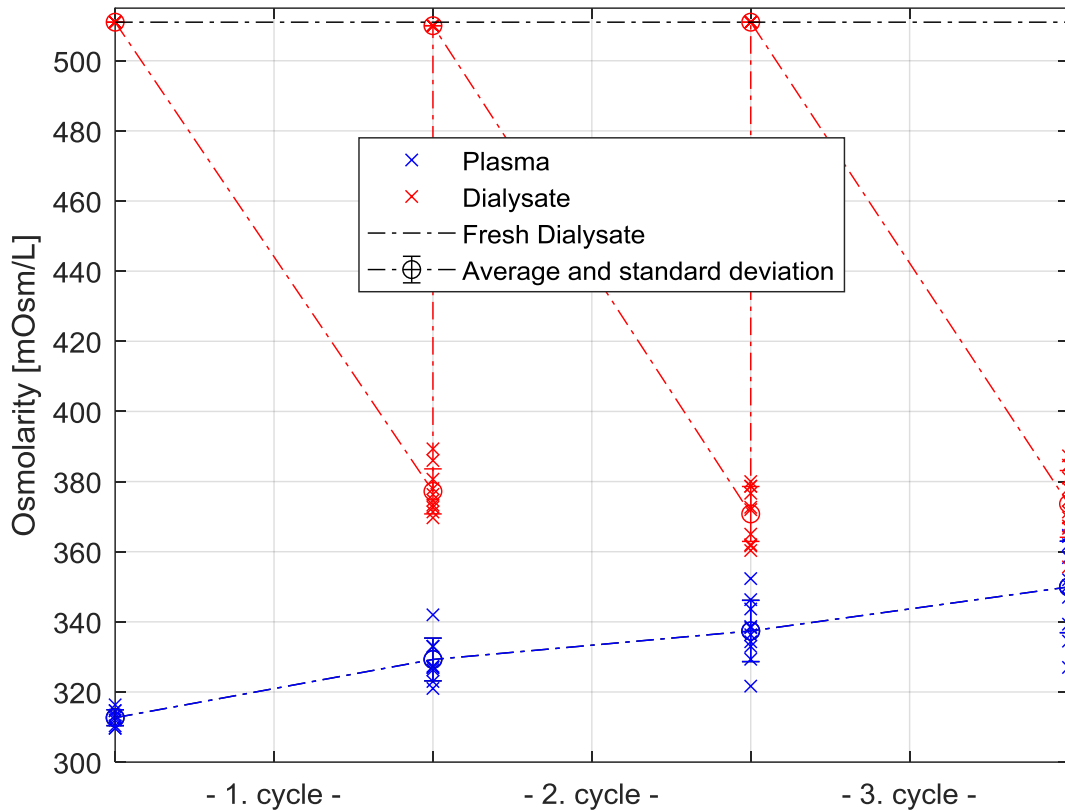


Figure 5-13: Change of the osmolarity from the beginning to the end of the experiment distinguished by the consecutive cycles performed.

Due to the high osmolarity of the dialysate, the high concentration gradient, respectively with fast dissipation, which is loading the animals' blood plasma with glucose, occurred. The glucose gets metabolized as mentioned in the section above. After every cycle the plasma osmolarity increases and the rat gets loaded with glucose, as the metabolization rate is not sufficient to keep the plasma osmolarity, respectively the plasma glucose concentration on steady state. Due to this increase in plasma osmolarity, the osmotic pressure gradient decreases, which is leading to lower UFV's, especially in combination with the lower hydration.

5.5 Osmolarity and UFV dependency

The osmolarity has a direct relationship with the dialysate glucose concentration (same matrix, only glucose concentration differs), which could be used for some simplifications for biophysical models. The results of this investigation as input for the models introduced (Chapter 3:) could be seen in Figure 5-14.

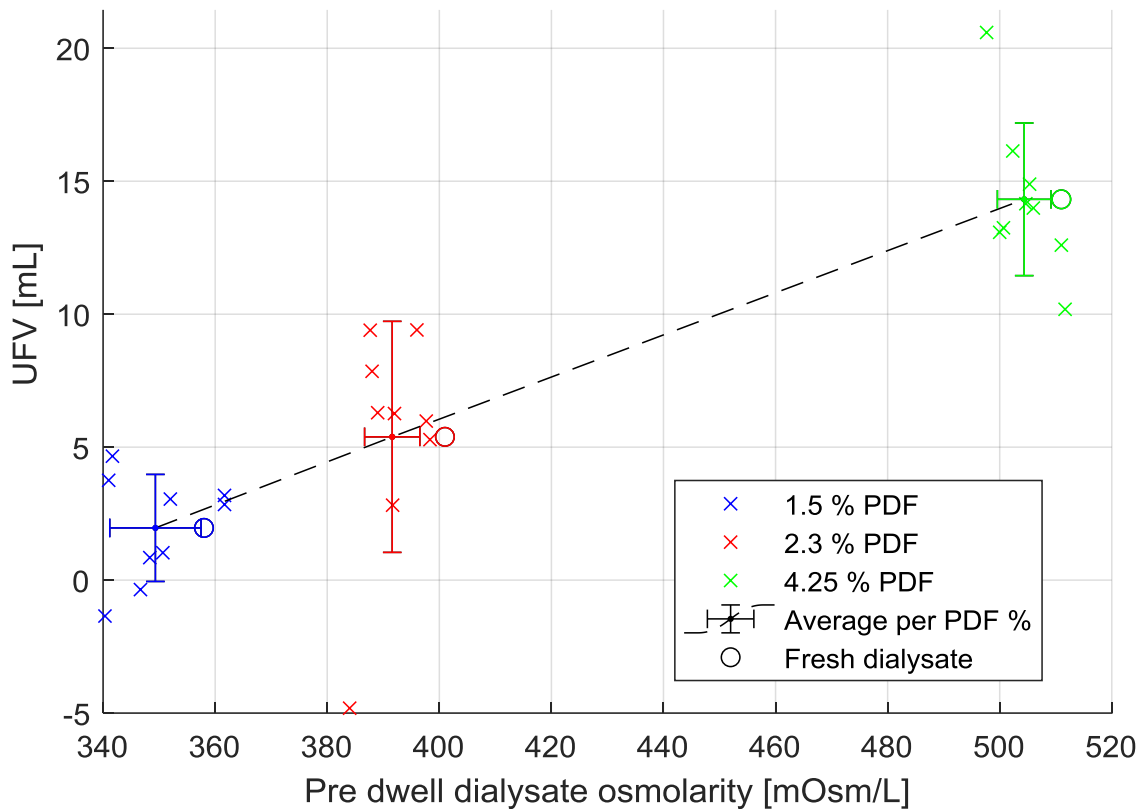


Figure 5-14: The UFV at the end of the dwell phase is obviously correlated ($R = 0.86$, $p < .05$) with the osmolarity measured for the dialysate in the cavity at the beginning of the dwell phase. The individual animals are shown for the different dialysates used against the resulting UFV's (x). Further, the average pre-dwell osmolarity and the average UFV per dialysate used is shown with the corresponding standard deviations (+). As reference, the fresh dialysate osmolarity (fill) for the different dialysate glucose concentrations dialysate's could be found (o).

These results reflect the state of the art, which is the basis for the further investigations made regarding IPP and UFV correlation, dependent on hydration and dialysate used.

5.6 Pressure / Volume - characteristics

The behaviour of the P/V-characteristics was examined in this section (5.3) regarding reproducibility, correlations and interactions with other factors as dialysate % and hydration.

Evaluation of the Pressure / Volume – characteristics

Common to all study phases is the determination of the P/V-characteristics by comparison of volume infused or drained, tracked by weight and the pressure measured inside the catheter line. The cavity was filled stepwise in ~ 5 mL steps, followed by a relaxation time (~15 s), and repeated, till the desired fill volume was reached or the drainage got stopped. As an example, the procedure is explained for the initial fill and drain of a random experiment, but the scheme is applicable to all experiments.

To create the cleaned-up pressure and volume signal, the data need to be processed in the way explained in this section. Both signals are shifted in time, till a consensus of the switching states of the valve occurring and the signals was achieved (Figure 5-15).

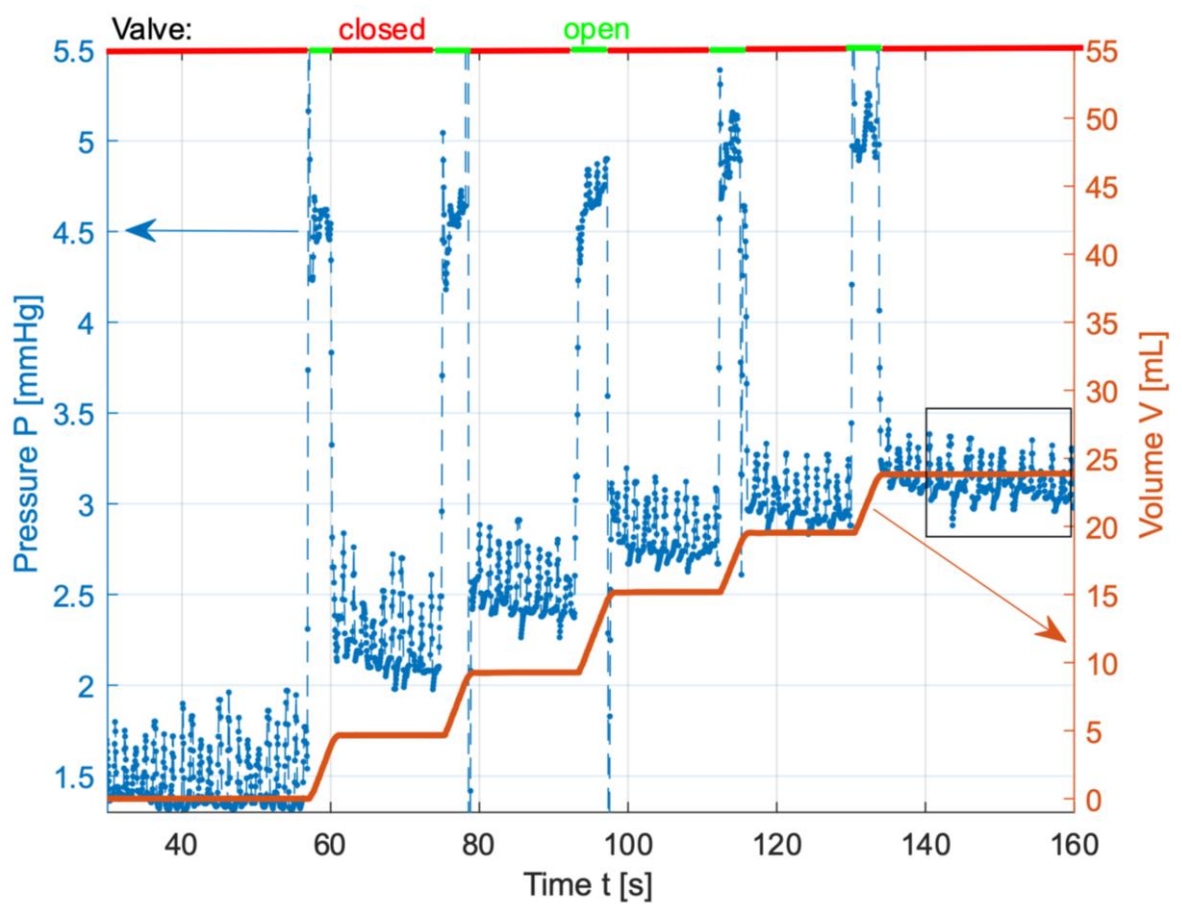


Figure 5-15: Example of the variation in intraperitoneal pressure (IPP) and volume measurements during the stepwise fill procedure (pressure: left axis, dashed blue line; fill volume: right axis, solid red line). A pressure offset that may be observed at zero fill volume arose due to the difference in height between the pressure gauge and the position of the catheter inside the abdominal cavity. A height difference of approx. 1.36 cm corresponds to 1 mmHg resulting from the specific weight of mercury. At each step when the valve was opened to deliver a volume increment during the fill phase, a transient pressure rise to approx. 4.5 to 5 mmHg in magnitude was observed. When the valve was closed, the measured pressure decreased rapidly to a new steady state value, representing the current IPP (3rd study phase).

During the stepwise increase of volume in the peritoneal cavity, if the valve is opened and the fluid flows inside the cavity, the pressure rises accordingly. This pressure change is a combination of the hydrostatic pressure caused by the water column inside the peritoneal cavity and the fill line and the dynamic pressure caused by fluid flow. Obviously, there is a relationship between volume filled to the peritoneal cavity and pressure measured in the catheter line. However, an additional phenomenon occurring is the slight decrease of pressure after the valve is closed during the relaxation time till the next fill step. As an explanation for this behavior the unfolding of the peritoneal cavity walls, a possible muscle relaxation or other physiological and physical influences can be assumed.

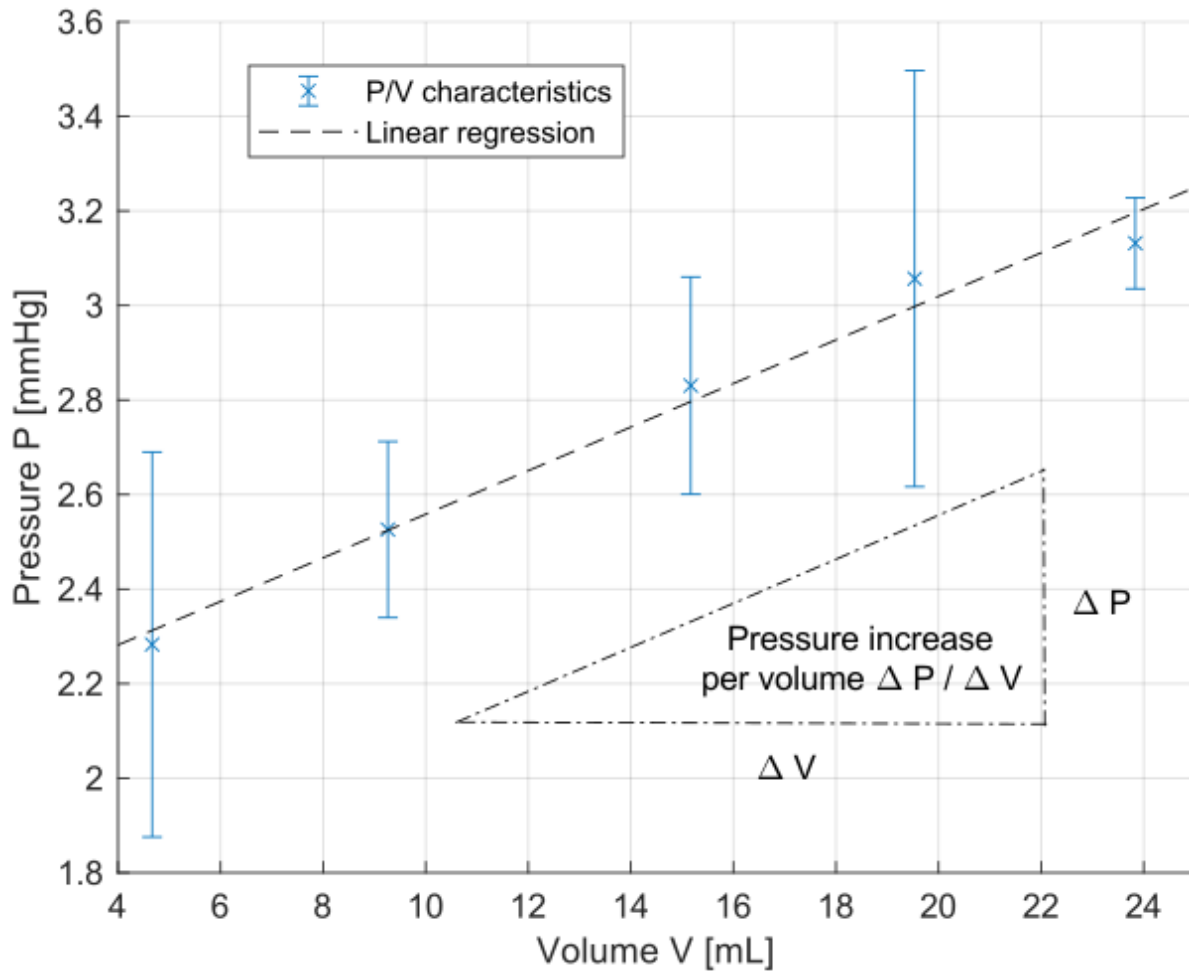


Figure 5-16: Example P/V characteristics for a rat in the linear range below 30 mL. Error bars were estimated from uncertainties in pressure recordings due to respiration. The slope $\kappa = \Delta P / \Delta V$ was determined by linear regression of the P/V characteristics for each rat (3rd study phase).

The simplest possibility to extract the P/V – characteristics from the pre-processed data is the calculation of the mean volume and mean pressure, respectively standard deviation for each of the plateaus, resulting in the P/V characteristics in Figure 5-16.

From the P/V – characteristics, the conclusion was drawn, that there is an obvious dependency between IPP and IPV in the expected range of 0 to 25 mL (3rd study phase), respectively 40 mL (2nd study phase) in our physiological rat model.

The main parameter, which characterizes this relationship of the individual rat, is the slope of the linear regression, which somehow depends on physiological properties like body weight, hydration and maybe others. For further investigations and model evaluations, the data generated by the mean value calculation are used (robust against measuring errors and outliers). The same calculations could be done for the drain phase with only slight differences. Again, both signals are superimposed in time dependent on the state of the valve (Figure 5-17).

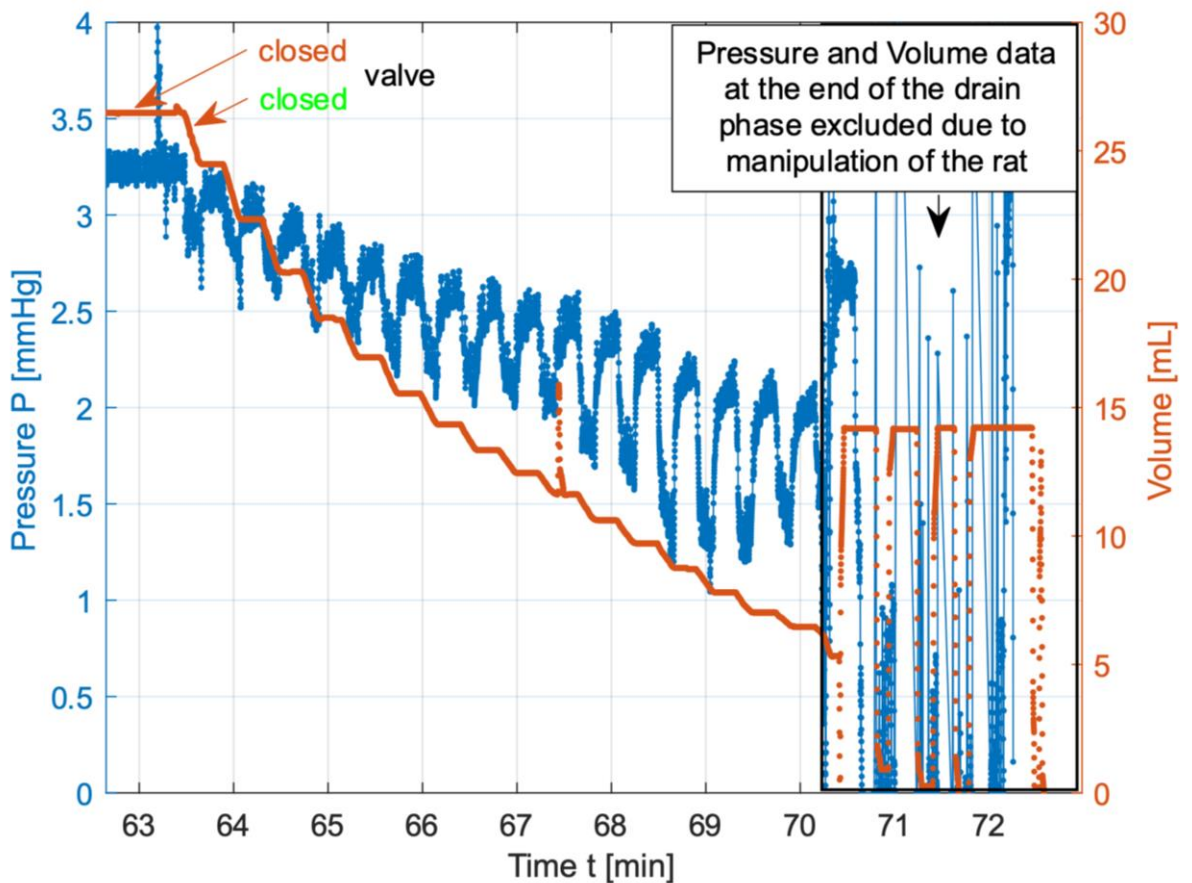


Figure 5-17: Temporal variation in pressure and volume during the drain phase only. Drainage performed in steps by control of the valve. To achieve complete drainage at the end of the drain phase, typically 5 mL of residual volume was removed by manipulating the position of the rat. This led to random fluctuations of pressure and volume (3rd study phase).

During the gradual reduction of the cavity volume, when the valve is open and the liquid flows to the outside, the pressure drops accordingly due to the dynamic negative pressure created by gravity (see Figure 5-17, blue curve). The hydrostatic pressure in the catheter line decreases with the water column height inside the abdomen by drainage. Concluding, there is an obvious relationship between volume drained from the peritoneal cavity and pressure measured in the catheter line, especially at the closed states of the valve.

Hysteresis of the P/V-characteristics

The pressure/volume curves of fill and drain differ from each other. The hysteresis in this system behavior in which the output variable, pressure in this case, does not depend solely on the independent input variable volume, but also on the previous state of the output variable. The system can thus - depending on the previous history - assume one of several possible states for the same input variable. This behavior is also called path dependence. Typical for hysteresis behavior is the occurrence of a hysteresis loop, which is created by moving the causative quantity back and forth between two different states, for the experiments in study phase 2 between 0- and 40-mL cavity volumes. If the data sets of the complete fill and drain cycles and the corresponding P/V characteristic of an individual animal were considered, the curves shown in Figure 5-18 could be generated.

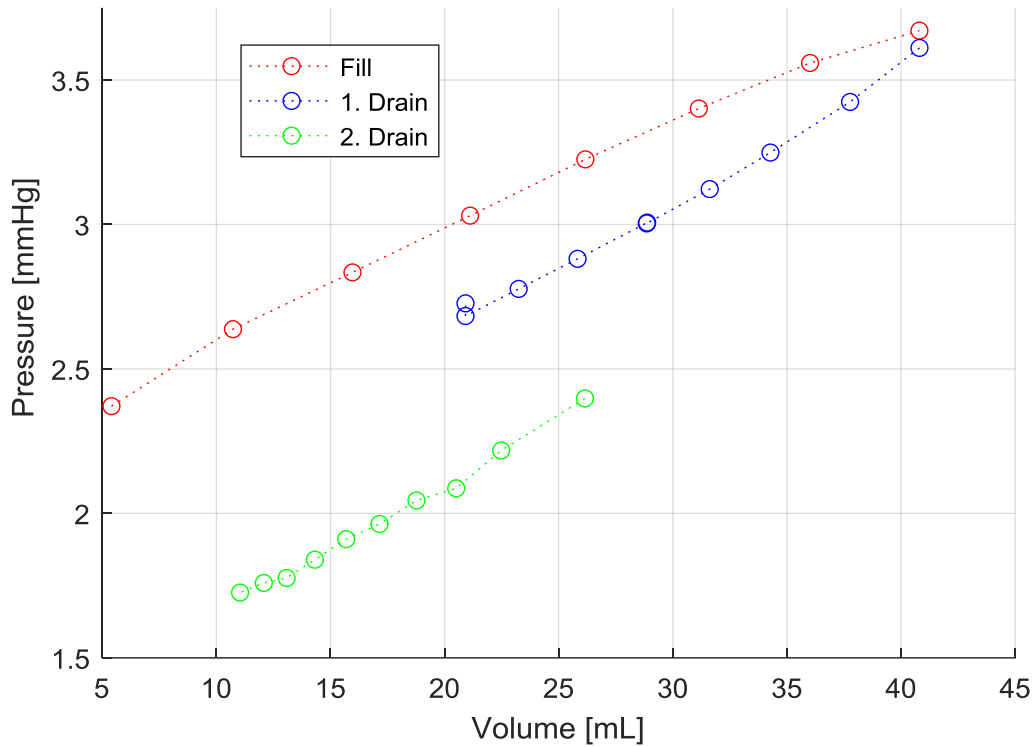


Figure 5-18: Comparison of the P/V-characteristics determined from fill and drain phases and conclusion of occurring hysteresis (2nd study phase).

Due to an offset shift of the green curve (2. drain) to overlap the blue curve would result in the hysteresis loop (Figure 5-19).

In comparison to the hysteresis, the standard deviations, fluctuations from respiration and bowel movements investigated are quiet high.

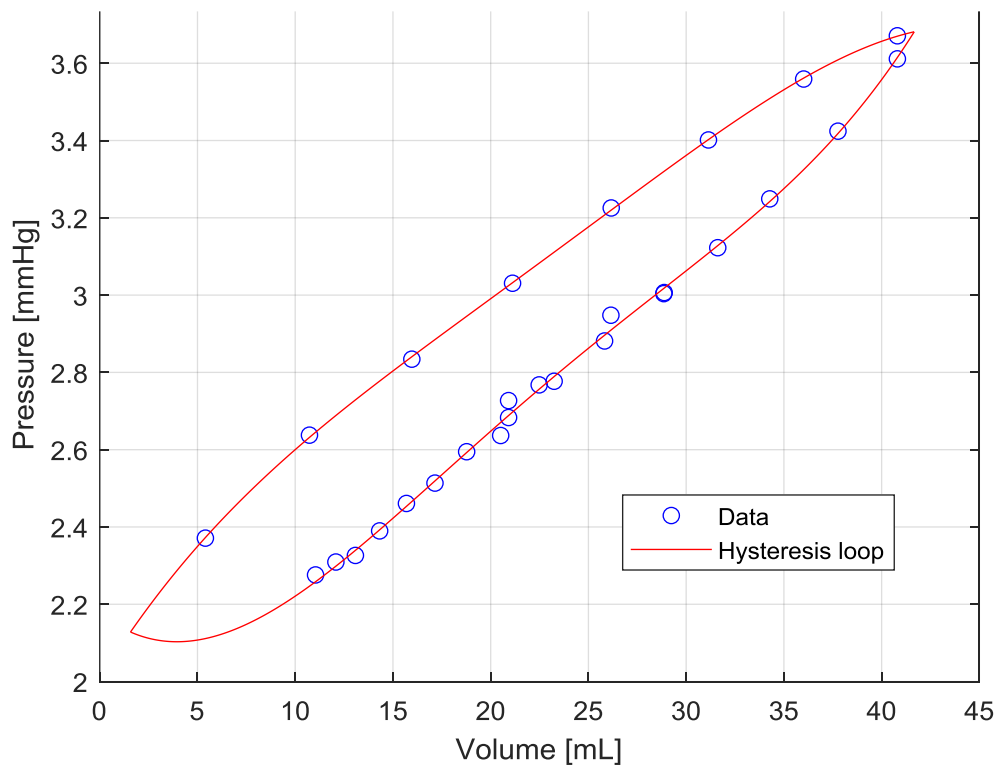


Figure 5-19: Resulting hysteresis loop of the P/V relationship (2nd study phase).

5.7 Calculation of the relative hydration in percent

In each experiment, the weight of the rat was measured before $w(t_0)$ and after the experiment $w(t_3)$, comprising three PD cycles. The difference $w(t_3) - w(t_0)$ was attributed to UFV, insensible losses, and urinary output. No defecation occurred during the experiments. It was assumed that prior to the first cycle, the rat was euvoletic (normally hydrated, $h_0 = 1$), and the initial measured body weight, $w(t_0)$ was regarded as 100 %. The hydration state at the end of the third cycle was determined from weight measurements, calculated as $h_3 = w(t_3)/w(t_0)$. The intermediate hydration states at the end of the 1st and 2nd cycles, were calculated by piecewise linear interpolation, whereby insensible losses were considered as constant over time. At the end of each PD cycle $i = \{1,2,3\}$, the dialysate fill and drain volumes were compared from which the respective UFV was determined. The mean rate of insensible losses over the whole experiment duration t_3 was defined by the difference of the measured individual weight loss $w(t_0) - w(t_3)$ and the sum of UFV_i at the i th cycle:

$$r = \frac{w(t_0) - w(t_3)}{t_3} - \frac{\rho}{t_3} \sum_{i=1}^3 UFV_i$$

Equation 5-2

Therefore, the hydration state after the first cycle was

$$h_1 = 1 - \frac{\rho UFV_1}{w(t_0)} - \frac{r}{w(t_0)} t_1$$

Equation 5-3

the state before the second cycle. The hydration state after the second cycle was

$$h_2 = 1 - \frac{\rho (UFV_1 + UFV_2)}{w(t_0)} - \frac{r}{w(t_0)} t_2$$

Equation 5-4

and after the third cycle

$$h_3 = 1 - \frac{\rho (UFV_1 + UFV_2 + UFV_3)}{w(t_0)} - \frac{r}{w(t_0)} t_3 = \frac{w(t_3)}{w(t_0)}$$

Equation 5-5

Table 5.7-I: Description of the used terms and the corresponding unit.

Term	Description	Unit
h_t	Relative hydration status at the t-th consecutive cycle performed	[%]
$w(t)$	Relative weight at the t-th consecutive cycle performed	[%]

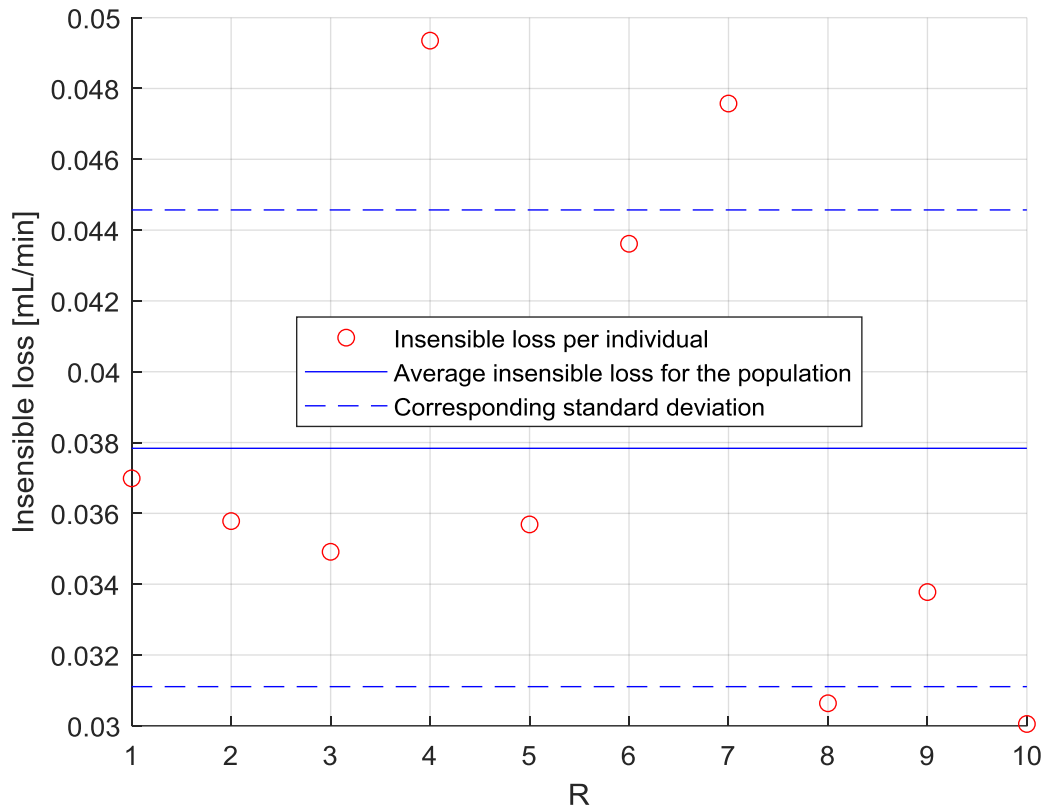


Figure 5-20: Insensible losses and average for the population of rats with standard deviation for S3.

From the calculations above the relative hydration was estimated after each consecutive cycle for the individual rat (Figure 5-21).

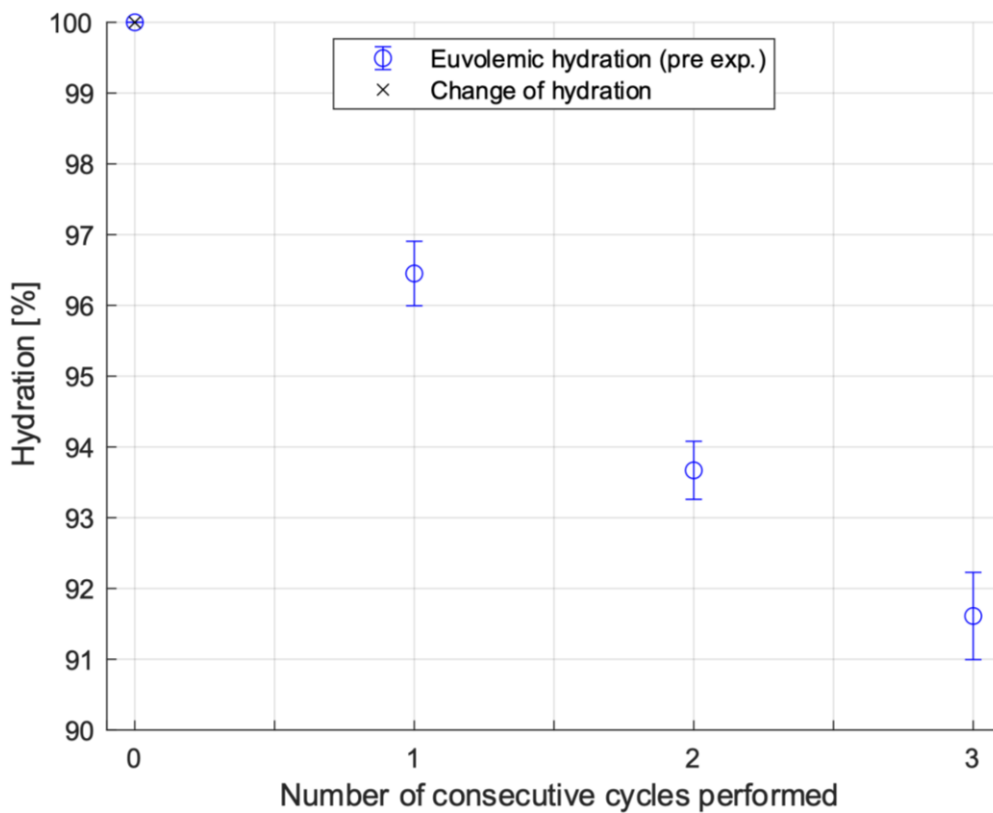


Figure 5-21: Relative hydration over the consecutive cycles performed (S3) for the population of rats with standard deviation.

In addition, the start weight was assumed to be same as a euvoletic state of hydration for each individual animal; respectively 100 % weight equals 100 % hydration because the rats are healthy individuals in euvoletic stage.

Change of the P/V characteristics dependent on dehydration

The relative hydration seems to influence the slope of the P/V relationship.

To investigate this in more detail, the slope for the linear regression from the fill procedure P/V curve of each individual animal was calculated and plotted against the corresponding hydration level (calculated as section 5.7), see Figure 5-22.

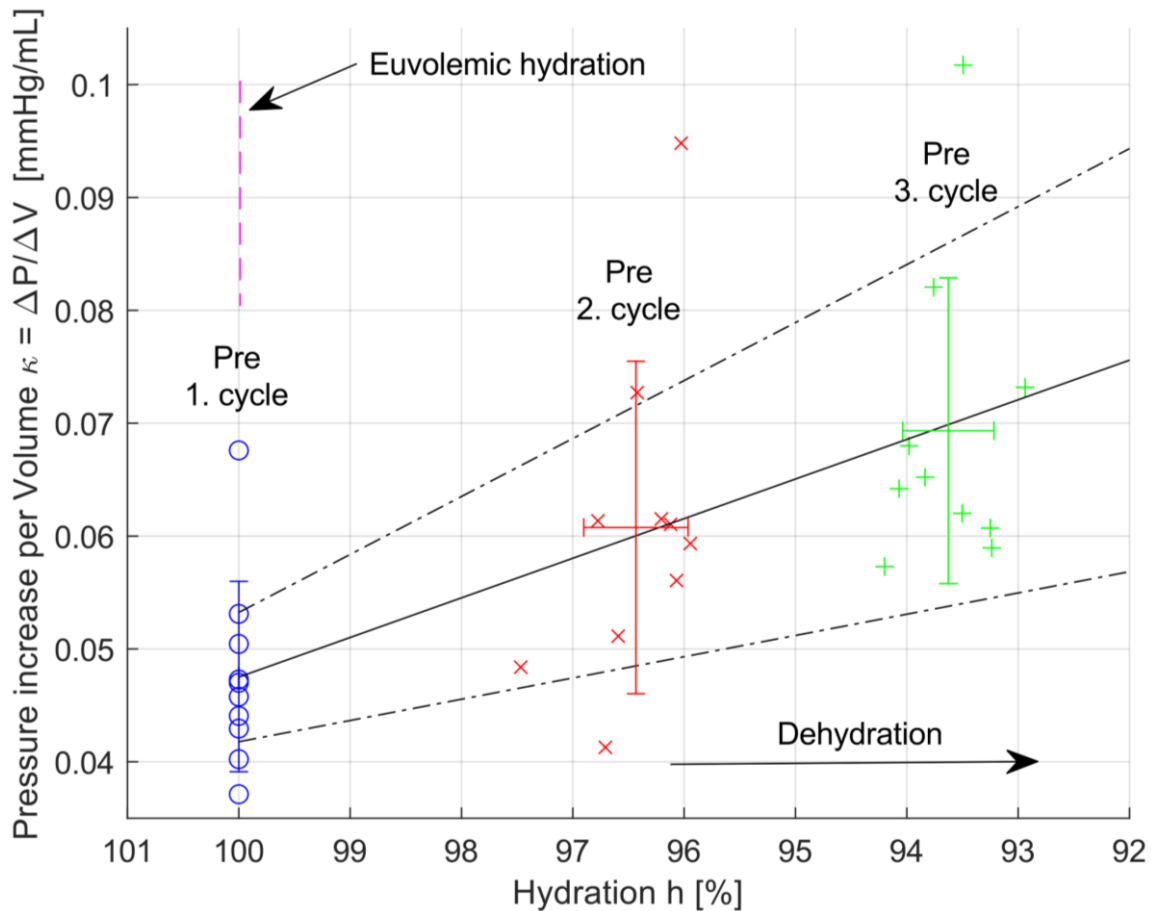


Figure 5-22: Pressure increase per volume as function of the relative hydration status ($R = 0.81$; $p < .01$). The slopes range from 0.037 to 0.102 mmHg/mL. The rats were considered euvoletic at the start of the first cycle. The slope increases with decreasing hydration status, shown as a solid line with $\Delta\kappa/\Delta h = 0.0035$ mmHg/mL/% (95% confidence intervals shown as dotted lines). Error bars reflect the corrected sample standard deviation of hydration and κ .

This behavior could be influenced of the dried out interstitial tissue, which could be stiffer with rising dehydration.

Table 5.7-II: Results of the linear mixed model evaluation regarding the κ and relative hydration relationship.

Parameter name	Estimate	Lower 95 %	Upper 95 %	Random effect (SD)
Intercept	0.0475	0.0418	0.0532	0.0009
Slope	0.0035	0.0018	0.0051	0.0014

We observed a strong association between κ and hydration status and considerable variation between individual animals.

Correlation between UFV and hydration status

The data generated during the 3rd study phase due intentionally dehydration of the rats by the consecutive cycles suggest that there is an obvious relationship between UFV and relative hydration of the individual animal, see Figure 5-23, confirming the hypothesis posted.

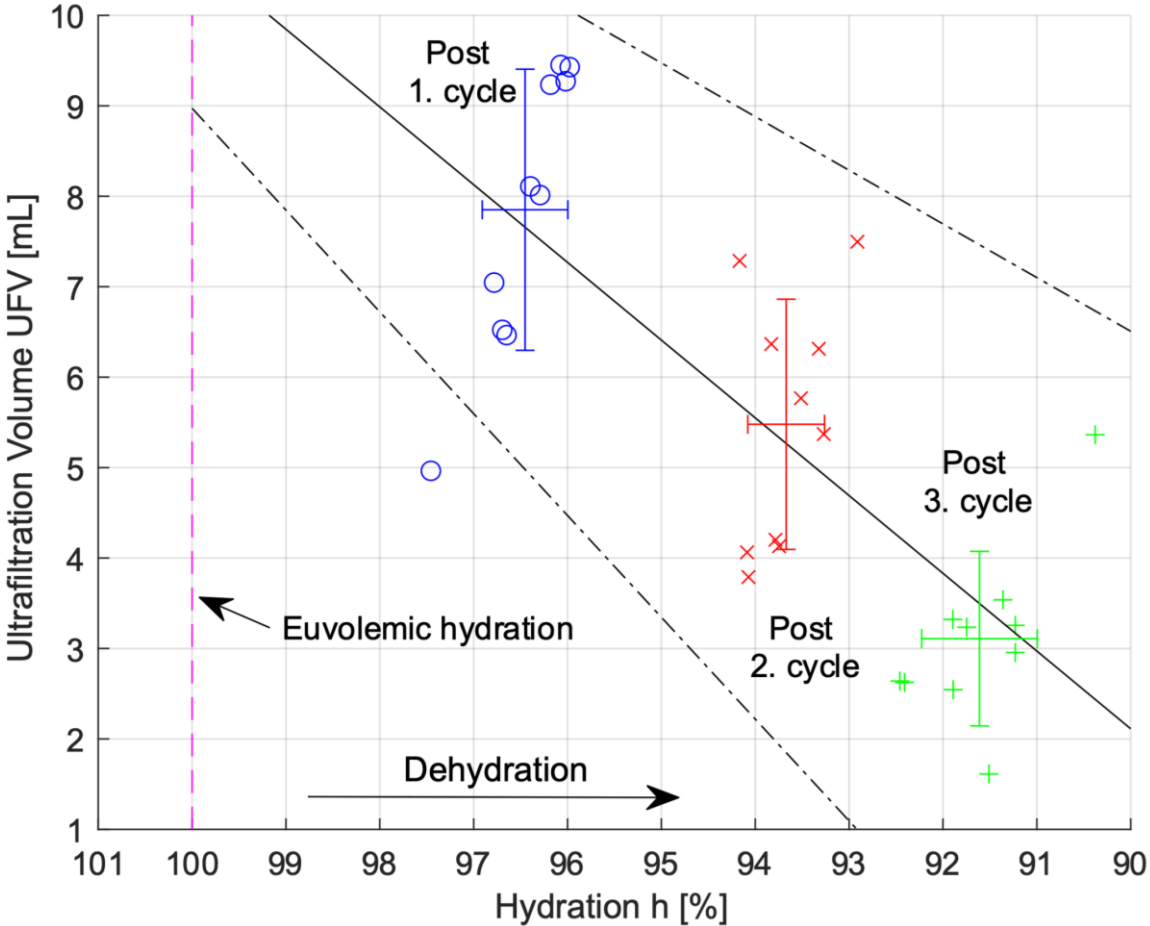


Figure 5-23: Decrease of UFV with increasing dehydration ($R = 0.82$; $p < .01$). The linear mixed effect model regression (straight line) yields a slope of ~ 0.86 mL%. (95% confidence intervals denoted by dotted lines) Error bars reflect the corrected sample standard deviation of the subjects.

To design a patient model, also called ‘Avatar’ (instead of ‘Bvatar’), this input also need to be considered for future models and expert systems (section 7.2).

Table 5.7-III: Results of the linear mixed model evaluation regarding the UFV and relative hydration status.

Parameter name	Estimate	Lower 95 %	Upper 95%	Random effect (SD)
Intercept	10.7	8.97	12.44	0.5
Slope	-0.86	-1.13	-0.59	0.027

Our results indicate a strong influence of hydration on the magnitude of the UFV, but there is considerable variation between animals.

5.8 Relationship of IPP and UFV during the dwell

Common to the study phases are the various dwells, resulting in an increase of intraperitoneal cavity volume, respectively UFV and the corresponding intraperitoneal pressure increase. From the data measured, the UFV and the increase in IPP during the dwell time could be calculated, representing the changes in IPP from the start of the dwell till the end of the dwell. These results could be used to get an impression of how good the IPV could be visualized real time during the treatment by measurements of the IPP. This could be an immense contribution to improve the PD treatment of patients today by measuring the pressure with an APD cyler in the catheter line during each treatment and simply plot IPP and IPV calculated from the P/V transfer function on the device or by a MSA.

Δ IPP and UFV for different dialysate glucose concentrations

Due to the different dialysate osmolarity, respectively glucose concentrations used for the second study phase, the relative UFV's are received as seen in Figure 5-14. The UFV's reached dependent on the dialysate osmolarity and the corresponding pressure change over the dwell are shown in Figure 5-24.

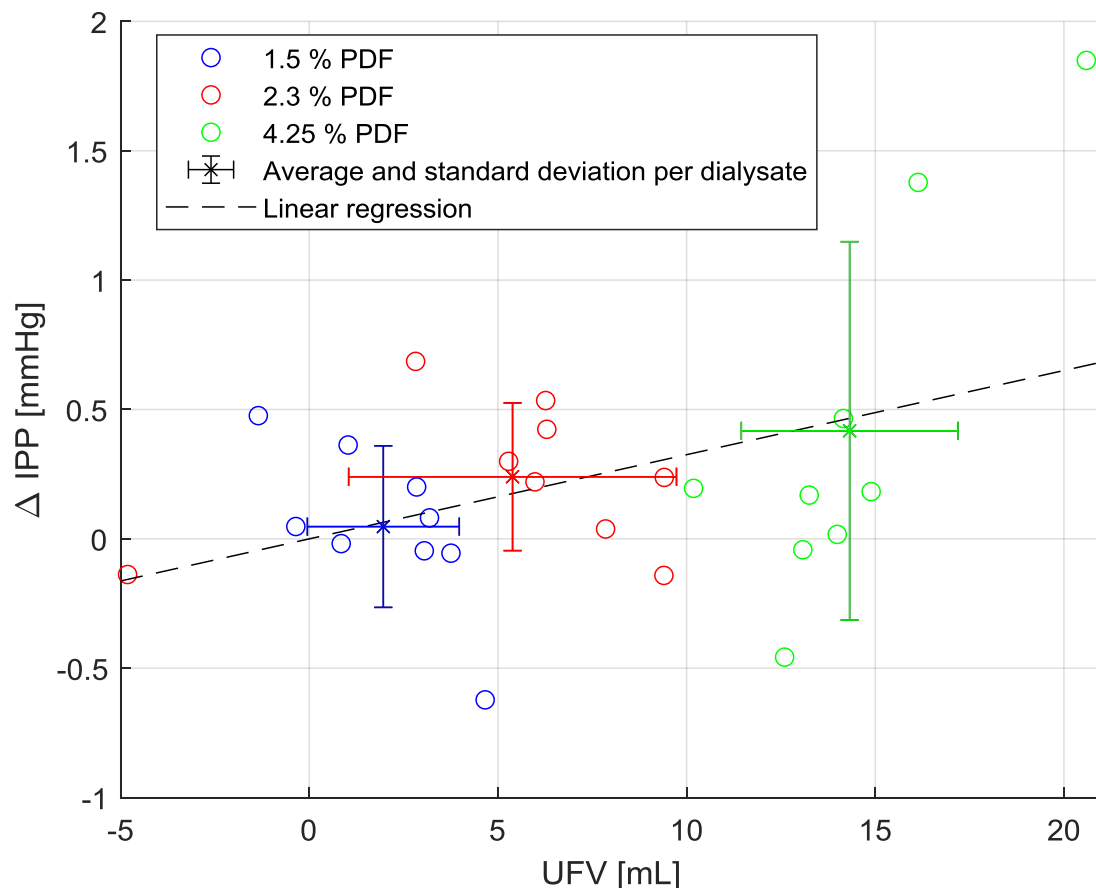


Figure 5-24: Measured pressure change in mmHg against UFV for the dwell phase in mL shown for each individual rat (o). The dialysate is represented by different colors, respectively blue for the 1.5%, red for the 2.3% and green for the 4.25% dialysate. Means and standard deviations (+) and the linear regression are added (---).

From the 2nd study phase an obvious but only low linear correlation ($R = 0.41$, $p = .036$) could be identified.

resulting in more accurate results assuming comparable resolution and standard deviation as for the animal study.

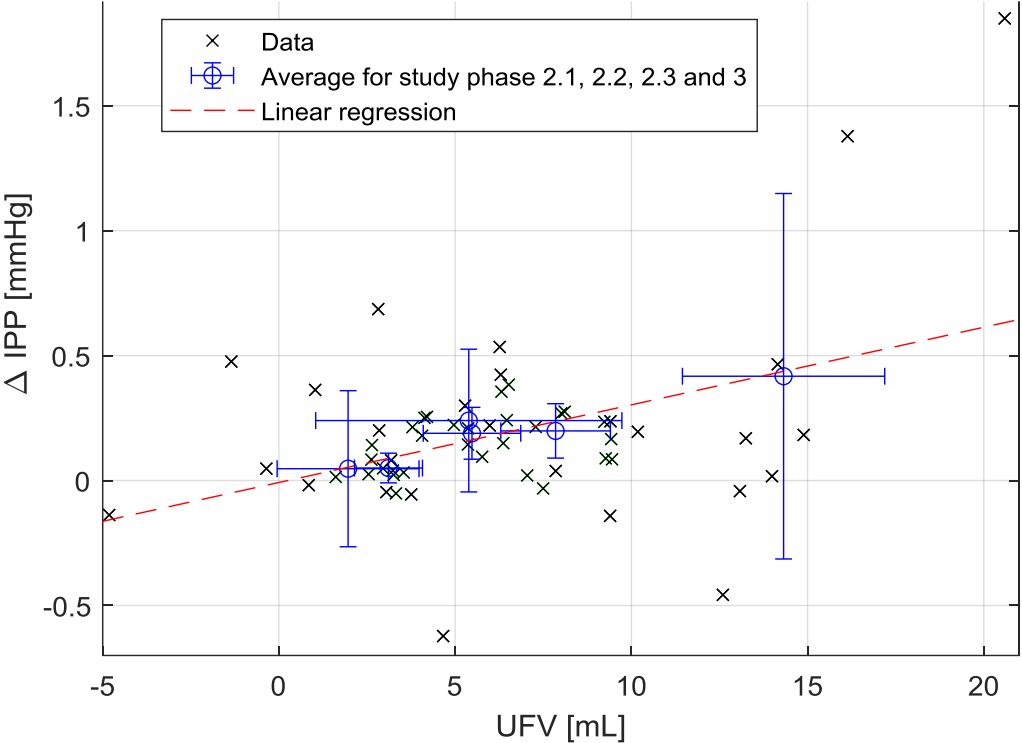


Figure 5-26: Measured pressure change in mmHg against the UFV at the end of the dwell in mL is shown for each individual rat (x) and (+) for the means with standard deviations respectively the different dialysate %'s or consecutive cycles performed. Additionally, the linear regression line is added (---).

From the 2nd and 3rd study phase data, contemplated together, a low linear correlation ($R = 0.41$, $p = .002$) could be identified. The fill and drain P/V relationships slopes and offsets for the 2nd study phase show no correlation with the dialysate % used. In contrast as shown in Figure 5-22 the P/V relationship slopes of the fill procedure of the 3rd study phase obviously correlates with the relative hydration of the rats, but also no relationship of the hydration and the offsets could be found. Also, for the corresponding drain P/V curves, no obvious correlation could be observed between slopes or offsets of the linear P/V behavior and the hydration. The averages for the P/V characteristics determined from the various datasets are transferred to the Table 5.8-I. Additionally, the linear regression parameters (slopes) of this section 5.8 are added to the table. The resolution/slope of all P/V curves of the study is in a comparable order of magnitude.

Table 5.8-I: Slope of the linear regression of the P/V characteristics for the different study phases and cycles measured.

Study phase	Slope of the linear regression [mmHg/mL]
Fill S2 (S2.1, S2.2, S2.3)	0.038
Drain S2 (S2.1, S2.2, S2.3)	0.035
Fill S3 1. cycle	0.048
Fill S3 2. cycle	0.061
Fill S3 3. cycle	0.069
Drain S3	0.056
Dwell S2	0.033

For further investigations the P/V relationship is needed, the parameters from the linear fit to the dwell data of S2 and S3 (Figure 5-26) is used for transferring from IPP to IPV and vice versa. With these parameters, from the pressure increase during the dwell time caused by UFV, we can directly calculate the theoretically UFV occurring inside the peritoneal cavity by simply rearranging the linear regression Equation 3-9.

$$(V^{PC}(t_{end}) - V_0^{PC}) = \frac{P_{Hy}^{PC}(V_{PC}(t_{end})) - P_0^{PC}}{\gamma}$$

Equation 5-6

In this Equation 5-6, the P_0^{PC} is the offset of the linear regression and γ is representing the slope respectively. The intraperitoneal pressure measured at the end of the dwell phase correlating to the cavity volume at the end of the dwell inside the cavity was declared as $P_{Hy}^{PC}(V_{PC}(t_{end}))$, respectively this is specific for the individual as for the population of rats. The resulting volume difference inside the peritoneal cavity ($V^{PC}(t_{end}) - V_0^{PC}$) is the UFV at the end of the dwell, calculated from the IPP, shown on the y-axis in Figure 5-27. This calculated UFV is in this figure compared to the measured UFV resulting from the drain procedure and simply subtracting the fill volume from the drained volume. The blue line is drawn as an angle bisector to show how it would look like, if perfect transfer function accuracy could be achieved in comparison (Figure 5-27) to the data collected.

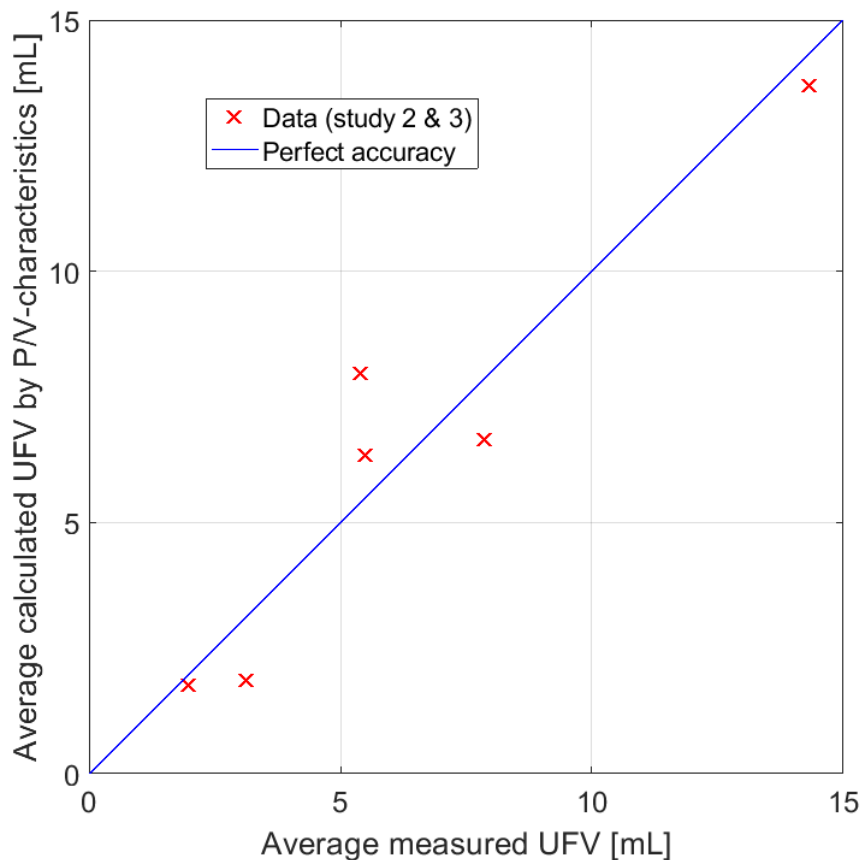


Figure 5-27: Calculated average UFV from the measured IPP from the P/V relationship for the population of rats from the different study phases and segments compared to the average measured UFV at the drain (x) and as a reference an angle bisector (-) to visualize the result of a perfect transfer function accuracy.

5.9 Pressure change during the dwell for different dialysates and corresponding volume estimated from the P/V characteristics

The continuous intraperitoneal pressure measurements of the second study phase during the dwell combined with the corresponding P/V transfer function enables the calculation of intraperitoneal volume, respectively UFV over time for the different dialysates used on basis of the IPP measured in the catheter line.

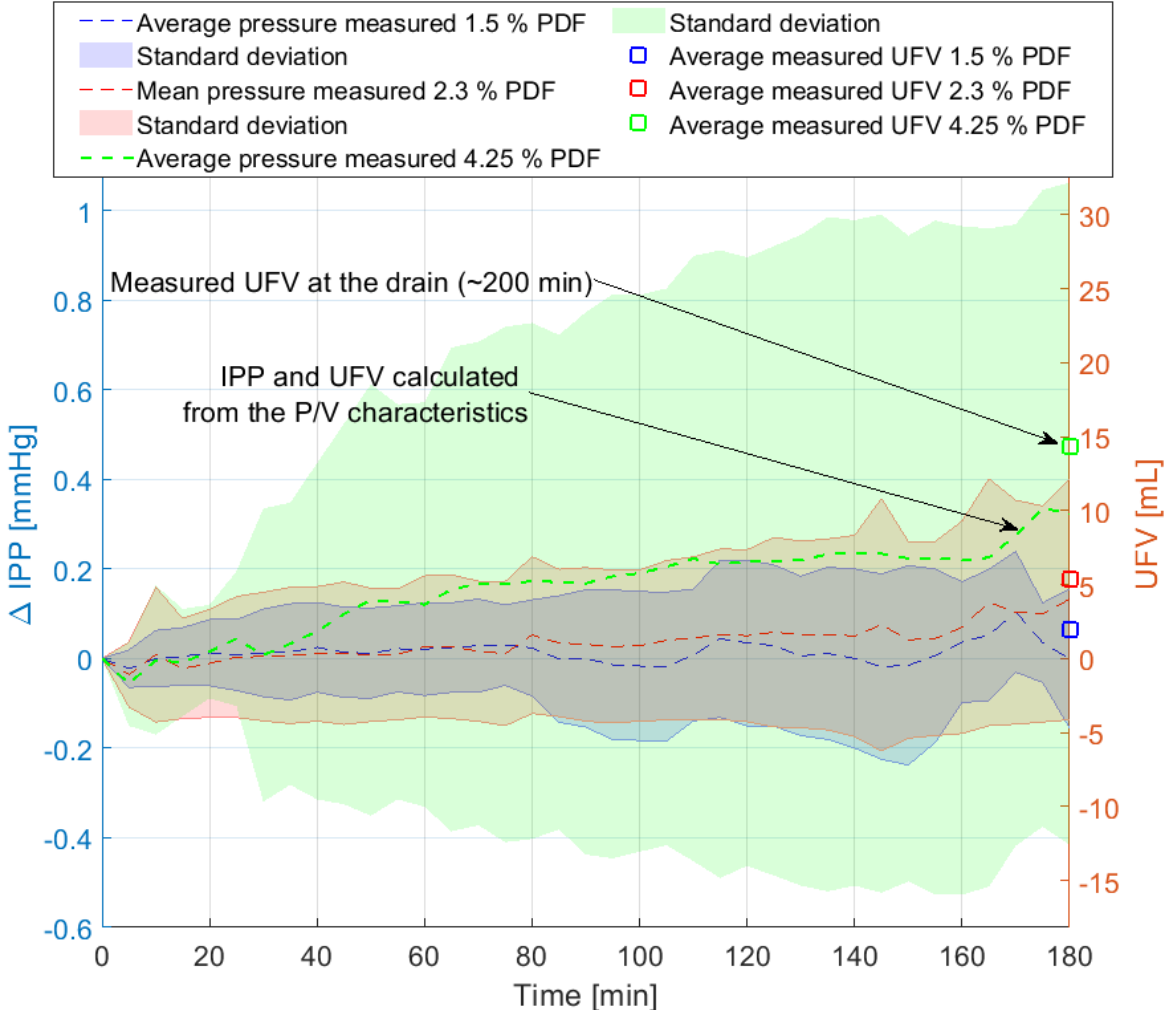


Figure 5-28: The intraperitoneal pressure, respectively the calculated UFV based on IPP as average for the dialysates used over time are shown. The corresponding standard deviations between individuals are also included. The P/V-characteristics (Table 5.8-I) of the second study phase (dwell) were used. Additionally, the measured UFV at the end of the experiment as averages for the various dialysates used are marked (□).

These data are used further in the following Chapter 6: for a first evaluation and test of the model approaches introduced.

Chapter 6: Comparison of the experimental results to the model approaches

In this chapter the model applications explained in Chapter 3: are applied to the data generated by the study in a general and simple fashion, considering the model concepts introduced. However, also the biophysical model could be further improved by adding for example the hydration level to the differential equations system or to the P/V characteristics and further taking additional compartments like blood plasma or interstitium into account.

6.1 Empirical model using the experimental data obtained

For the empirical model evaluation, the MATLAB Regression Learner toolbox was used (Version 2021a Update 2) for model evaluation. For the parameter identification and optimization, the whole set of measured data was used as starting point. Therefore, the dialysate osmolarity, just like plasma osmolarity and glucose concentration, before and after the dwells, IPP changes and residual volumes, dwell times and urine outputs were considered [16].

Osmolarity (2nd study phase)

The second study phase delivers a matrix with data of size 27 x 11 including the 11 variables (27 experiments), especially as 10 predictor variables, the dialysate osmolarity pre and post dwell, same as plasma osmolarity and glucose concentration, IPP change during the dwell, residual volume, and urine output at the end of, respectively during the experiment and of course the response variable UFV. First just a linear regression was made using all variables. An effect, or main effect, of a predictor represents an effect of one predictor on the response from changing the predictor value while averaging out the effects of the other predictors. From this step, the influence of our various predictor variables could be investigated. However, in most cases it is reasonable to take the dependencies of these variables with each other into account (Chapter 5:) to reduce the dimensionality by redundant information sitting inside these dependencies. To do this, the regression learner was used to find the minimum set of predictor variables and the linear model suitable for this data set. Moreover, the cross validation was used to avoid over fitting.

The variable sets with major influence for determination of the model parameters could be reduced to 2 predictor variables and identified as pre dwell dialysate osmolarity and residual volume for the second study phase. Thus, the linear regression model generated delivers a good predictive capability for the UFV shown in Figure 6-1.

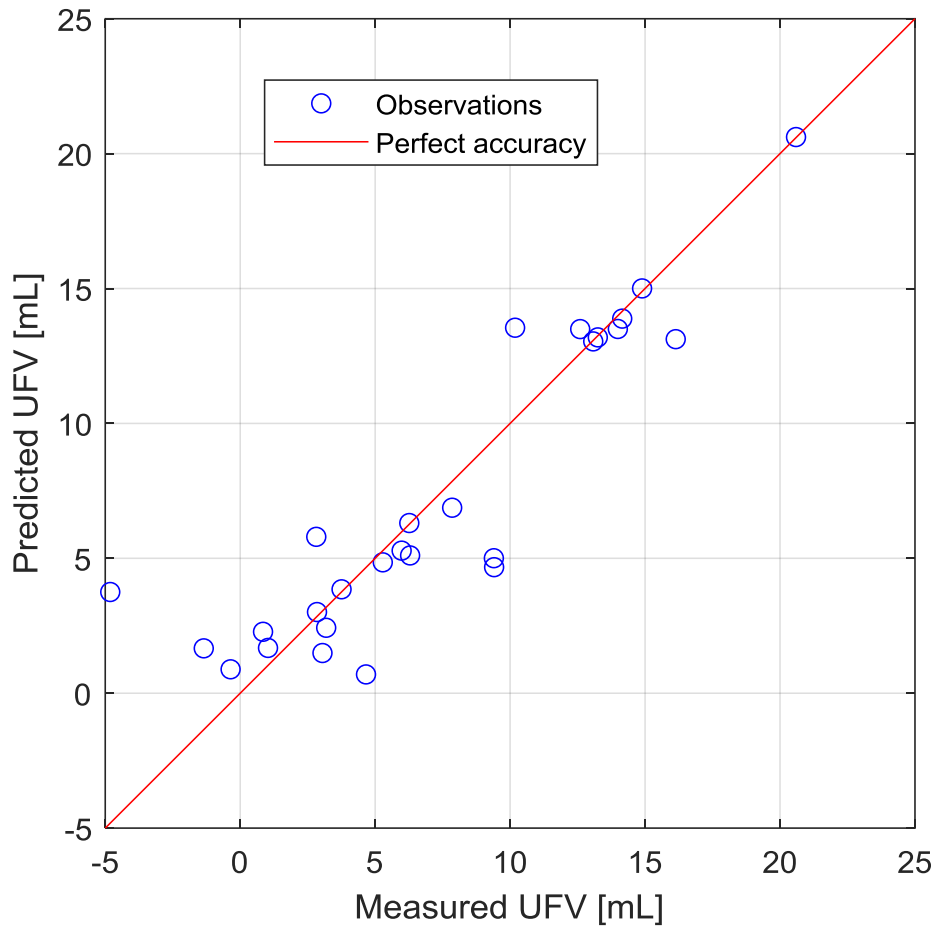


Figure 6-1: Prediction accuracy of the linear model showing observations and perfect prediction, comparing the true response against the predicted response (R-squared: 0.82)

For visualization the following 3D plot (Figure 6-2) dependent on the predictor variables which have the highest main effects on the response variable, respectively pre dwell dialysate osmolarity and residual volume, are used.

Accordingly, the linear regression model could be described by Equation 6-1, as

$$V_{UF_{measured}}(t_{end}) = a + b C_{Osm}^{PC}(t_1) + c V_{Res}(t_{end})$$

Equation 6-1

by usage of the estimated coefficients shown in Table 6.1-I.

Table 6.1-I: Estimated values of the Equation 6-1 coefficients with the affiliated term.

Coefficients	Affiliation	Estimate	Unit
a (Intercept)	Error term/Offset	-25.715	[mL]
b	$C_{Osm}^{PC}(t_1)$	0.077	[mL / mOsm/L]
c	$V_{Res}(t_{end})$	0.972	[-]

Using these equations with the suitable coefficients, the contour plot (Figure 6-2) could be created, comparing the input data from the studies, pronounced as designed experiments and the predicted UFV from the linear regression model, resulting in a usable predictive capability.

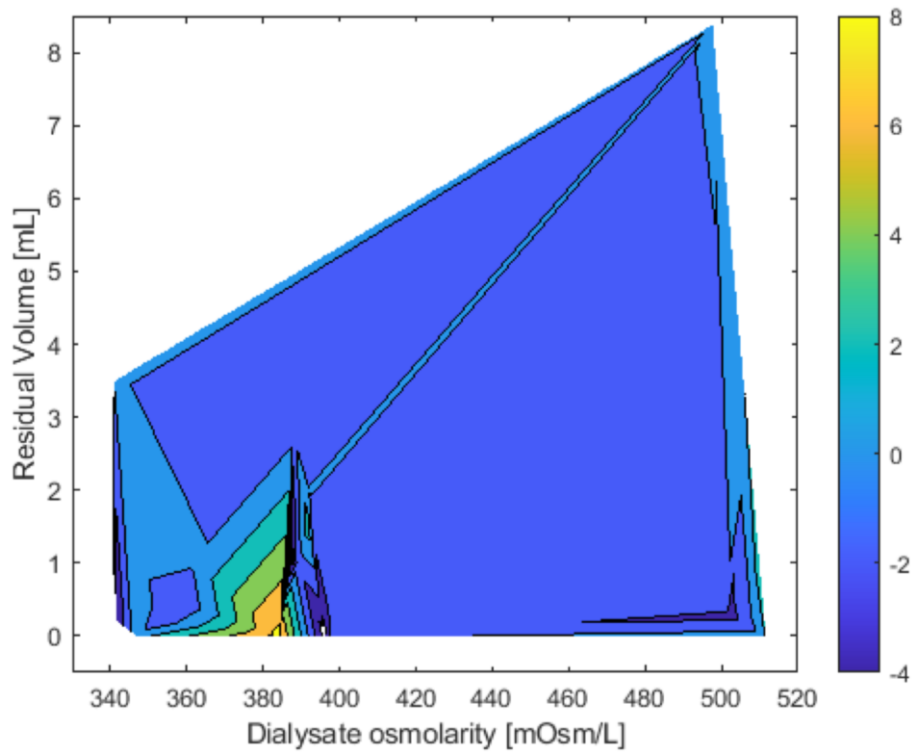


Figure 6-2: Comparison of data generated from the designed experiments (rat exp.) and the predicted response from the linear model based on the residual volume and pre dwell dialysate osmolarity.

Hydration (3rd study phase)

The third study phase results in a matrix with data of size 30 x 8 including the 8 variables (10 experiments with 3 cycles each), especially as 7 predictor variables: the relative hydration, the dialysate osmolarity post dwell, same as plasma osmolarity and glucose concentration, IPP change during the dwell, cycle time and of course the response variable UFV.

The variable sets with major influence for determination of the model parameters could be identified as relative hydration and plasma glucose concentration pre-dwell for the third study phase. Thus, the linear regression model generated delivers a moderate predictive capability for the UFV shown in Figure 6-3.

Accordingly, the linear regression model could be described by Equation 6-2, as

$$V_{UF_{measured}}(t_{end}) = a + b RH(t_2) + c C_{Glucose}^{Plasma}(t_0)$$

Equation 6-2

by usage of the estimated coefficients shown in Table 6.1-II.

Table 6.1-II: Estimated values of the Equation 6-2 coefficients with the affiliated term.

Coefficients	Affiliation	Estimate	Unit
a (Intercept)	Error term/Offset	-4.905	[mL]
b	$RH(t_{end})$	0.149	[mL/%]
c	$C_{Glucose}^{Plasma}(t_0)$	-0.01	[mL / mOsm/L]

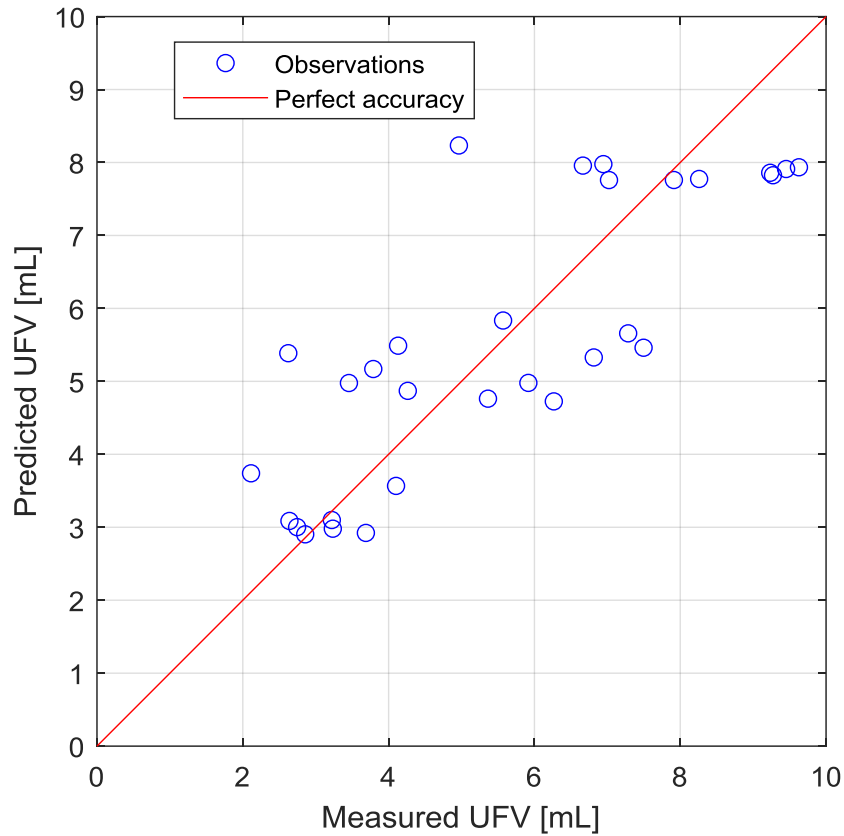


Figure 6-3: Prediction accuracy of the linear model showing observations and perfect prediction, comparing the true response against the predicted response (R -squared: 0.66).

For further visualization, again the 2 main effects are used to create the contour plot (Figure 6-4) dependent on the predictor variables, which have the highest main effects on the response variable, respectively relative hydration, and plasma glucose concentration pre-dwell.

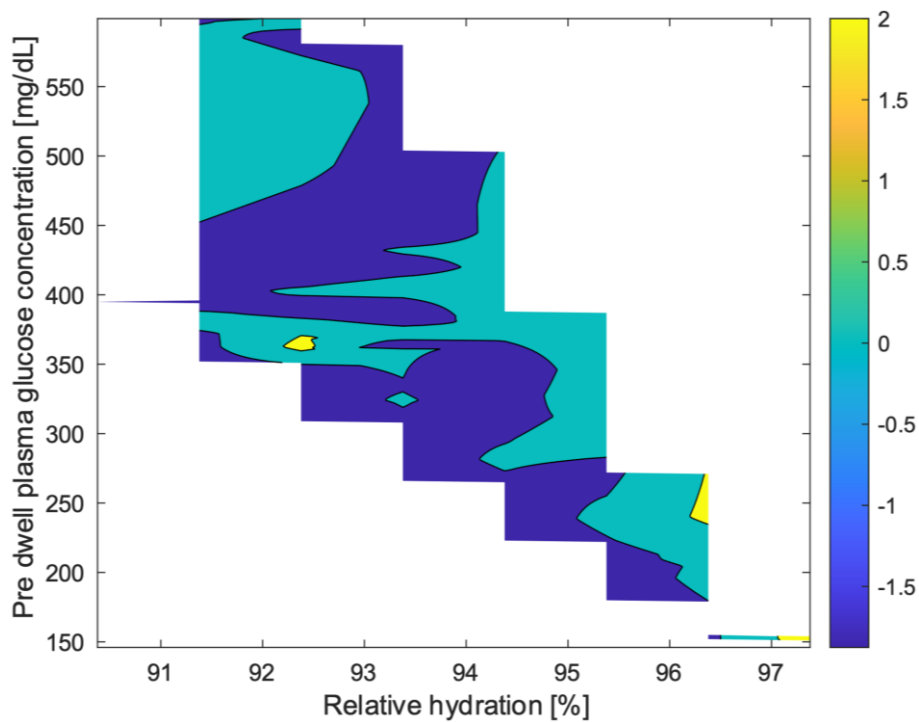


Figure 6-4: Data generated from the designed experiments (rat exp.) and the predicted response from the linear model based on the relative hydration and pre dwell plasma glucose concentration.

Using the Equation 6-2 with the suitable coefficients of Table 6.1-II, the 3D plot (Figure 6-4) could be created, comparing the measured and the predicted UFV from the linear regression model, resulting in a moderate predictive capability.

Combinations (2nd & 3rd study phase)

Linear model:

If finally, the second and third study phase's results are together packed into a matrix with data of size 57 x 8 including the 8 variables and a linear regression as for the previous models was made using all common variables for both study phases.

$$V_{UF_{measured}}(t_{end}) = a + b C_{Osm}^{PC}(t_1) + c P_{Meas}^{PC}(t_2) + d C_{Osm}^{Plasma}(t_1) + e C_{Osm}^{Plasma}(t_2) + f C_{Glucose}^{Plasma}(t_1) + g ResVol + h t_{dwell} + i UrinVol$$

Equation 6-3

by usage of the estimated coefficients shown in Table 6.1-III.

Table 6.1-III: Estimated values of the Equation 6-3 coefficients with the affiliated term.

Coefficients	Affiliation	Estimate	Unit
a (Intercept)	Error term/Offset	18.935	[mL]
b	$C_{Osm}^{PC}(t_1)$	0.076	[mL / mOsm/L]
c	$P_{Meas}^{PC}(t_2)$	0.415	[mL / mmHg]
d	$C_{Osm}^{Plasma}(t_1)$	-0.038	[mL / mOsm/L]
e	$C_{Osm}^{Plasma}(t_2)$	-0.076	[mL / mOsm/L]
f	$C_{Glucose}^{Plasma}(t_1)$	-0.002	[mL / mOsm/L]
g	<i>ResVol</i>	0.977	[-]
h	t_{dwell}	-0.043	[mL / min]
i	<i>UrinVol</i>	11.63	[-]

Also, for this model a useful predictive capability could be generated for the rat population, in dependence on the main influencing factors shown in Table 6.1-III and Equation 6-3.

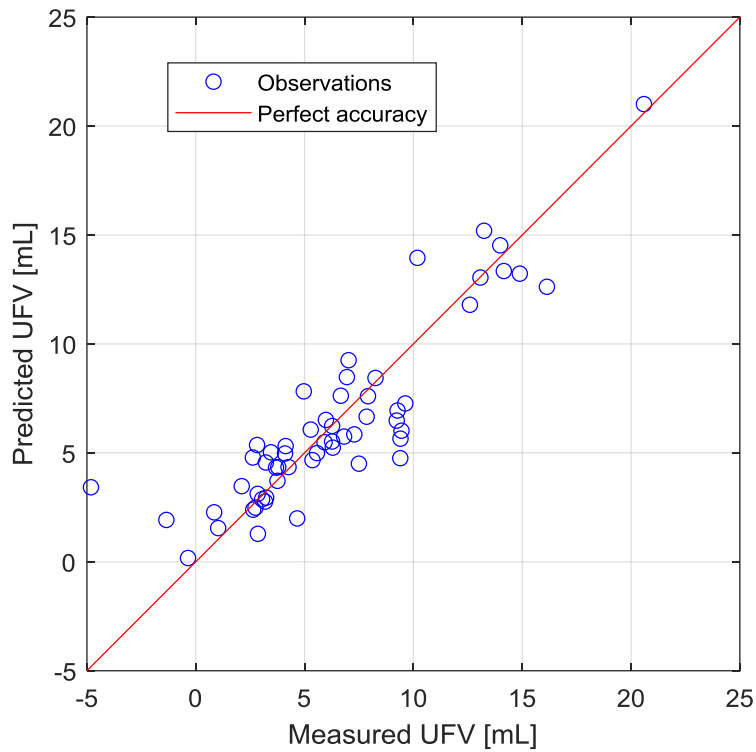


Figure 6-5: Prediction accuracy of the linear model showing observations and perfect prediction, comparing the true response against the predicted response (R-squared: 0.79).

Linear model with interactions:

For comparison and completeness the same was done with the linear model with interactions approach and the results are visualized in Figure 6-6.

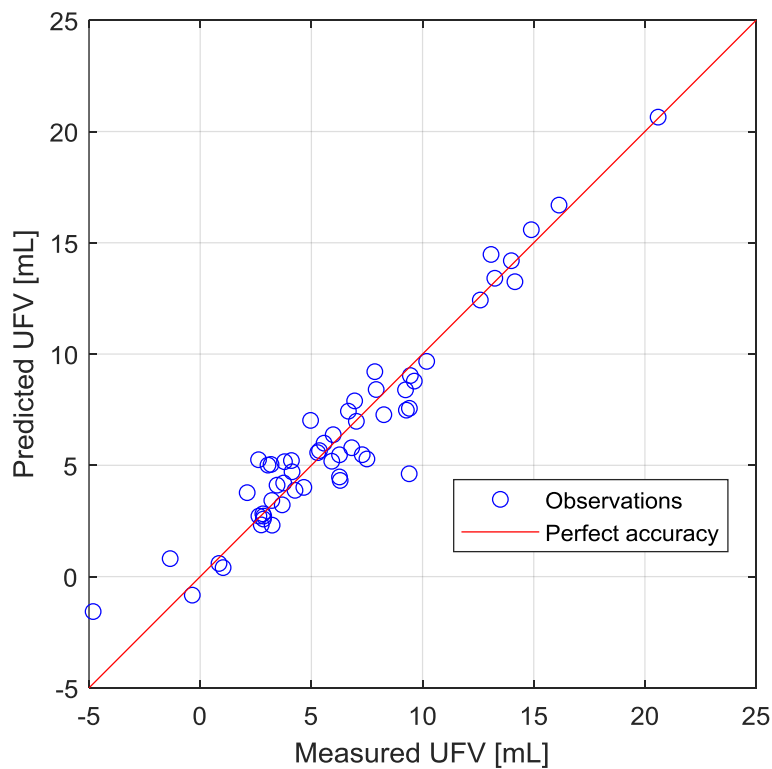


Figure 6-6: Prediction accuracy of the linear model, taking interactions into account, showing observations and perfect prediction, comparing the true response against the predicted response (R-squared: 0.92).

6.2 Biophysical model

For the biophysical model the data of the dwell phase from Figure 5-28 are used for a first evaluation and identification of the membrane parameters of the rat population. The phenomenological Equation 3-30 with same coefficients for all dialysate %'s was used to smooth the curves and for offset correction as seen in Figure 6-7. From this point the same transfer function of section 5.9 was used for P/V calculations combined with the least square's method to determine the model parameters from the corrected curves.

Single cycle model

The single cycle model could describe the corrected curves by usage of the phenomenological model and could provide a potentially good predictive capability (see Figure 6-7). The major advantage compared to the multicyle model is the capability of better handling of nonlinearities as shown in Chapter 3:. However, the average volume curves during the dwell could be described by the model with usage of the same membrane parameters for each dialysate used. Only the initial osmotic pressure gradient varies depending on the dialysate used. This principle also shown for the *Bvatar* could be considered and to further improve the model, it could be combined with empirical regression concepts; respectively machine learning to also handle different fill volumes e.g. these very practical concepts should be further investigated in a suitable patient study, as planned in the follow-up project.

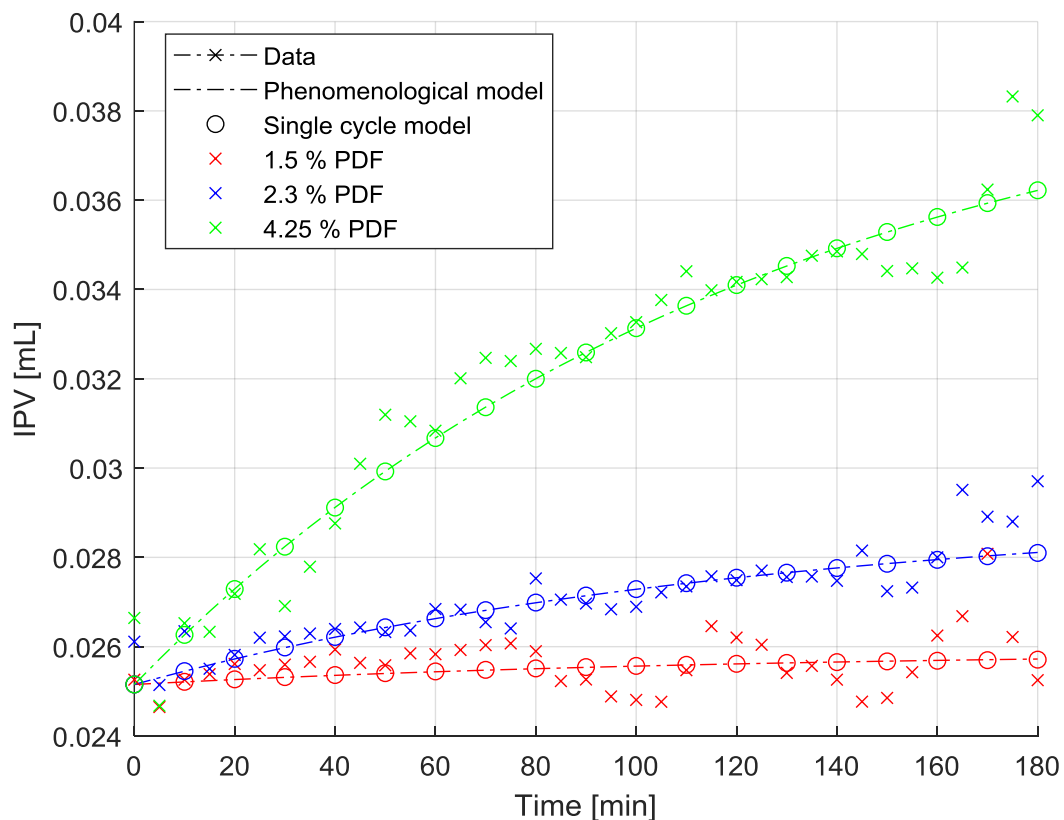


Figure 6-7: Average intraperitoneal volume over the dwell time for the used dialysates calculated by the pressure signal measured and transferred by the P/V characteristics. Further the curves are smoothed, and offset shifted by usage of the phenomenological model and finally the single cycle biophysical model was fitted to identify the rat population's membrane parameters.

Multicycle model

For the model parameter identification of the multicycle model, Equation 3-13 was used because the blood osmolarity (~ 310 mOsm/L) need to be considered in contrast to the *Bvatar* experiments, where it is simply 0 mOsm/L at the start of the experiment.

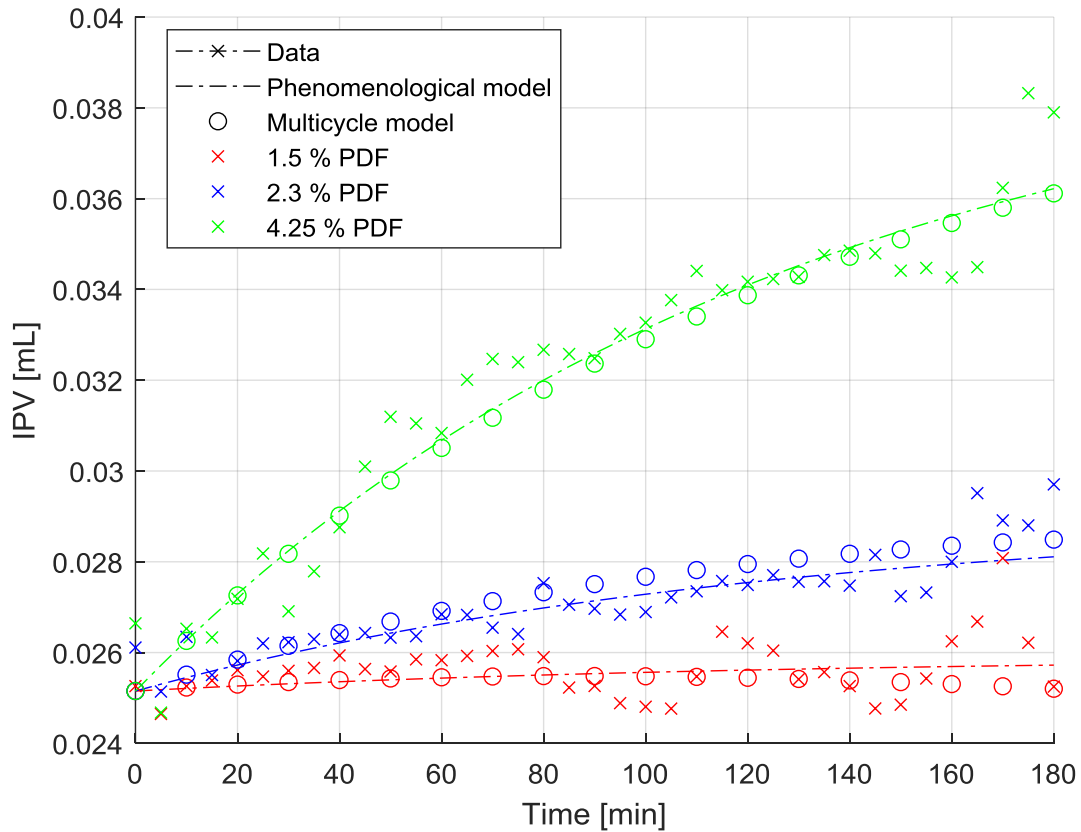


Figure 6-8: Average intraperitoneal volume over the dwell time for the used dialysates ($N=9$ per dialysate %) calculated by the pressure signal measured and transferred by the P/V characteristics. Further the curves are smoothed, and offset shifted by usage of the phenomenological model and finally the multicycle biophysical model was fitted to identify the rat population's membrane parameters.

Compared to the single cycle model, the parameter identification doesn't leave space for handling nonlinearities compared to the single cycle model approach, but nevertheless a good approximation over all curves with a suitable parameter set could be achieved.

Chapter 7: Summary and outlook

7.1 Summary

The main goal of this thesis was to establish a rat model for the PD treatment data generation, especially for investigation of biophysical and empirical model approaches built on basis on an *in vitro* test system called *Bvatar*. The physiological rat *in vivo* model was established at the Institute for Clinical and Experimental Surgery, Saarland University, Homburg, to investigate these concepts and as basis for future studies. The main simplifications of the introduced models are the reduction of concentration gradients of individual solutes to osmols and usage of a continuous measurement of IPP during the whole treatment procedure. The results of this study are used to verify the resulting model approaches and investigate the hypotheses posted, as influence of hydration on the UFV, which could in fact by wrong interpretation be a major reason for ultrafiltration failure, which is one of the big causes for dropout in PD.

7.2 Outlook

The concepts introduced need to be investigated in a more sophisticated patient study. Such a study is planned in near future at the RENAL RESEARCH INSTITUTE in New York. Moreover, from this data generated the algorithms and models to build up an Avatar model of the patient should be evaluated, and an expert system need to be built up step by step due to cooperation of an interdisciplinary team of nephrologists, physicians, data scientist, and the industry.

Feedback hydration control system (Expert systems)

The biggest problem today is to choose the right dialysate OA concentration, fill volume and dwell time to target the individual patient's needs. Due to a feedback control system with quasi continuous input of hydration status measured by body composition monitor (BCM) or known dry weight concepts, a target hydration status or body weight defined by the nephrologist and the ultrafiltration volume (UFV) response of every treatment, the treatment could be optimized for the individual patient without trial-and-error prescriptions. The feedback controller should cause an oscillation around the target hydration status to solve the big problem of overhydration and dehydration in PD treatment. The treatment schedule created from this concept should be also sufficient to remove enough uremia toxins, because this is less complicated to achieve in dialysis treatment today and could be tested by established quality assurance tests (e.g., peritoneal equilibration test, PET).

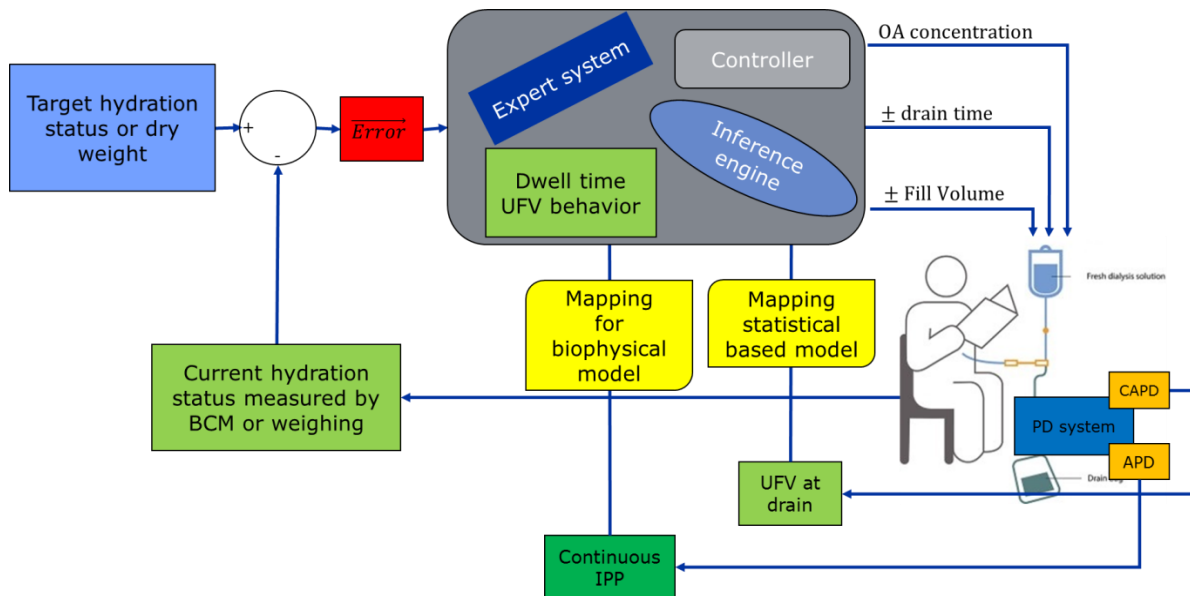


Figure 7-1: Schematic representation of an expert system with inference engine for feedback hydration control

Figure 7-1 demonstrates schematically the function of the algorithms used. First the target hydration status needs to be set in the clinic by a nephrologist and fed into the system. For the regular treatment, the patients need to measure their hydration status or body weight various often, in the best case at the start of every cycle. The resulting deviation (Error) of every hydration evaluation from the target hydration status is calculated and saved to a vector, same holds if body weight, BCM or dry weight concepts are used. This vector is used to calculate the control signal for the feedback control system, for example a PID-controller could be used for a first evaluation in simulations, as it is the simplest controller. An input, which would be also very useful and should in best case be collected every cycle, is the continuous IPP measurement during APD or the drained dialysate volume (CAPD) to get information about the patient-specific UFV and membrane characteristics behavior and the peak time of the peritoneal cavity volume. With the data generated by the controller, the inference engine could change the treatment conditions for the following cycle dependent on the control signal and the knowledge base information feed in. For the timing of the drain, the shortest possible dwell time, respective drain should be set at the peak of the UFV in the peritoneal cavity to also achieve sufficient clearance of toxins. Dependent on the residual renal function of the patient the lowest OA concentration possible to keep the patient in the range of euvoletic hydration should be used to avoid very long dwells and unnecessary glucose absorption and sodium loading of the patient [86].

Literature

- [1] Fresenius, Dialyse - Fresenius, <https://www.fresenius.de/dialyse>, (12.05.2022).
- [2] Hörl, M. P. (2003). *Dialyseverfahren in Klinik und Praxis: Technik und Klinik*. Georg Thieme Verlag.
- [3] Kuhlmann, U., Böhrer, J., Luft, F. C., Kunzendorf, U., & Alschner, M. D. (Eds.). (2015). *Nephrologie: Pathophysiologie-Klinik-Nierenersatzverfahren*. Georg Thieme Verlag.
- [4] Fresenius, Behandlungsmöglichkeiten bei chronischer Nierenerkrankung - Fresenius Medical Care, <https://www.freseniusmedicalcare.com/de/patientenfamilien/behandlungsmoeglichkeiten/>, (12.05.2022).
- [5] Fresenius, Fresenius- Home Therapies Product Catalog 2017, https://FreseniusMedicalCarena.com/content/dam/FreseniusMedicalCarena/live/support/documents/product-catalogs/HomeTherapies_1000378-F_2017__r6_new.pdf, (12.05.2022).
- [6] Baxter, Renal Care - Behandlung von Nierenerkrankungen, <https://www.baxter.de/de/medizinische-fachkraefte/renal-care-behandlung-von-nierenerkrankungen>, (12.05.2022).
- [7] Rippe, B., Stelin, G., & Haraldsson, B. (1991). Computer simulations of peritoneal fluid transport in CAPD. *Kidney international*, 40(2), 315-325, DOI: 10.1038/ki.1991.216.
- [8] Vonesh, E.F., Story, K.O., & O'Neill, W. (1999). A Multinational Clinical Validation Study of Pd Adequest 2.0. *Peritoneal Dialysis International*, 19, 556 – 571, DOI:10.1177/089686089901900611
- [9] Flessner, M. F., Fenstermacher, J. D., Dedrick, R. L., & Blasberg, R. G. (1985). A distributed model of peritoneal-plasma transport: tissue concentration gradients. *American Journal of Physiology-Renal Physiology*, 248(3), 425-435, DOI: 10.1152/ajprenal.1985.248.3.F425.
- [10] Rippe, B., & Stelin, G. (1989). Simulations of peritoneal solute transport during CAPD. Application of two-pore formalism. *Kidney international*, 35(5), 1234-1244, DOI: 10.1038/ki.1989.115.
- [11] Öberg, C. M., & Rippe, B. (2017). Optimizing automated PD using an extended 3-pore model. *Kidney international reports*, 2(5), 943-951, DOI:10.1016/j.ekir.2017.04.010.

- [12] Cano, F., Rojo, A., Azocar, M., Ibacache, M. J., Delucchi, A., Ugarte, F., Delgado, I. (2013). The mini-PET in pediatric PD: A useful tool to predict volume overload? *Pediatric Nephrology*, 28(7), 1121-1126, DOI: 10.1007/s00467-013-2447-2.
- [13] Fresenius, Interpreting the Peritoneal Equilibration Test (PET) | FRESENIUS MEDICAL CARENA, <https://Fresenius Medical Carena.com/insights/education/interpreting-the-peritoneal-equilibration-test-pet/>, (12.05.2022).
- [14] Chamney P. W., Wabel. P., Wolf. K. (2017), Apparatus for performing PD, Patent: US20200353148A1.
- [15] Masuhr, K. F., Masuhr, F., & Neumann, M. (2013). *Duale Reihe Neurologie*. Georg Thieme Verlag.
- [16] MathWorks, MATLAB & Simulink - Deutschland, https://de.mathworks.com/products/matlab.html?s_tid=hp_products_matlab, (12.05.2022).
- [17] Azar, A. T. (2013). *Modeling and Control of Dialysis Systems* (Vol. 1). Berlin, Germany: Springer.
- [18] Antony, J. (2014). *Design of experiments for engineers and scientists*. Elsevier.
- [19] Jacques, J., & Fraix-Burnet, D. (2014). Linear regression in high dimension and/or for correlated inputs. *European Astronomical Society Publications Series*, 66, 149-165, doi:10.1051/eas/1466011.
- [20] Karaca- Mandic, P., Norton, E. C., & Dowd, B. (2012). Interaction terms in nonlinear models. *Health services research*, 47, 255-274, DOI: 10.1111/j.1475-6773.2011.01314.x.
- [21] Frampton, J. E., & Plosker, G. L. (2003). Icodextrin: a review of its use in PD. *Drugs*, 63(19), 2079–2105, DOI:10.2165/00003495-200363190-00011.
- [22] Albinus, M., Amschler, G., Amschler, U., Angerer, E., Barthel, W., Bauer, A., Müller, K. (Eds.). (1994). *Hagers Handbuch der pharmazeutischen Praxis*. Springer Berlin Heidelberg.
- [23] Devuyst, O., & Ni, J. (2006). Aquaporin-1 in the peritoneal membrane: Implications for water transport across capillaries and PD. *Biochimica et Biophysica Acta (BBA)-Biomembranes*, 1758(8), 1078-1084, DOI: 10.1016/j.bbamem.2006.02.025.
- [24] Fournier, R. L. (2017). *Basic transport phenomena in biomedical engineering*. CRC press.
- [25] ARGE Niere Österreich, Peritonealdialyse (CAPD) – Verein Niere Oberösterreich, <https://ooe.argeniere.at/peritonealdialyse/>, (12.05.2022).

- [26] Khanna, R., & Krediet, R. T. (Eds.). (2009). *Nolph and Gokal's textbook of PD*. Springer Science & Business Media.
- [27] Verger, C. (1985). Relationship between peritoneal membrane structure and its permeability: Clinical implications. In *Advances in PD 1985* (87-95). Toronto University Press, Toronto.
- [28] Armada, E. R., Villamañán, E., López-de-Sá, E., Rosillo, S., Rey-Blas, J. R., Testillano, M. L., López-Sendón, J. (2014). Computerized physician order entry in the cardiac intensive care unit: effects on prescription errors and workflow conditions. *Journal of critical care*, 29(2), 188-193, DOI: 10.1016/j.jcrc.2013.10.016.
- [29] Fresenius, sleep safe harmony – so individuell wie Ihre Patienten - Fresenius Medical Care, <https://www.freseniusmedicalcare.com/de/medizinisches-fachpersonal/heimtherapien/apd/sleepsafe-harmony/>, (12.05.2022).
- [30] Scanziani, R., Dozio, B., Baragetti, I., & Maroni, S. (2004). Intraperitoneal hydrostatic pressure and flow characteristics of peritoneal catheters in automated PD. *Nephrology Dialysis Transplantation*, 19(3), 754-754, DOI:10.1093/ndt/gfh145.
- [31] Struijk, D. G., & Krediet, R. T. (2003). European best practice guidelines: adequacy in PD. *Contributions to nephrology*, 140, 170-175, DOI: 10.1159/000071437.
- [32] Schreiber, C., Al-Chalabi, A. N., Tanase, O., & Kreyman, B. (2009). Grundlagen der Nieren- und Leberdialyse. In *Medizintechnik* (1519-1584). Springer, Berlin, Heidelberg.
- [33] Johnson, D. W., Hawley, C. M., McDonald, S. P., Brown, F. G., Rosman, J. B., Wiggins, K. J., Badve, S. V. (2010). Superior survival of high transporters treated with automated versus continuous ambulatory PD. *Nephrology Dialysis Transplantation*, 25(6), 1973-1979, DOI: 10.1093/ndt/gfp780.
- [34] Himmelfarb, J., & Sayegh, M. H. (2010). *Chronic kidney disease, dialysis, and transplantation E-book: a companion to Brenner and Rector's The Kidney*. Elsevier Health Sciences.
- [35] Devuyst, O., Ni, J., & Verbavatz, J. M. (2005). Aquaporin- 1 in the peritoneal membrane: implications for PD and endothelial cell function. *Biology of the Cell*, 97(9), 667-673, DOI: 10.1042/BC20040132.
- [36] Devuyst, O., & Rippe, B. (2014). Water transport across the peritoneal membrane. *Kidney international*, 85(4), 750-758, DOI: 10.1038/ki.2013.250.
- [37] Nolph, K. D., & Twardowski, Z. J. (1989). The PD system. *PD*, 13-27.
- [38] Bręborowicz, A., Bręborowicz, M., & Oreopoulos, D. G. (2003). Glucose-induced changes in the phenotype of human peritoneal mesothelial cells: effect of L-2-oxothiazolidine carboxylic acid. *American Journal of Nephrology*, 23(6), 471-476, DOI:10.1159/000074667.

- [39] Erixon, M., Wieslander, A., Lindén, T., Carlsson, O., Forsbäck, G., Svensson, E., Kjellstrand, P. (2006). How to avoid glucose degradation products in PD fluids. *PD International*, 26(4), 490-497, DOI:10.1177/089686080602600414.
- [40] Twardowski, Z. J. (2006). Pathophysiology of peritoneal transport. *PD: A Clinical Update*, 150, 13-19, DOI:10.1159/000093443.
- [41] Ronco, C., Dell'Aquila, R., & Rodighiero, M. P. (Eds.). (2006). *PD: A clinical update* (Vol. 150). Karger Medical and Scientific Publishers.
- [42] Lee, H. Y., Choi, H. Y., Park, H. C., Seo, B. J., Do, J. Y., Yun, S. R., Shin, S. K. (2006). Changing prescribing practice in CAPD patients in Korea: increased utilization of low GDP solutions improves patient outcome. *Nephrology Dialysis Transplantation*, 21(10), 2893-2899, DOI: 10.1093/ndt/gfl393.
- [43] Heimbürger, O., Waniewski, J., Werynski, A., & Lindholm, B. (1992). A quantitative description of solute and fluid transport during PD. *Kidney international*, 41(5), 1320-1332, DOI: 10.1038/ki.1992.196.
- [44] Popovich, R. P., Pyle, W. K., & Moncrief, J. W. (1981). Kinetics of peritoneal transport. In *PD* (79-123).
- [45] Jaffrin, M. Y., Odell, R. A., & Farrell, P. C. (1987). A model of ultrafiltration and glucose mass transfer kinetics in PD. *Artificial Organs*, 11(3), 198-207, DOI: 10.1111/j.1525-1594.1987.tb02660.x.
- [46] Devuyst, O., & Goffin, E. (2008). Water and solute transport in PD: models and clinical applications. *Nephrology Dialysis Transplantation*, 23(7), 2120-2123, DOI: 10.1093/ndt/gfn298.
- [47] Struijk, D. G., & Khanna, R. (2020). Monitoring the functional status of the peritoneum. *Nolph and Gokal's Textbook of PD*, 1-31.
- [48] Mehrotra, R., Ravel, V., Streja, E., Kuttykrishnan, S., Adams, S. V., Katz, R., Kalantar-Zadeh, K. (2015). Peritoneal equilibration test and patient outcomes. *Clinical Journal of the American Society of Nephrology*, 10(11), 1990-2001, DOI: 10.2215/CJN.03470315.
- [49] Rodrigues, A. S., Silva, S., Bravo, F., Oliveira, J. C., Fonseca, I., Cabrita, A., & Krediet, R. T. (2007). Peritoneal membrane evaluation in routine clinical practice. *Blood purification*, 25(5-6), 497-504, DOI: 10.1159/000113009.
- [50] Blake, P., Burkart, J. M., Churchill, D. N., Daugirdas, J., Depner, T., Hamburger, R. J., Soderbloom, R. (1996). Recommended clinical practices for maximizing PD clearances. *PD international*, 16(5), 448-456, DOI:10.1177/089686089601600507.
- [51] Jörres, A., Lage, C., Witowski, J., & Bender, T. O. (2007). Quality assurance in PD. *PD international*, 27(2_suppl), 16-20, DOI:10.1177/089686080702702s02.
- [52] Misra, M., & Khanna, R. (2014, November). The clinical interpretation of peritoneal equilibration test. In *Seminars in Dialysis*, Vol. 27, No. 6, 598-602, DOI: 10.1111/sdi.12285.

- [53] Wang, T., Heimbürger, O., Cheng, H. H., Waniewski, J., Bergström, J., & Lindholm, B. (1997). Effect of increased dialysate fill volume on peritoneal fluid and solute transport. *Kidney international*, 52(4), 1068-1076, DOI: 10.1038/ki.1997.430.
- [54] Chien, C. C., Wang, H. Y., Chien, T. W., Kan, W. C., Su, S. B., & Lin, C. Y. (2010). A reference equation for objectively adjusting dwell volume to obtain more ultrafiltration in daily practice of PD. *Renal Failure*, 32(2), 185-191, DOI: 10.3109/08860220903541127.
- [55] Fischbach, M., Issad, B., Dubois, V., & Taamma, R. (2011). The beneficial influence on the effectiveness of automated PD of varying the dwell time (short/long) and fill volume (small/large): a randomized controlled trial. *PD international*, 31(4), 450-458, DOI: 10.3747/pdi.2010.00146.
- [56] Twardowski, Z. J., Prowant, B. F., Nolph, K. D., Martinez, A. J., & Lampton, L. M. (1983). High volume, low frequency continuous ambulatory PD. *Kidney international*, 23(1), 64-70, DOI: 10.1038/ki.1983.12.
- [57] Fischbach, M., Zaloszc, A., Schaefer, B., & Schmitt, C. P. (2014). Optimizing PD prescription for volume control: the importance of varying dwell time and dwell volume. *Pediatric Nephrology*, 29(8), 1321-1327, DOI: 10.1007/s00467-013-2573-x.
- [58] Rutkowski, B., Tam, P., van der Sande, F. M., Vychytil, A., Schwenger, V., Himmele, R., Ouimet, D. (2016). Low-sodium versus standard-sodium PD solution in hypertensive patients: a randomized controlled trial. *American Journal of Kidney Diseases*, 67(5), 753-761, DOI: 10.1053/j.ajkd.2015.07.031.
- [59] Flessner, M. F. (2009). Peritoneal ultrafiltration: physiology and failure. In *PD-From Basic Concepts to Clinical Excellence*, Vol. 163, 7-14, Karger Publishers, DOI:10.1159/000223773.
- [60] Hayes, W., & Paglialonga, F. (2019). Assessment and management of fluid overload in children on dialysis. *Pediatric Nephrology*, 34(2), 233-242, DOI: 10.1007/s00467-018-3916-4.
- [61] Aukland, K., & Reed, R. K. (1993). Interstitial-lymphatic mechanisms in the control of extracellular fluid volume. *Physiological reviews*, 73(1), 1-78, DOI: 10.1152/physrev.1993.73.1.1.
- [62] Dasgupta, I., Keane, D., Lindley, E., Shaheen, I., Tyerman, K., Schaefer, F., Moissl, U. (2018). Validating the use of bioimpedance spectroscopy for assessment of fluid status in children. *Pediatric Nephrology*, 33(9), 1601-1607, DOI: 10.1007/s00467-018-3971-x.
- [63] Wabel, P., Chamney, P., Moissl, U., & Jirka, T. (2009). Importance of whole-body bioimpedance spectroscopy for the management of fluid balance. *Blood purification*, 27(1), 75-80, DOI: 10.1159/000167013.

- [64] Fischbach, M., Zaloszc, A., Schaefer, B., & Schmitt, C. P. (2014). Optimizing PD prescription for volume control: the importance of varying dwell time and dwell volume. *Pediatric Nephrology*, 29(8), 1321-1327, DOI: 10.1007/s00467-013-2573-x.
- [65] Ronco, C., Verger, C., Crepaldi, C., Pham, J., De los Ríos, T., Gauly, A., Van Biesen, W. (2015). Baseline hydration status in incident PD patients: the initiative of patient outcomes in dialysis (IPOD-PD study). *Nephrology Dialysis Transplantation*, 30(5), 849-858, DOI: 10.1093/ndt/gfv013.
- [66] Tipler, P. A., & Mosca, G. (2019). *Physik: für Studierende der Naturwissenschaften und Technik*. Springer-Verlag.
- [67] Morelle, J., Sow, A., Fustin, C. A., Fillée, C., Garcia-Lopez, E., Lindholm, B., Devuyt, O. (2018). Mechanisms of crystalloid versus colloid osmosis across the peritoneal membrane. *Journal of the American Society of Nephrology*, 29(7), 1875-1886, DOI: 10.1681/ASN.2017080828.
- [68] Flessner, M. F. (1994). Osmotic barrier of the parietal peritoneum. *American Journal of Physiology-Renal Physiology*, 267(5), F861-F870, DOI: 10.1152/ajprenal.1994.267.5.F861.
- [69] Zakaria, E. R., Lofthouse, J., & Flessner, M. F. (1999). *In vivo* effects of hydrostatic pressure on interstitium of abdominal wall muscle. *American Journal of Physiology-Heart and Circulatory Physiology*, 276(2), H517-H529, DOI: 10.1152/ajpheart.1999.276.2.H517.
- [70] Kramme, R. (Ed.). (2016). *Medizintechnik: Verfahren-Systeme-Informationsverarbeitung*. Springer-Verlag.
- [71] Zakaria, E. R., Lofthouse, J., & Flessner, M. F. (2000). Effect of intraperitoneal pressures on tissue water of the abdominal muscle. *American Journal of Physiology-Renal Physiology*, 278(6), F875-F885, DOI: 10.1152/ajprenal.2000.278.6.F875.
- [72] Díaz, V. P., Ballesteros, S. S., García, E. H., Casado, E. D., Callejo, I. H., & Perales, C. F. (2017). Intraperitoneal pressure in PD. *Nefrología (English Edition)*, 37(6), 579-586, DOI: 10.1016/j.nefro.2017.05.014.
- [73] Dejardin, A., Robert, A., & Goffin, E. (2007). Intraperitoneal pressure in PD patients: relationship to intraperitoneal volume, body size and PD-related complications. *Nephrology Dialysis Transplantation*, 22(5), 1437-1444, DOI: 10.1093/ndt/gfl745.
- [74] Wolberg, J. (2006). *Data analysis using the method of least squares: extracting the most information from experiments*. Springer Science & Business Media.
- [75] Nolph, K. D., Mactier, R., Khanna, R., Twardowski, Z. J., Moore, H., & McGary, T. (1987). The kinetics of ultrafiltration during PD: The role of lymphatics. *Kidney international*, 32(2), 219-226, DOI: 10.1038/ki.1987.195.
- [76] Yáñez-Mó, M., Lara-Pezzi, E., Selgas, R., Ramírez-Huesca, M., Domínguez-Jiménez, C., Jiménez-Heffernan, J. A., López-Cabrera, M. (2003). PD and epithelial-to-

- mesenchymal transition of mesothelial cells. *New England Journal of Medicine*, 348(5), 403-413, DOI: 10.1056/NEJMoa020809.
- [77] Milan Manani, S., Baretta, M., Giuliani, A., Virzì, G. M., Martino, F., Crepaldi, C., & Ronco, C. (2020). Remote monitoring in PD: benefits on clinical outcomes and on quality of life. *Journal of nephrology*, 33(6), 1301-1308, DOI: 10.1007/s40620-020-00812-2.
- [78] Widerøe, T. E., Smeby, L. C., Dahl, K., & Jørstad, S. (1988). Definitions of differences and changes in peritoneal membrane water transport properties. *Artificial Organs*, 12(3), 210-218, DOI: 10.1111/j.1525-1594.1988.tb02756.x.
- [79] Van Biesen, W., Heimbürger, O., Krediet, R., Rippe, B., La Milia, V., Covic, A., & Vanholder, R. (2010). Evaluation of peritoneal membrane characteristics: clinical advice for prescription management by the ERBP working group. *Nephrol Dial Transplant*, 25(7), 2052-62, DOI: 10.1093/ndt/gfq100.
- [80] Lameire, N., Van Biesen, W., Van Landschoot, M., Wang, T., Heimbürger, O., Bergström, J., Beelen, R. H. (1998). Experimental models in PD: a European experience. *Kidney International*, 54(6), 2194-2206, DOI: 10.1046/j.1523-1755.1998.00179.x.
- [81] Lameire, N., Van Biesen, W., Mortier, S., & De Vriese, A. (2006). What did we learn from animal models in PD?. *PD: A Clinical Update*, 150, 70-76, DOI: 10.1159/000093504.
- [82] Flessner, M. F., Dedrick, R. L., & Schultz, J. S. (1985). A distributed model of peritoneal-plasma transport: analysis of experimental data in the rat. *American Journal of Physiology-Renal Physiology*, 248(3), F413-F424, DOI: 10.1152/ajprenal.1985.248.3.F413.
- [83] Grzegorzewska, A. E., Moore, H. L., Nolph, K. D., & Chen, T. W. (1991). Ultrafiltration and effective peritoneal blood flow during PD in the rat. *Kidney international*, 39(4), 608-617, DOI: 10.1038/ki.1991.72.
- [84] Zakaria, E. R., & Rippe, B. (1993). Osmotic barrier properties of the rat peritoneal membrane. *Acta physiologica scandinavica*, 149(3), 355-364, DOI:10.1111/j.1748-1716.1993.tb09631.x.
- [85] Konner, K., Keller, F., Cetto, C., Langer, S., Hepp, W., Thon, P., Böhner, H. (2009). Dialyseshuntchirurgie. In *Dialyseshunts* (119-276). Steinkopff.
- [86] Keane, D., Chamney, P., Heinke, S., & Lindley, E. (2016). Use of the body composition monitor for fluid status measurements in subjects with high body mass index. *Nephron*, 133(3), 163-168, DOI: 10.1159/000446193.

Appendix

Bvatar

Tab. I: Parameters determined to fit the data from the *Bvatar* experiments to the various model approaches

<i>Phenomenological model (Equation 3-30)</i>					
V_0 [L]	$a_1 [1e^{-3} L]$		$a_2 \left[\frac{1e^{-3} L}{min} \right]$	$k \left[\frac{1}{min} \right]$	
0.101	5% dialysate	1.8	0.004	0.041	
	7.5% dialysate	2.5			
	10% dialysate	3.8			
	15% dialysate	4.8			
<i>Biophysical multicycle model (Section 3.3)</i>					
$\widetilde{L}_p S$ [L]	$\widetilde{P}_{Osm} S \left[\frac{L}{min} \right]$	$\widetilde{\sigma}$ [-] (Offset)	$\widetilde{J}_{CL} \left[\frac{L}{min} \right]$		
1.9883 e-6	0.0035	0.0058 (0)	0		
<i>Biophysical single cycle model (Section 3.3)</i>					
$\widetilde{L}_p S$ [L]	$\Delta\pi_{Osm}^{Eff} (\widetilde{C}_{Osm}^{PDF})$ [mmHg]	$\widetilde{J}_{CL} \left[\frac{L}{min} \right]$	$\widetilde{\sigma}$ [-] (Offset)	$\widetilde{K}_{Osm} S$ [-]	
1.9395 e-6	5% dialysate	30.178	0	0.0059 (0.689)	0.0343
	7.5% dialysate	43.794			
	10% dialysate	65.251			
	15% dialysate	93.804			

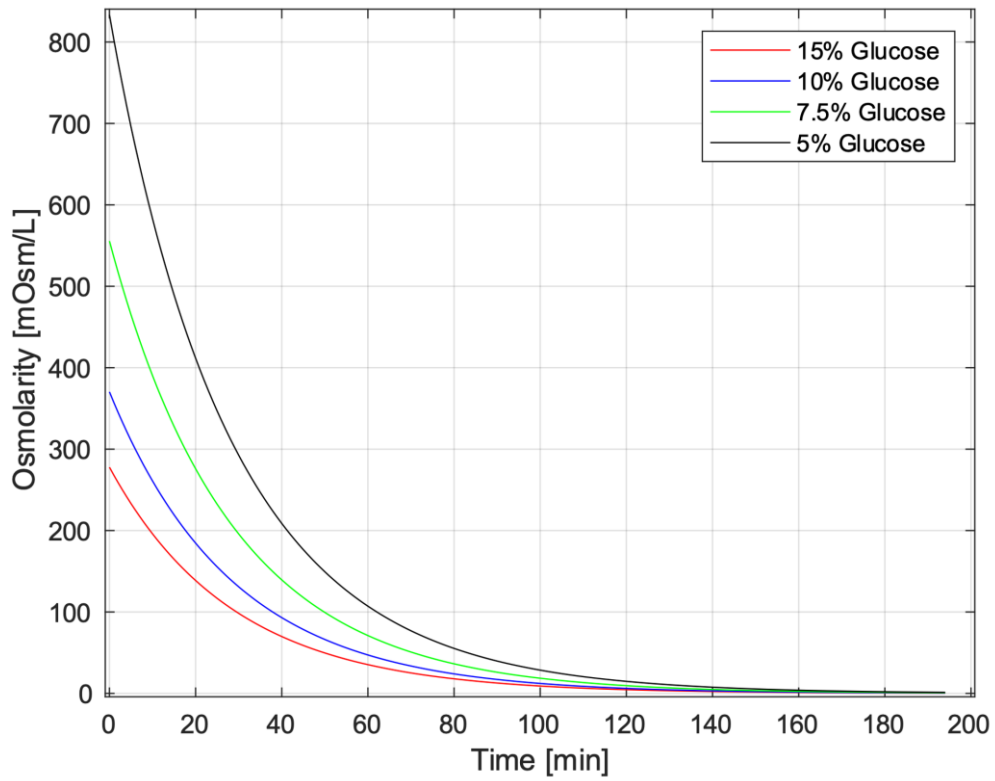


Fig. I: Multi-cycle model osmolarity over time.

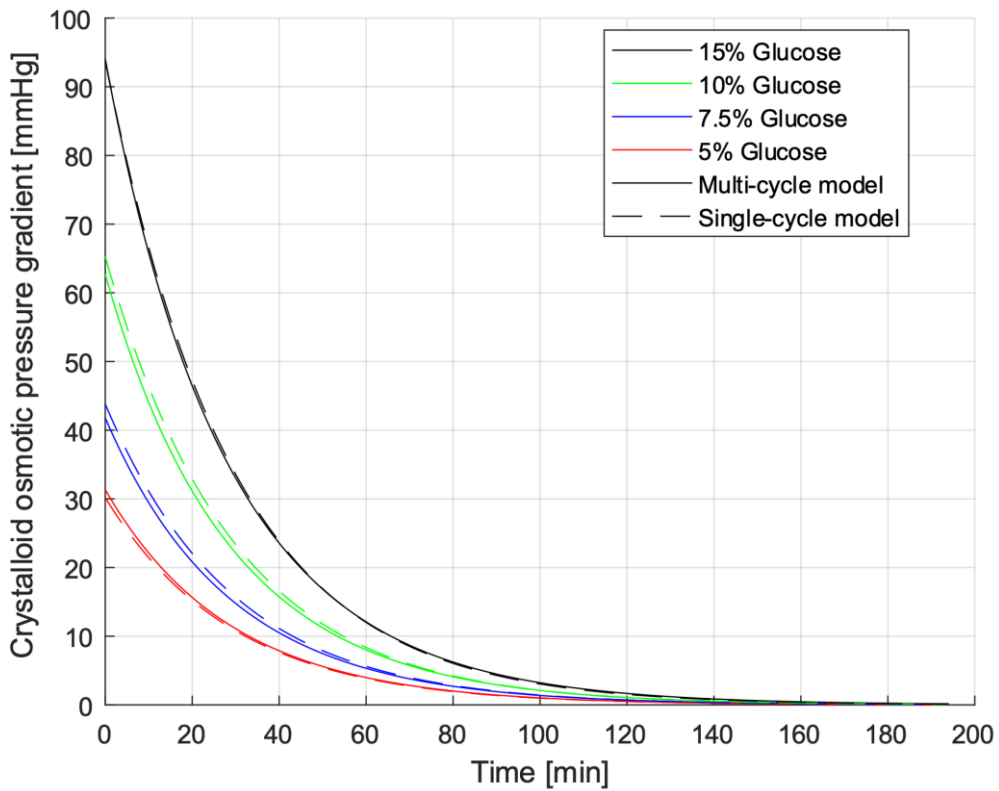


Fig. II: Multi-cycle and single-cycle model crystallloid osmotic pressure gradient over time.

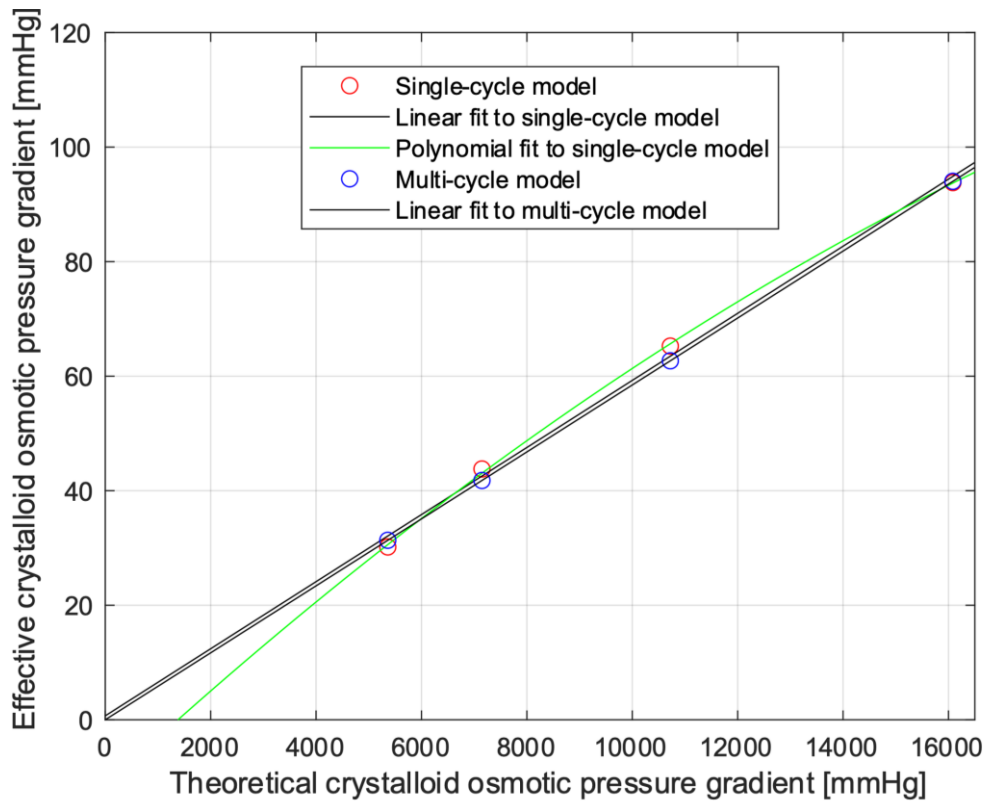


Fig. III: Representation of the relationship of unscaled to scaled osmotic pressure shown in Figure 3-6 for the models evaluated for the Bvatar.

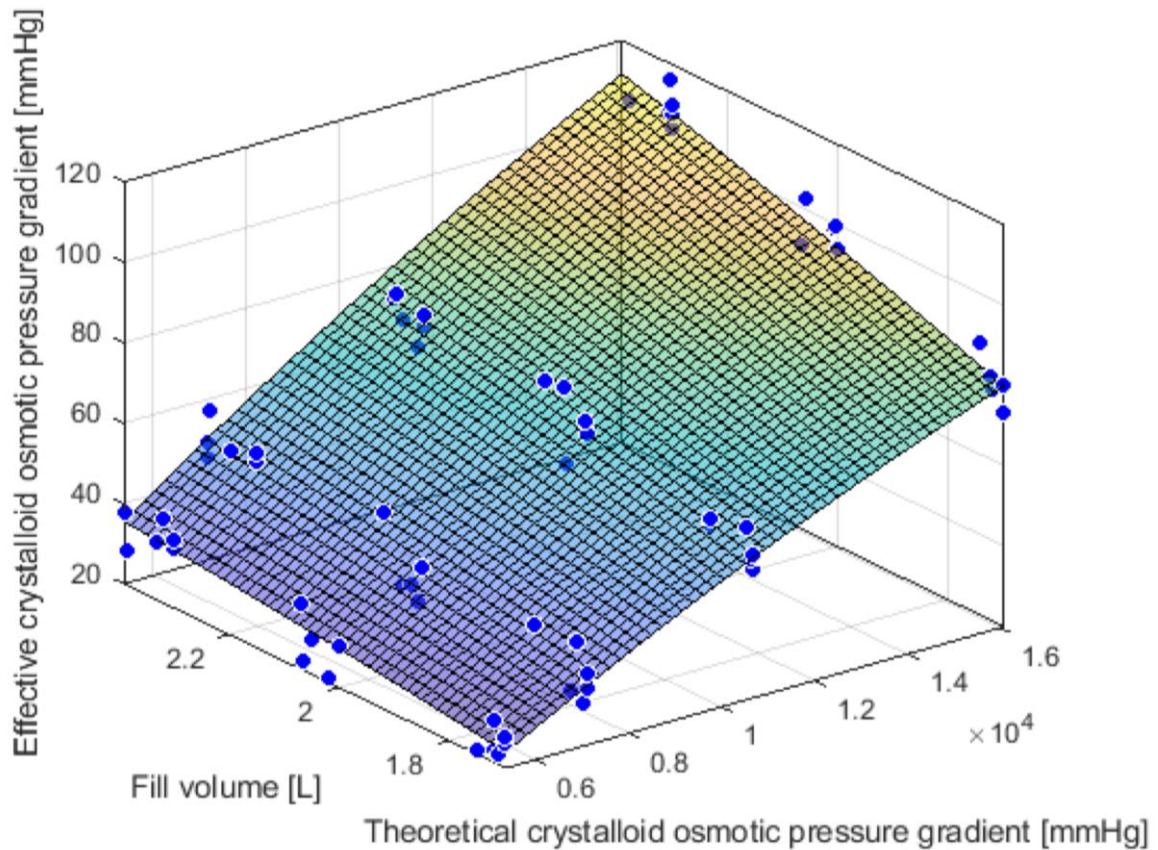


Fig. IV: Exemplary surface for calculation of the effective crystalloid osmotic pressure gradient by fill volume and theoretical crystalloid osmotic pressure gradient for the single-cycle model.

Animal study – Single-cycle model

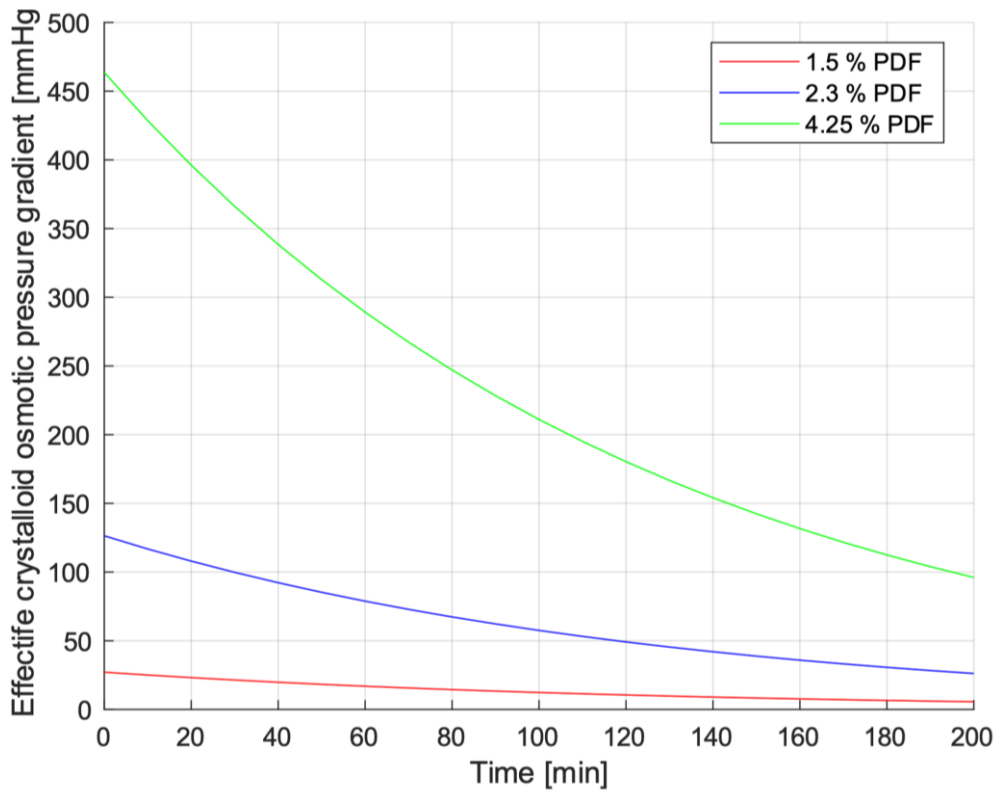


Figure V: Corresponding to Section 6.2, Figure 6-7 regarding the change of the effective crystalloid osmotic pressure gradient.

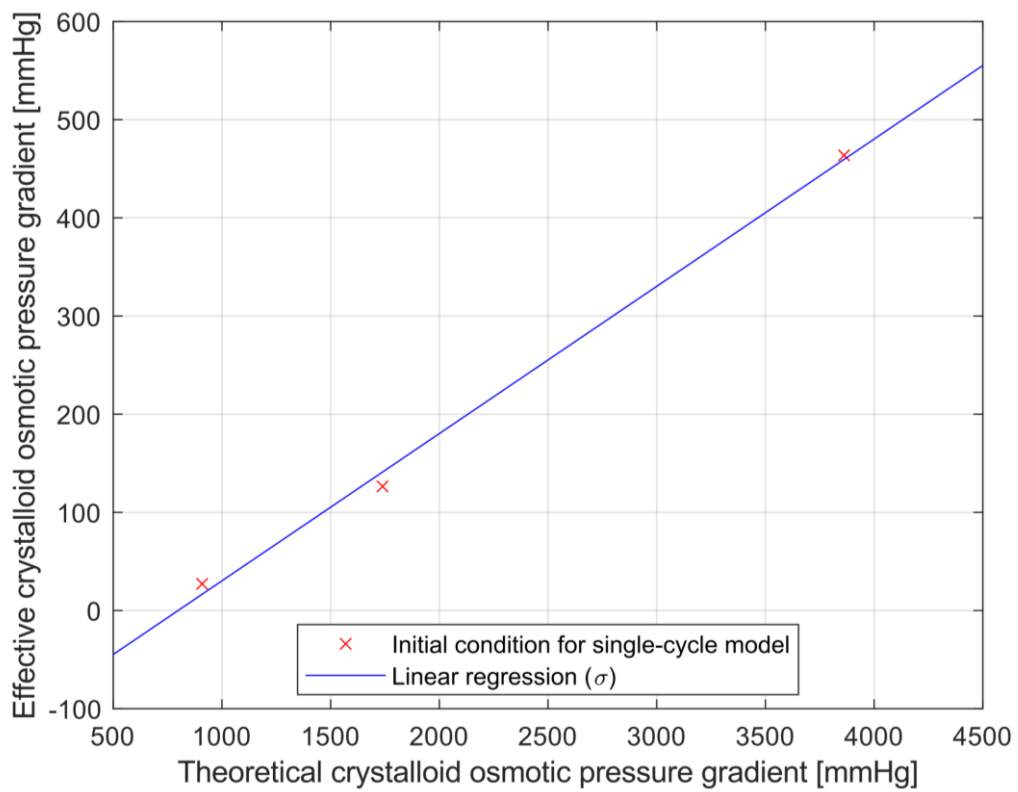


Figure VI: Single-cycle model determination of agglomerated reflection coefficient.

Animal study – Multi-cycle model

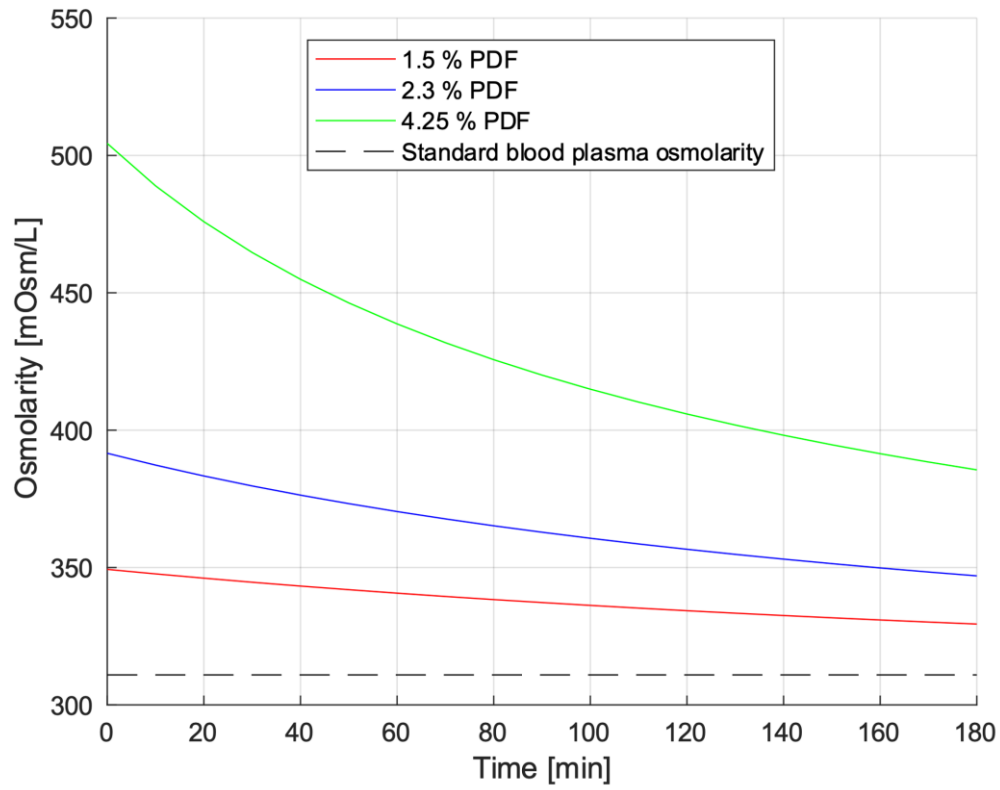


Figure VII: Corresponding to Section 6.2, Figure 6-8 regarding the change of the osmolarity over time for the different dialysate's used.

Acknowledgement

First and foremost, I would like to thank my doctoral supervisor, Prof. Dr. Christian Wagner, who immediately made himself available to supervise my work and Dr. Thomas John, who was always a great support to me with his advice and tips.

I would like to thank Prof. Dr. Matthias W. Laschke for his willingness to take on the task of second examiner.

I would like to express my special thanks to Dr. Robert Berlich and Dr. Jochen Huppert of Fresenius Medical Care for allowing me to work on this interesting topic and the possibility to visit a lot of interesting congresses as well as to my supervisors Dr. Paul Chamney and Dr. Lisa Strahl for their support throughout the entire period of my doctorate.

I would like to thank them for the numerous discussions and support throughout my doctoral studies, as well as Dr. Thomas John, who actively supported me during the final phase of my doctoral thesis at Fresenius Medical Care.

I would especially like to thank Mirjam Jakob and Nora Toggweiler for their cooperation and excellent support through their work also started for a PhD thesis at Fresenius Medical Care. Further, I would like to thank the members of the AG Wagner, especially Rishab Handa and Dr. Alexander Kiehm for their moral support and motivation to always keep going.

Other thanks go to the training workshop, especially Torsten Brill and Thorsten Lauer, who always supported me in mechanical and electrical questions concerning the test systems and setups.

During the practical part at Fresenius Medical Care, I was supported by the whole departments GRD/PEC-SCC, Sterile Solutions/Packaging/Accessories Development and GRD/PEC-CaTS, Cassettes and Tubing Systems as well as all students of the last four years.

I would like to thank them for their cooperation and the nice working atmosphere.

Furthermore, I would like to thank the Fresenius Medical Care's Biocompatibility, Microbiology, Analytical, Application Engineering, Home Team, Law Department as well as Patent department for their help and support.

I would like to thank the group at the Institute for Clinical and Experimental Surgery, Saarland University, Homburg, especially Prof. Dr. Matthias Laschke for the friendly integration during the animal experiments. Furthermore, I would like to thank the group members of the Renal Research Institute in New York for their cooperation and fruitful discussions, especially MD Peter Kotanko for his support and the possibility to visit their clinic.

Finally, I would like to thank my friends, my girlfriend Sabrina and my whole family for their understanding, constant support, patience, distraction, and motivation.

Thank you!